Boosting baseline plant immunity using non-self RNAs

Joshua Hoti

MSc in Computational Biology

2025

School of Biosciences,

Division of Natural Sciences,

The University of Kent,

Canterbury

Page count: 149

Table of Contents

List of Abbreviations:

	Abbreviation	Definition
1.	RdDM	RNA-directed DNA methylation
2.	VIRE	Virulence Protein
3.	ACC	Aminocyclopropane-1-Carboxylic Acid
4.	ACD	Accelerated Cell Death
5.	ACS	Aminocyclopropane-1-Carboxylic Acid Synthase
6.	ADP	Adenosine Diphosphate
7.	AGO	Argonaute
8.	ANOVA	Analysis Of Variance
9.	AP	Apetala
10	ATP	Adenosine Triphosphate
11	BAK	Brassinosteroid Insensitive 1 (Bri1)-Associated Receptor Kinase
12	BIK	Botrytis-Induced Kinase
13	BIR	Bak1-Interacting Receptor-Like Kinase
14	BRI	Brassinosteroid Insensitive
15	BSA	Bovine Serum Albumin
16	CAB	Chlorophyll A/B Binding Protein
17	CCA	Circadian Clock-Associated Protein
18	CDPK	Calcium Dependent Protein Kinase
19	CERK	Chitin Elicitor Receptor Kinase

20	CFU	Colony Forming Units
21	CHN48	Chitinase A Gene
22	CML	Calmodulin-Like Protein
23	COI	Coronatine-Insensitive
24	DA	Dehydroabietinal
25	DCL	Dicer-Like Protein
26	DEG	Differentially Expressed Genes
27	DNA	Deoxyribonucleic Acid
28	DRM	Domains Rearranged Methyltransferase
29	EDS	Enhanced Disease Susceptibility
30	EMS	Ethyl Methanesulfonate
31	ERF	Ethylene Response Factor
32	ET	Ethylene
33	ETI	Effector-Triggered Immunity
34	FDH	Formate Dehydrogenase
35	FDR	False Discovery Rate
36	FLS	Flagellin-Sensing
37	FRK	Flg22-Induced Receptor-Like 1
38	GFP	Green Fluorescent Protein
39	GO	Gene Ontology
40	GSEA	Gene Set Enrichment Analysis
41	GSH	Glutathione

42	GSTU	Glutathione S-Transferases
43	GTP	Guanosine Triphosphate
44	HEM	Homozygous EMS Mutant
45	HIGS	Host-Induced Gene Silencing
46	HLH	helix–loop–helix
47	HP	Hairpin
48	ICS	Isochorismate Synthase
49	IDT	Independent DNA Technologies
50	IG	Indolic Glucosinolates
51	JA	Jasmonic acid
52	JAI	Jasmonate Insensitive
53	JAZ	Jasmonate-ZIM domain
54	KANR	Kanamycin Resistance
55	KYP	Kryptonite (protein)
56	LAP	Leucine Aminopeptidase
57	LBA	Luria Bertani Agar
58	LBB	Luria Bertani Broth
59	LRR	Leucine Rich Repeat
60	MAPK	Mitogen Activated Protein Kinase
61	MES	2-(N-Morpholino)Ethanesulfonic Acid
62	MIN7	HopM Interactor7
63	MS	Murashige and Skoog

64	MYC	Myelocytomatosis
65	NAD	Nicotinamide Adenine Dinucleotide
66	NCBI	National Center For Biotechnology Information
67	NEB	New England Biolabs
68	NHP	N-Hydroxy Pip
69	NLR	Nucleotide-Binding Leucine-Rich Repeat
70	NO	Nitric Oxide
71	NPR	Nonexpresser Of PR-Genes
72	OD	Optical Density
73	OH	Hydroxyl-
74	ORA	Octadecanoid-Responsive Arabidopsis Protein
75	OX	Overexpression
76	PAMP	Pathogen Associated Molecular Pattern
77	PBS	avrPphB Susceptible
78	PCR	Polymerase Chain Reaction
79	PD	Plasmodesmata
80	PDF	Plant Defensin
81	PDLP	Plasmodesmata-Located Protein
82	PIN	Proteinase Inhibitor
83	PR	Pathogenesis-Related Protein
84	PRR	PAMP-recognition receptor
85	PTI	PAMP-Triggered Immunity

86	QTL	Quantitative Trait Loci
87	RAC	Rac-Family GTPase
88	RBD	RNA Binding Protein
89	RBOHD	Respiratory Burst Oxidase Homolog Protein
90	RDR	RNA-Dependent RNA Polymerase
91	RICK	Receptor-like Cytoplasmic Kinase
92	RIN	RPM1-Interacting protein
93	RISC	RNA-Induced Silencing Complex
94	RLK	Receptor-Like Kinase
95	ROS	Reactive Oxidative Species
96	RPM	Resistance To Pseudomonas syringae Pv Maculicola
97	RPS	Resistant to Pseudomonas syringae
98	SA	Salicylic Acid
99	SAR	Systemic Acquired Resistance
10	SERK	Somatic Embryogenesis Receptor Kinase
10	SGS	Suppressor Of Gene Silencing
10	SIGS	Spray-Induced Gene Silencing
10	SOBIR	Suppressor Of Bir
10	T-DNA	Transfer DNA
10	T3SS	Type Iii Secretion System
10	TAE	Tris-Acetate-EDTA
10	TAIR	The Arabidopsis Information Resource

10	TGA	TGACG-Binding
10	TGS	Transcriptional Gene Silencing
11	TIR	Transport Inhibitor Response
11	TML	Too Much Love
11	TOC	Timing Of Cab Expression
11	TOE	Target Of Eat
11	TPL	Topless Protein
11	TPR	Topless-Related
11	TSPI	Triosephosphate Isomerase 1
11	UDP	Uridine Diphosphate Glycosyltransferase
11	UGT	Uridine Diphosphate Glucuronosyltransferase
11	VIP	VIRE2 Interaction Protein
12	VST	Variance Stabilising Transformation
12	WRKY	WRKY DNA-binding domain transcription factor family
12	WT	Wild-Type
12	YEB	Yeast-Extract Broth
12	YFP	Yellow Fluorescent Protein
12	ZIM	Zinc finger protein
12	ZIP	Basic Leucine Zipper

Declaration

I confirm that the wording of this report is entirely my own. No part of the report has been copied from scientific journals, web sites or any other sources. AI tools have NOT been used in the generation of text for this thesis. The AI tool ChatGPT has been used for signposting and troubleshooting in the iterative process of developing programming scripts for data analysis.

Acknowledgements

I'm grateful to the University of Kent's School of Biosciences, part the division of Natural Sciences, for hosting this Master's Project. I'm also thankful to my supervisors, Dr Helen Cockerton and Dr Sara Lopez-Gomollon, and the other members of my supervisory board, Dr Jose Ortega Roldan and Dr Hollie Larnach, for their unwavering support and guidance over the past two years. In particular, I appreciate Dr Cockerton and Dr Larnach for their invaluable mentorship in the laboratory, which helped me conduct much of the project's work.

I also want to thank the remaining members of the Cockerton lab group: Harry Meades, Dr Cindayniah Godfrey, Dr Sarah Blackburn, Simon Thundow, and Keely Masser, as well as Dr Andrew Armitage at the Natural Resources Institute, University of Greenwich. Their assistance in understanding statistical tests, providing R bioinformatics resources, and helping me set up a GitHub repository was crucial for my academic progress.

I would also like to thank Dr Deniz Göl at Cranfield University for suggesting the application of Spray-Induced Gene Silencing in *Arabidopsis thaliana*, which provided the direction for the second year of my project and helped me develop my own disease assay protocol using agroinfiltration.

I finally want to thank the wider members of the Kent Fungal Group of laboratories for their guidance and support throughout the project. Their encouragement to present my work and receive constructive feedback has been instrumental in my academic development.

Data Availability

All scripts and datasets generated and used in this project can be found on GitHub at: https://github.com/NRI-pathogenomics/Josh-s-R-Protocols.

1. Abstract

Plants and pathogens engage in a molecular arms race that determines infection outcomes. RNA interference is a defence mechanism used by both host plants and pathogens during infection and the subsequent disease response. Recent studies have also demonstrated that double-stranded RNAs (dsRNAs) play an important role in triggering defence responses to viral infection, by acting as Pathogen Associated Molecular Patterns (PAMPs) which are recognised by host plants. There is also evidence to suggest that non-self RNAs may also protect the plants against infection with fungal pathogens. One study observed that mutant *Arabidopsis thaliana* lines expressing dsRNA hairpins, targeting the Green Fluorescent Protein (GFP) gene, appeared to show enhanced resistance to infection with *Verticillium dahliae*. However, it was unclear why expression of the GFP hairpin in *A. thaliana* appeared to protect the mutant plant from infection, despite not targeting the genes of crucial virulence factors in the fungus.

In this project, we sought to validate the findings of these previous studies and investigate whether expression of non-self RNA hairpins enhances plants' resistance to disease. We transiently expressed the hairpin in *A. thaliana* leaves and infected the transformed plants with the plant pathogen *Pseudomonas syringae*, to test of the introduction of the hairpin reduced the severity of disease symptoms in transformed plants. To further explore whether non-self RNA hairpins elicit the upregulation of defence pathways in host plants, we analysed RNASeq data from a study that used RNA hairpins against *S. sclerotiorum* in *A. thaliana*. This analysis revealed differentially expressed genes (DEGs) in hairpin-expressing versus wild-type plants prior to infection.

Although our disease assay was variable, when the controls succeeded, we demonstrated that the GFP hairpin did not reduce leaf damage after *P. syringae* infection in transformed plants. This contradicts previous observations of the GFP hairpin conferring a protective effect in *A. thaliana*. However, our analysis of RNASeq data revealed that the hairpin targeting the fungal *Anhydrolase-3* gene enhanced baseline immunity in *A. thaliana*. At 0 d.p.i., the hairpin-expressing line showed an upregulation of baseline defence pathways compared to the wild-type, suggesting improved natural disease response to *S. sclerotiorum*. We hypothesised that, besides reducing *S. sclerotiorum* virulence by targeting , the hairpin also acted as a PAMP, leading to upregulation of defence pathways and enhancing the plant's natural response to *S. sclerotiorum*.

Plant pathogens pose a significant threat to global food security. However, the use of commercial antimicrobial agents on crops is unsustainable due to the increasing difficulties associated with antimicrobial resistance, stricter

legal regulations on chemical use, and the negative impacts many agricultural antimicrobials have on human health and the environment. Therefore, RNA technology is gaining traction in the agricultural sector as a means of developing chemical-free disease management strategies.

2. Introduction

2.1 Plant-Pathogen Interactions

Unlike animals, plants lack circulating cells and an adaptive immune system. However, through the use of a more specialised innate immune system, plants have evolved specific responses to various pathogens and can even build up prolonged memory for future infections (Spoel *et al.* 2012; Zhang *et al.* 2024). Plant immunity can be split into two overlapping responses: the Pathogen-Associated Molecular Pattern Triggered Immunity (PTI) response and the Effector-Triggered Immunity(ETI) response (Figure 1).

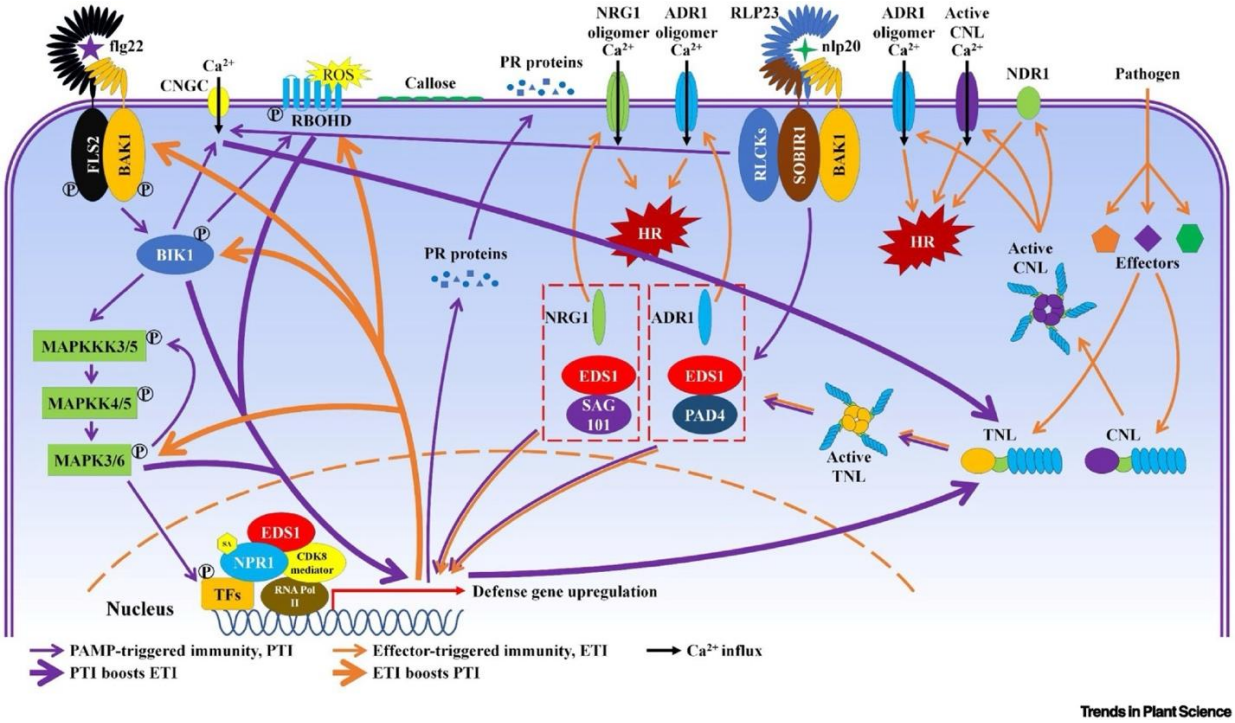

Figure 1: The PAMP-Triggered Immunity (PTI) and Effector-Triggered Immunity (ETI) pathways which underpin the immune response of plant cells. PTI-related interactions are shown in purple, ETI related interactions are shown in orange. As illustrated, the two pathways converge and potentiate the other (Chang *et al.* 2022).

2.1.1 PAMP-Triggered Immunity (PTI) and Pathogen Associated Molecular Patterns (PAMP)

There are many pathogen-derived molecules that plants recognise as Pathogen Associated Molecular Patterns (PAMPs) and each one triggers different pathways to mount an appropriate response to the type of invading pathogen (bacterial, fungal, oomycete or viral). The PAMP Triggered Immunity (PTI) pathway in plants is the first layer of a complex immune system that protects local and systemic tissue from invasion by a pathogen.

This pathway is governed by various transmembrane Pattern Recognition Receptors (PRRs), which detect a variety of PAMPs from invading pathogens in a gene-for-gene like fashion: PRRs encoded by host resistance (*R*) genes are responsible for detecting PAMPs encoded by avirulence genes in the invading pathogen (Zipfel *et al.* 2005). Upon detection of a PAMP, *PRR*s phosphorylate a variety of signalling molecules, which in turn phosphorylate MITOGEN ACTIVATED PROTEIN KINASE (MAPK) proteins, which activate transcription factors, which leads to an upregulation of defence pathway genes (Bigeard, Colcombet and Hirt, 2015). Different PAMPs elicit different signalling molecules, with the most well-known signalling pathway being the response to *flg22* (Felix *et al.* 1999; Bigeard, Colcombet and Hirt, 2015). In the *flg22* response pathway, the transmembrane Leucine Repeat Rich (LRR)-receptor kinase FLAGELLIN-SENSING-2 (FLS2) associates with the regulatory LRR-receptor kinase BRASSINOSTEROID INSENSITIVE 1 (BRI1)-ASSOCIATED RECEPTOR KINASE 1 (BAK1) to form heteromeric coreceptors, which detect *flg22* in invading pathogens (Couto *et al.* 2016). The FLS2-BAK1 complex also binds to BOTRYTIS-INDUCED KINASE-1 (BIK1) (Li *et al.* 2023) during normal cell signalling. Once bound to *flg22*, the FLS2 activates BAK1, which phosphorylates BIK1, releasing it from The *FLS2-BAK1* complex into the cytosol (Couto and Zipfel, 2016; Chi *et al.* 2021; Li *et al.* 2023). BIK1 then begins phosphorylating transmembrane Ca^{2+} ion channels, triggering an influx of Ca^{2+} ions into the host plant cells, leading to downstream reactive oxidative species (ROS) production by CA^{2+} DEPENDENT RESPIRATORY BURST OXIDASE HOMOLOG (RBOH) proteins (Chi *et al.* 2021).

This influx also leads to activation of CALCIUM DEPENDENT PROTEIN KINASE (CDPK) enzymes which work synergistically with MAPKs (Seybold *et al.* 2014), though the intermediate signalling that occurs between PRR activation and MAPK signalling in the PTI response pathway has yet to be characterised (Couto and Zipfel, 2016). MAPKs, namely MAPK-3, -4 and -6 have been linked to phosphorylation of transcription factors and other metabolites involved in the PTI response. For example, the transcription factor *VIRE2 INTERACTION PROTEIN 1 (VIP1)*, which upregulates the *PATHOGENESIS-RELATED PROTEIN-1* (*PR1)* gene*,* is one such gene that MAPK-3 phosphorylates in response to fungal pathogens such as *Verticillium dahliae* (Zhang *et al.* 2019). MAPK-3 and MAPK-6 function redundantly, sharing several key PTI-related functions, such as the phosphorylation of aminocyclopropane-1-carboxylic acid (ACC) SYNTHASE-2 and -6 (ACS-2 and -6), enzymes which are responsible for converting f-S-adenosyl-L-Met to 1- ACC (Thulasi Devendrakumar, Li and Zhang, 2018). ACC is a precursor to the phytohormone ethylene, which triggers the plant's defence responses to attack

from insect parasites and necrotrophic pathogens (Padmanabhan, Zhang and Jin, 2009). MAPK-3, -4 and -6 have all been linked to phosphorylation of transcription factors such as WRKY-33, which is responsible for camalexin biosynthesis, a phytoalexin that acts as a broadly targeting antimicrobial agent against a range of bacterial and fungal pathogens (Bigeard, Colcombet and Hirt, 2015; Thulasi Devendrakumar, Li and Zhang, 2018). Camalexin and other phytoalexins have also been linked to the synthesis of Tryptophan-derived indolic glucosinolates (IGs), which act as molecular triggers for callose deposition and the subsequent closure of stomata, restricting pathogen entry to the host tissue (Clay *et al.* 2009; Ahuja, Kissen and Bones, 2012; Thulasi Devendrakumar, Li and Zhang, 2018; Nguyen *et al.* 2022).

Phytohormones also play a key role in the PTI response. Salicylic Acid (SA), jasmonic acid (JA) and ethylene (ET) are the three main phytohormones involved in both PTI and the Effector-Triggered Immunity(ETI) Pathway (Chang *et al.* 2022). Each phytohormone is upregulated in response to different types of pathogens: SA is expressed in response to biotrophic pathogens, while JA and ET are expressed in response to necrotrophic pathogens (Nguyen, Nguyen and Nguyen, 2024).

In *Arabidopsis thaliana,* SA is produced in the chloroplasts by the ISOCHORISMATE SYNTHASE-1 (ICS1) enzyme and in the cytosol by the *avrPphB* SUSCEPTIBLE3 (PBS3) enzyme, with chloroplastic SA being trafficked to the cytosol by the ENHANCED DISEASE SUSCEPTIBILITY 5 (EDS5) transporter protein (Ishihara *et al.* 2008; Rekhter *et al.* 2019; Tian *et al.* 2024). SA accumulates and binds to its cytosolic receptor protein, NONEXPRESSER OF PR-GENES 1 (NPR1) (Wu *et al.* 2012). This leads to NPR1's trafficking to the nucleus, where it interacts with transcription factors in the TGACG-BINDING (TGA) family, resulting in the upregulation of SA-related defence genes. (Nguyen *et al.* 2024). SA-related defence pathways include: ROS production (free radical nitric oxide in particular), Ca^{2+} influxes and MAPK cascades (Saleem, Fariduddin and Castroverde, 2021).

JA is produced by the plant upon being wounded, producing α-Lipoxygenase (LOX) enzymes which convert linolenic acid into JA (Nguyen, Nguyen and Nguyen, 2024). ET is produced when its precursor molecules 1-aminocyclopropane-1-carboxylic acid (ACC) is oxidised by AC-OXIDASE enzymes (Chen *et al.* 2021). The bioactive form of JA ((+)-7-iso-JA-Ile) induces the formation of the CORONATINE-INSENSITIVE-1(COI1)-jasmonate (JAZ)-ZIM domain co-receptor complex, which triggers ubiquitination and subsequent breakdown of

JAZ repressors, such as JASMONATE-INSENSITIVE-3 (JAI3), allowing for the activation of JAZ-repressed transcription factors which proceeds to activate JA-associated resistance pathways (Chini *et al.* 2007, 2018; Chen *et al.* 2021).

The main functions of JA, in the form of (+)-7-iso-JA-Ile, are to induce the closure of stomata and to interact with various signalling metabolites and other molecules to upregulate the plant's baseline immunity (Hewedy *et al.* 2023). JA elicits two types of response: one targeting insect parasites and one targeting necrotrophic pathogens (Zhang *et al.* 2017).

In the response to insects, JAZ binds to a series of transcription factors in the basic helix–loop–helix (bHLH) group IIIe, specifically: MYELOCYTOMATOSIS (MYC)-2, -3, -4, and -5 (J. Wang *et al.* 2019; Song *et al.* 2022). These MYCs upregulate the production of glucosinolates, which, when metabolised by insects, form toxic compounds like thiocyanates, isothiocyanates, or nitriles, killing the invading parasite. (Schweizer *et al.* 2013). Additionally MYC2 and -10 have been linked to upregulation of *PROTEINASE INHIBITOR II* (*PIN2*) and *LEUCINE AMINOPEPTIDASE* (*LAP*) genes, which plants secrete when being fed on to cause digestive tract disruption to the invading insect (Boter *et al.* 2004).

In the response to necrotrophic pathogens, JA works synergistically with ethylene to upregulate of APETALA2/ ETHYLENE RESPONSE FACTOR (AP2/ERF) domain transcription factors such as ERF1, OCTADECANOID-RESPONSIVE ARABIDOPSIS 59 (ORA59) and BASIC LEUCINE ZIPPER (bZIP) transcription factor-family protein TGA5, which leads to an upregulation of defence proteins such as PLANT DEFENSIN 1.2 (PDF1.2) (Zarei *et al.* 2011; Zhu, 2014; Zhang *et al.* 2017). Plant defensins have been predominantly linked to antifungal responses (Stotz and and Wang, 2009), acting in one of several proposed mechanisms: oligomerising and perforating in the cell wall of the pathogen to form pores, peptides individually perforating the membrane to form pores, or altering the phospholipid membrane's permeability to ions and plant-derived peptides leading to increased ROS production and programmed cell death in the fungal cells (Lacerda *et al.* 2014).

2.1.2 Effector-Triggered Immunity (ETI) and effectors

Throughout evolution, pathogens have evolved to inhibit PATHOGEN RECOGNITION (PR) proteins and, consequently, block the PTI response. Biomolecules responsible for inhibition of PR proteins are called effectors

(Laflamme *et al.* 2020). In response to the evolution of effectors in pathogens, plants have developed countermeasure pathways which comprise the Effector-Triggered Immunity(ETI) Response.

The ETI is a second layer of the plant's immune response, triggered either when the plant detects the secreted effector proteins themselves or the disruption to the cellular and extracellular environments caused by effector proteins(Cui *et al.* 2015; Couto *et al.* 2016). The ETI provides a more specific immune response, where specific effector proteins are recognised by complementary plant resistance (R) proteins, typically NUCLEOTIDE-BINDING LEUCINE-RICH REPEAT (NLR) receptors (Cui *et al.* 2015; Yu *et al.* 2017; Yuan *et al.* 2021), in a gene-to-gene like fashion (Jones *et al.* 2006). The ETI is a far stronger and more sustained response than the PTI (Yu *et al.* 2024), with some studies suggesting that ETI works to restore pathogen-suppressed PTI responses by upregulating basal immunity-related pathways (Jones *et al.* 2006; Cui *et al.* 2015).

During normal cell signalling, NLRs are kept in an "off" state, however, upon binding to their complementary effector (or host-derived Damage Associated Molecular Patterns), conformational changes within the NLRs occur resulting in downstream signalling (Baudin *et al.* 2017). For example, in *Arabidopsis thaliana*, the two main NLRs involved in the response to infection with *Pseudomonas syringae* are: RESISTANT TO PSEUDOMONAS SYRINGAE-2 (RPS2) and RESISTANCE TO PSEUDOMONAS SYRINGAE PV *MACULICOLA* 1 (RPM1) (Gao *et al.* 2013). RPM1 is activated when *P. syringae* effectors, AvrB and AvrRPM1 trigger an accumulation of the phosphorylated negative immune regulator protein, RPM1-Interacting protein 4 (RIN4), by increasing the kinase activity of the Receptor-like Cytoplasmic Kinase (RICK) enzyme (Liu *et al.* 2011; Lu *et al.* 2024). It is this accumulation of phosphorylated RIN4 that is detected by RPM1 and leads to ETI-related signalling (Liu *et al.* 2011; Chung *et al.* 2011). RPS2 signalling is induced by the absence of RIN4, as the *P. syringae* effector AvrRpt2 targets RIN4 for degradation (Mackey *et al.* 2003). As RIN4 negatively regulates RPS2 protein, the decrease in RIN4 levels causes activation of RPS2-signalling, triggering the ETI response (Axtell *et al.* 2003; Mackey *et al.* 2003).

Downstream signalling from NLRs is poorly understood, as there is a distinct knowledge gap between the activation of NLRs and the subsequent defence response, with little detail known about the signalling pathways that occur in between (Qi *et al.* 2013; Bentham *et al.* 2017; Su *et al.* 2018). Nevertheless, some details of the downstream process following NLR signalling has been discovered. For example, RPS2 leads to an upregulation

of MAPK-3/6, which causes a global downregulation of photosynthesis genes across the plant (Su *et al.* 2018). Additionally, the transcription factors WRKY-8, WRKY-28, and WRKY-48 are proposed to regulate downstream gene expression from RPS2 and RPM1, reportedly being regulated by CA^{2+}-DEPENDENT PROTEIN KINASE (CDPK) -4, -5, -6, and -11 (Jacob, Vernaldi and Maekawa, 2013). Pathways activated by downstream signalling of NLRs during the ETI response include: programmed cell death (the hypersensitive response) (Yuan *et al.* 2021), ROS production (Tsuda *et al.* 2010), prolonged Ca^{2+} signalling (Wang *et al.* 2021; Köster *et al.* 2022) and *MAPK* signalling (Nabi *et al.* 2024).

It was once thought that the PTI and ETI formed separate arms of the plant immune system (Kim, Song and Lee, 2022; Locci and Parker, 2024), however, in recent years it has become more apparent that there is a strong synergistic relationship between the two (Tsuda *et al.* 2010; L. Zhang *et al.* 2023; Yu *et al.* 2024). On one side of this crosstalk, ETI signalling causes mass production of effector-targeted molecules to restore PTI signalling, resulting in the potentiation of PTI-related responses such as: ROS production, callose deposition, prolonged phosphorylation, increased accumulation of proteins such as BIK1, RBOHD and MAPKs, biosynthesis of defence-related phytohormone and secondary metabolites (Dalio *et al.* 2021; Ngou *et al.* 2021). On the other side of this crosstalk, the PTI pathway has been demonstrated to be essential for ETI signalling. For example, PAMP Recognition Receptors have been demonstrated to be involved in the ETI-mediated programmed cell death response in infected tissue. Studies investigating *Arabidopsis* knockout mutants for PRR/co-receptors, *fls2-efr-cerk1* (*fec*) and *bak1-bkk1-cerk1* (*bbc*), showed that the absence of these PRRs and PRR co-receptors, which detect bacterial PAMPs, led to impaired programmed cell death responses during infection with *P. syringae* pv. tomato (*Pst*) DC3000 (Yuan, Jiang, *et al.* 2021; Chang *et al.* 2022).

2.1.3 Localised and systemic acquired resistance

Upon initial infection, plants will raise an appropriate response to the type of pathogen in the local infected tissue – this is the localized immune response. During the localised response, Systemic Acquired Resistance (SAR) signalling molecules such as salicylic acid will accumulate in the primary infected leaf (Ádám *et al.* 2018; Kachroo *et al.* 2020), particularly in the petiole regions, connecting to the plants' phloem (Ádám *et al.* 2018). Other than Salicylic acid, other signalling molecules accumulate including: methyl-SA (MeSA) (Park *et al.* 2007), azelaic acid (AzA) (Yu *et al.* 2013), GLYCEROL-3-PHOSPHATE (G3P) (Shine *et al.* 2019), dehydroabietinal (DA) (Chaturvedi *et al.* 2012), free radical nitric oxide (•NO), and reactive oxygen species (ROS) (Wang *et al.* 2014),

pipecolic acid (Pip) (Návarová *et al.* 2012), N-hydroxy Pip (NHP) (Hartmann *et al.* 2018), pinene volatiles (Wenig *et al.* 2019), and extracellular nicotinamide adenine dinucleotide phosphate (eNADP) (Wang *et al.* 2019).

Signalling molecules are transported first into the apoplast via transpiration (Lim *et al.* 2020), to induce PR gene expression in the surrounding uninfected leaf tissue (Maruri-López *et al.* 2019) before being loaded into the phloem to be transported to distal regions of the plant (Lim *et al.* 2020). Interestingly, Lim *et al.* (2020) reported that, while SA accumulation in the uninfected distal regions of the plant was essential for SAR, transport of SA from the infected to uninfected tissue was not. Therefore, they concluded that an intermediate signalling molecule may be being transported to induce SA production in distal regions of the plant (Lim *et al.* 2020). The result is a long lasting systemic resistance response, with PR genes being upregulated in healthy tissue (Park *et al.* 2007; Vlot, Dempsey and Klessig, 2009), to reduce the likelihood of repeat infection by the same pathogen.

2.2 RNA Immunity

RNA silencing is used ubiquitously in eukaryotes as a form of post-transcriptional gene regulation. The term "RNA immunity" covers a broad range of RNA-elicited response pathways that are part of both the PTI and ETI pathways. Two major pathways are: the dsRNA-triggered PTI response (Amari *et al.* 2020) and the RNA-interference (RNAi) response (Fusaro *et al.* 2006; Ellendorff *et al.* 2009). The RNAi response is one application of RNA silencing in plants, whereby targeted RNAs provide pathogen-specific protection for both local and systemic infections and trigger pathways which induce prolonged immunity, whereas dsRNAs in the dsRNA-triggered PTI response induces a more general systemic response by temporarily upregulating defence pathways to make the plant more responsive to foreign molecular patterns (Necira *et al.* 2024).

2.2.1 Small RNAs (sRNAs) and their discovery

Small RNAs (sRNAs) were first discovered in *Caenorhabditis elegans* when it was discovered that the *lin-4* gene encoded a small RNA, produced from a longer hairpin intermediate, which worked to repress protein production from *lin-4* mRNA (Lee *et al.* 1993; Dexheimer *et al.* 2020) playing a regulatory role in *C. elegans* cell differentiation and development (Wightman *et al.* 1993; Dexheimer *et al.* 2020). sRNAs and RNA-interference (RNAi) are part of an ancient pathway, believed to have evolved in unicellular organisms before the emergence of the metazoan clade 700 million years ago (Bråte *et al.* 2018; Dexheimer *et al.* 2020). Analogous components of the RNA interference (RNAi) machinery are believed to have first arisen in prokaryotes and archaea (Shabalina

et al. 2008). It has been reported that sRNAs and RNAi may have first evolved as a means of defence against viruses and genomic parasites such as transposable elements (Obbard *et al.* 2009).

2.2.2 sRNAs and RNA-interference (RNAi) in plants

Messenger RNA (mRNA) is the chemical message from the nucleus, transcribed from an organism's DNA which is then trafficked to the ribosomes. The ribosomes then read the sequence of codons that makes up the mRNA strand and translate the encoded message into produce protein strands. RNA interference (RNAi) serves as a regulatory mechanism for metabolic pathways. There are several types of regulatory sRNAs: microRNA (miRNAs) and small interfering RNAs (siRNAs). Both are typically generated from double stranded RNAs (dsRNAs) by Dicer proteins (Wilson *et al.* 2013) and then loaded into Argonaute-family (AGO) endonuclease proteins to form the core of the RNA-induced silencing complex (RISC) (Hu *et al.* 2013; Wilson *et al.* 2013). The RISC complex, influenced by the template provided by the miRNA/siRNA guide strand at its core, will then target specific mRNA strands for degradation (Iwakawa *et al.* 2022).

In plants, small RNAs (sRNAs) are an important regulator of immune pathways, playing multiple roles in genomic regulation (Padmanabhan, Zhang and Jin, 2009). For example, *miR393* is an miRNA produced in response to the detection of *flg22* and negatively regulates auxin by targeting the mRNAs that encode auxin receptors transport inhibitor response 1 (TIR1) and Auxin-signalling F-Box 1 (ABF1) protein, inhibiting their production (Dharmasiri, Dharmasiri and Estelle, 2005; Navarro *et al.* 2006; Padmanabhan, Zhang and Jin, 2009; Dubey *et al.* 2023). miRNAs are also involved in plant-microbe symbiosis events. For example, during nodulation events with rhizobia bacteria in the roots of leguminous plants, the immune system can hinder the success of nodulation if plant's defences are triggered by rhizobacteria colonisation (Ratu *et al.* 2021). Therefore, both the bacteria (Jiménez-Guerrero *et al.* 2022), and the plant have developed mechanisms to suppress the immune system during symbiosis (Luo *et al.* 2024). For example, *miR2111* is translocated to the roots to inhibit the symbiosis suppressor TOO MUCH LOVE (TML) to allow symbiosis to occur (Tsikou *et al.* 2018). Zou *et al.* (2020) reported that miRNAs can work in an age-dependent fashion, such as *miR172b* which represses the negative regulators for the expression of the *flg22* receptor *FLS2* gene, TARGET OF EAT 1 (TOE1) and TOE2. The levels of *miR172b* increases between days 2 and 6 of growth in *Arabidopsis thaliana*, leading to an increase in *FLS2* production as the plant ages (Zou, Wang and Lu, 2020).

The RNAi pathway is also used as a defence from viral and eukaryotic pathogens in the PTI and ETI pathways.

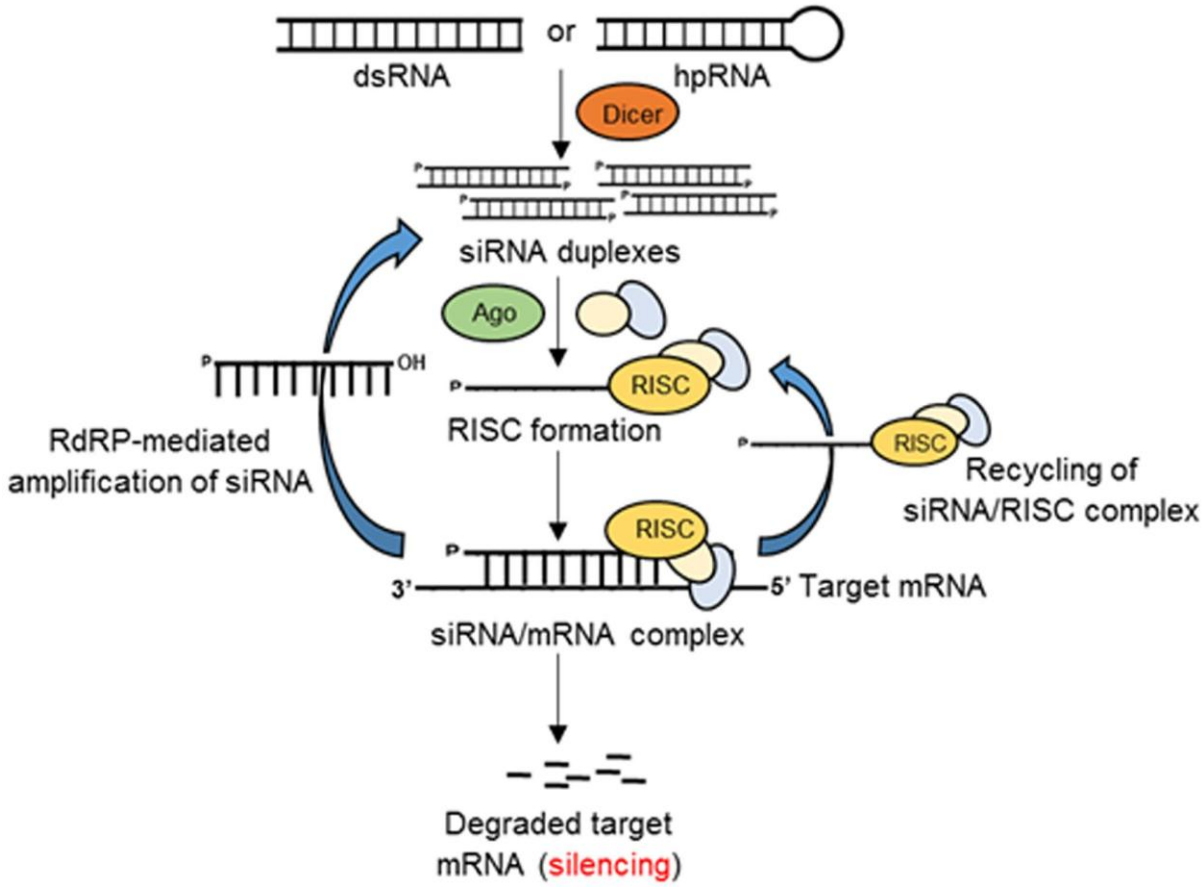

Figure 2: The production of small interfering RNAs (siRNAs) from double-stranded RNAs (dsRNAs). dsRNAs are cleaved by Dicer-like enzymes (green) producing siRNAs, which are incorporated into the RISC complex (purple) and leading to recognise and degrade target messenger RNA (mRNA) transcripts. Taken from Majumdar *et al.* (2017).

As shown in Figure 2, dsRNAs released from the pathogen trigger the RNA-interference pathway by interacting with Dicer-like Proteins (DCLs), which break down the dsRNAs into small interfering RNAs (siRNAs) to help degrade pathogenic messenger RNA (mRNA) within the cytosol of invaded host cells (Whitehead *et al.* 2011; Niehl *et al.* 2016).

In the case of viral infection, viruses multiply within the host plant cell, hence why the RNAi pathway is crucial for the antiviral response in plants (Muhammad *et al.* 2019). During the antiviral RNAi response, viral-derived siRNAs are generated from the viral dsRNA intermediates, by multiple DCLs operating on cytosolic viral RNAs in the infected cells (Wang *et al.* 2011). Different clades of DCLs produce different lengths of siRNAs: DCL2

produces 22-nt long siRNAs, DCL-3 produces 24-nt long siRNAs and DCL4 produces 21-nt long siRNAs (Fusaro *et al.* 2006). Once produced, siRNAs are then loaded into AGO1 and AGO2 (Wang *et al.* 2011). RNA viruses produce dsRNAs as an intermediate step before hijacking transcriptional machinery, therefore DCL4 is the primary DCL protein driving the antiviral response supported by the partially redundant function of DCL2 and -3 (Gasciolli *et al.* 2005; Fusaro *et al.* 2006). DCL2 and -4 work to cleave viral-derived dsRNA into 21-nt siRNAs to trigger targeted lysis of viral mRNAs via RISC-mediated RNA degradation (Xie *et al.* 2004; Jin *et al.* 2022). In the case of DNA viruses, such as geminiviruses (Catoni *et al.* 2018), their genetic material localises to the infected plant cell nucleus which acts as the virus's site of transcription (Pooggin, 2013). The antiviral response to DNA viruses is driven by several different mechanisms which silence viral gene expression *de novo*. One such route requires the use of small RNAs. This defence pathway uses the RNA-DEPENDENT RNA POLYMERASE-6 (RDR6) and SUPPRESSOR OF GENE SILENCING-3 (SGS3) proteins which produce dsRNAs from the DNA virus's genome to trigger the production of siRNAs (Béclin *et al.* 2002; Ye *et al.* 2015). The plant's expression profile during viral infection will also change, in part due to the production of miRNAs. RNA POLYMERASE III (Pol III) processes host-derived RNAs into double stranded pre-miRNAs (Du *et al.* 2019) which are then cleaved into single-stranded miRNAs by DCL1 (Kurihara *et al.* 2004). Once siRNAs are loaded into the RISC complex, they guide the AGO proteins at its core to bind complementary viral mRNA transcripts, leading to the catalytic degradation of viral RNA (Muhammad *et al.* 2019). In the case of miRNAs, they target host RNAs which are either positive regulators of pathways, leading to downregulation of genes that relate to metabolic pathways that make a plant more susceptible to an invading pathogen (Wang *et al.* 2018), or negative regulators of pathways that are linked to immunity-related pathways such as ROS production and phytohormone modulation (Val-Torregrosa *et al.* 2022; Fahad *et al.* 2025). Hence, by targeting these RNAs for degradation, miRNAs can alter a plant's expression profile to enhance the plant immune response (Huang, Yang and Zhang, 2016). Another mechanism of DNA virus repression is epigenetic modification of viral chromatin, via RNA-directed DNA methylation (RdDM) (Jin *et al.* 2022). RNA POLYMERASE IV (Pol IV) and RNA-DEPENDENT RNA POLYMERASE-II (RDR2) work sequentially to form short dsRNA precursors, which are then processed by DCL3 to form 24-nt siRNAs (Huang *et al.* 2021; Jin *et al.* 2022). These siRNAs are then loaded into AGO4 and -6 proteins, which recruit Domains Rearranged Methyltransferase 2 (DRM2) to viral chromatin (Coursey *et al.* 2018; Pougy *et al.* 2025). DRM2 facilitates the cytosine methylation on viral chromatin formed by DNA viruses, such as geminiviruses (Coursey *et al.* 2018). Pol V also synthesises long non-coding (lncRNA) scaffold RNAs, using viral chromatin as a template (Zhang *et al.* 2019; Veluthambi *et al.* 2021). These lncRNAs then recruit the

RdDM complex to target viral loci (Gallego-Bartolomé *et al.* 2019) facilitating the recruitment of histone methyltransferases, such as KRYPTONITE (KYP), which deposit H3K9me2 repressive markers on viral chromatin (Sun *et al.* 2015). This results in heterochromatinization of the viral mini-chromosomes and transcriptional gene silencing (TGS) of the viral genome (Jackel *et al.* 2016).

Some fungi are also susceptible to host plant RNAi defences. Studies on species of fungal pathogens such as *Botrytis cinerea* and *Verticillium dahliae* have suggested that these pathogens may engage in a bidirectional cross-talk with their host plants, each one possibly passing RNAs derived from the other's genome to inhibit the immune response (pathogen-to-host) or to stem the growth of invading fungal cells (host-to-pathogen) (Wang *et al.* 2016). The current model of this bidirectional cross-talk involves the passing of sRNAs between host and pathogen cells via extracellular vesicles, where the fungus passes its own mRNAs to hijack the replication machinery of the plant to enhance the production of fungal proteins during infection, and it is this hijacking that presents plants with the opportunity to produce siRNAs against key fungal genes, which are then passed by the plant to the fungus by extracellular vesicles (Cheng *et al.* 2023). For defence against pathogens in the *Verticillium* genus, this bidirectional transfer of RNAs has been proven to be essential for the antifungal response during infection (Ellendorff *et al.* 2009). Despite what is already known about bidirectional crosstalk between host plants and fungal pathogens, the exact mechanisms of RNA transfer between the two has yet to be properly identified.

Cross-kingdom signalling has been exploited by various studies looking into development of alternative antifungal strategies. Duanis-Assaf *et al.* (2022) demonstrated that application of dsRNAs exogenously to the site of infection can stem the growth of *B.cinerea* in the fruit, leaf and petal tissue of various host species, and can even reduce the concentration of commercial fungicide required to inhibit fungal growth.Walker *et al.* (2023) demonstrated that a genetically modified line of *Arabidopsis thaliana* expressing an RNA hairpin designed to target a key pathogenicity factor in the fungus *Sclerotina sclerotiorum* led to significantly reduced lesion size during infection and an overall improved resistance response compared to the Col-0 wild-type. These two studies alone demonstrate the two main approaches to RNAi strategies to disease management: Host-Induced Gene Silencing (HIGS) (Walker *et al.* 2023) and Spray-Induced Gene Silencing (SIGS) (Duanis-Assaf *et al.* 2022). In both cases, pathogen-targeting dsRNAs are passed from the host to the pathogen, cleaved into 21-22 nt-long siRNAs and incorporated into the RISC complex in the fungal pathogens' cells (Cheng *et al.* 2023), leading to reduced pathogenicity. RNAi-induced pathogenicity reduction in invading fungal species can be achieved through various

means such as: targeting pathogenicity factor genes (Walker *et al.* 2023), indirectly targeting transcription factors that regulate pathogenicity factors (such as the *sge1* gene in *V. dahliae*) (Song and Thomma, 2016), or by targeting the expression of enzymes responsible for elongation and maintenance of components of the fungal cell wall (Caracuel *et al.* 2005; Mouyna *et al.* 2005).

2.2.3 Double-stranded RNA (dsRNA) as a PAMP

In recent years, double stranded RNA (dsRNA) has also become a widely known PAMP for the plant viral immunity pathway. dsRNAs are recognised by the plant during viral infection and activate the PTI response in a DCL-independent manner (Niehl *et al.* 2016). Nucleic acid induced PTI and peptide-induced PTI signalling pathways are different, with dsRNAs triggering the SOMATIC EMBRYOGENESIS RECEPTOR KINASE-1 (SERK1) coreceptor-mediated signalling pathway (Niehl *et al.* 2016) which is distinct from bacterial response pathways. dsRNA-triggered callose deposition is triggered independently from ROS signalling, when BOTRYTIS-INDUCED KINASE-1 (BIK1) signalling is elicited by the detection of Salicylic Acid (SA) by PLASMODESMATA-LOCATED PROTEIN 1 and 3 (PDLP1 and -3) and Ca^{2+} ion sensing by CALMODULIN-LIKE PROTEIN 4 (CML4) resulting in defence upregulation such as plasmodesmata closure (Huang *et al.* 2021).

There is evidence that non-self RNAs also have a 'priming' effect on the host plant, by causing an accumulation of ethylene and jasmonic acid which cause a baseline upregulation of plant immune defences (Whitehead *et al.* 2011). This increase in baseline immunity is believed to lead to improved systemic acquired resistance to infection with pathogens in the plant (Serrano-Jamaica *et al.* 2021), although few studies have investigated this 'priming' effect in much detail, as it is often overlooked as a side-effect of RNAi techniques, rather than as a viable disease prevention tool. This priming effect may also be a confounding variable when it comes to interpreting the findings from path assays which have used RNAi to screen the functions of effectors and pathogenicity genes, if the siRNAs targeting these genes in the pathogen are themselves immunogenic in the host plant producing them.

2.3 The host: *Arabidopsis thaliana*

Arabidopsis thaliana is one of the most studied model organisms for plant research. Its initial use was established before the development of modern genomics and renewed interest in the species during 1970s led to it becoming a standard model species for plant science research (Koornneef *et al.* 2010). The first recorded use of the species in modern science has been attributed to Friedrich Laibach, whose 1907 PhD thesis reported the number of

chromosomes the species to be 5 (Laibach 1907; Koornneef *et al.* 2010), an observation that was confirmed by later karyotyping studies on Col-0 and other mutant lines (Leutwiler, Hough-Evans and Meyerowitz, 1984).

In plant science research, the benefits of *A. thaliana* include: a small nuclear genome, virtually no dispersed repetitive nucleotide sequences, a generation time of 4 to 5 weeks and (by 1985) mutations that affect hormone synthesis and responses, enzyme pathways, and embryonic developmental processes have been identified and characterized (Meinke *et al.* 1979; Meyerowitz *et al.* 1985). Because of its unique properties as a model organism, various genetic tools have been developed using *A. thaliana*. For example, chemical and fast neutron mutagenesis provide the means of carrying out forward genetic screens and transformation methods such as transposon-induced and T-DNA insertion (by *A. tumefaciens*) mutagenesis allow for the production of loss-of-function mutation lines for most genes, to be used in reverse genetic studies (Sozzani *et al.* 2011).The wealth of forward and reverse genetic studies allowed for the development of various comprehensive genomic databases for *A. thaliana's* genome, which have provide a starting point for many plant genetic studies (Friesner *et al.* 2025). T-DNA insertional mutagenesis can be applied to forward genetics, to disrupt gene sequences across the *A. thaliana* genome, using the insertional sequence as a tag to identify the causative genotype linked to a focal phenotype. That said, forward genetic studies using T-DNA insertional mutagenesis in *A. thaliana* have previously been limited by the need to phenotype tens of thousands of individual plants to properly characterise mutant lines, and the limitations of gene insertion methods like T-DNA insertion creating variation in the lines due to a lack of homozygosity within the mutant populations produced (Wang *et al.* 2016; Carrère *et al.* 2023). To overcome these limitations, a recent study mutated *A. thaliana* via ethyl methanesulfonate (EMS) mutagenesis and produced fully characterised homozygous EMS mutant (HEM) lines by single seed descent, streamlining the characterisation process by using whole genome sequencing, and produced a HEM collection of homozygous mutants which are genetically stable and sharable, enabling large-scale phenotyping on a small, consistent set of samples (Carrère *et al.* 2023). Additionally, while the *A. thaliana* Col-0 genome has been sequenced (The Arabidopsis Genome Initiative, 2000) older reference genomes still contained large missing segments and had a higher number of errors due to being produced by older sequencing methods, leading to more comprehensive reference genomes being produced using newer, more precise sequencing methods such as Oxford-Nanopore and Hi-Fi sequencing (Wang *et al.* 2022). Newer reference genomes have provided a greater insight into the genome organisation and functions of individual genes in the Col-0 genome. In addition, pan-genome studies have performed whole genome sequencing of cultivars other than Col-0, to better characterise the differences within the genomes of *A. thaliana*

cultivars from different environments from around the world and analyse how these differences between cultivars allow them to survive under the various biotic and abiotic stresses found in their preferred environments (Kileeg *et al.* 2024).

2.4 The pathogen: *Pseudomonas syringae*

Pseudomonas syringae is a gram-negative bacterium and one of the most researched and well-documented plant pathogens to date, with a broad host range (Morris *et al.* 2019) and over 40 known host-specific pathogenic strains (Young *et al.* 2010). As such, it serves as a highly effective model for research into: understanding host-pathogen interactions, phytobacterial virulence mechanisms, adaptation of pathogens to their preferred host, microbial evolution, ecology and epidemiology (Xin *et al.* 2018).

P. syringae provides a useful insight into the emergence of disease in domesticated crops, a famous example being the emergence of canker disease in Kiwifruit caused by *P. syringae pv. actinidiae* (*Psa*), in the 1980s (McCann *et al.* 2013). Disease emergence in crop plants has been linked to the domestication of crop plants by early humans, during the Holocene period 11.5 thousand years ago (Stukenbrock *et al.* 2008). However, this fact often limits disease emergence studies, as pathogens do not typically leave evidence of emergence and diversification such as fossils (Gibbs *et al.* 2008). Canker disease is the exception as its host, the Kiwifruit, was only domesticated in the 1930s, 50 years prior to the first outbreaks of the disease (McCann *et al.* 2013), not only making the emergence of *Psa* much easier to study, but also highlighting the economic significance of the *Pseudomonas* genus in terms of *Psa* ecology and evolution (Donati *et al.* 2020).

P. syringae has 50 known pathovars to date, which share a common ancestor approximately 150-183 million years ago (O'Brien *et al.* 2012). Not all pathotypes are pathogenic and some exist as plant commensals (Xin, Kvitko and He, 2018). The lifecycle of pathogenic *P. syringae* can be split into an epiphytic phase, where they live and potentially proliferate on the surface of a plant (Arnold *et al.* 2019), and an endophytic stage, when the bacteria gains entry to the leaves via openings such as stomata or wounds in the epidermis to infect and cause disease in their host plants (Melotto *et al.* 2006).

Once in the apoplastic space, *P. syringae* has two objectives: suppress plant immunity and alter the apoplastic space by releasing nutrients from mesophyll cells to create a favourable environment for reproduction (Xin,

Kvitko and He, 2018). *P. syringae* alters the apoplastic space via a process called "water-soaking", where the mesophyll cells release vast quantities of water and nutrients into the apoplast (Aung, Jiang and He, 2018). The two key water-soaking inducing virulence factors employed by *P. syringae* are AvrE and HopM1 (Aung, Jiang and He, 2018; Hu *et al.* 2022). AvrE is secreted into the mesophyll cells via the Type-III secretion system (T3SS) and causes lesion formation by inducing necrosis of the mesophyll cells which releases their contents into the apoplastic space (Badel *et al.* 2006; Cunnac, Lindeberg and Collmer, 2009). HopM1 targets the HOPM interactor 7 (MIN7) Trans-Golgi Network adenine dinucleotide phosphate (ADP) ribosylation factor–guanine nucleotide exchange factor, a critical component of the vesicle trafficking system which disrupts the plants' ability to modulate water availability in the apoplast (Xin *et al.* 2016). The molecular components of the endophytic stage of *P. syringae's* life cycle have been highly characterised over the years, making it one of the most well studied pathosystems to use in host-plant interaction research.

Entry to the leaves is met by resistance from the host plant, as Pathogen Associated Molecular Patterns (PAMPs) such as *flg22* on the *P. syringae* cell surface are sensed by PRRs. FLAGELLIN-SENSING-2 (FLS-2) receptors in the membranes of stomatal guard cells, triggering stomatal closure and downstream signalling to upregulate plant defences in response to the pathogen (Zeng *et al.* 2010).

P. syringae supresses the PAMP-Triggered (Section 2.1.1) and Effector-Triggered (Section 2.1.2) immune responses, using a T3SS to introduce jasmonic acid (JA) modulating effector proteins such as: HopX1, AvrB (Gimenez-Ibanez *et al.* 2014; Lee *et al.* 2015) and coronatine (Uppalapati *et al.* 2005). These effectors keep JA levels high which prevents Salicylic Acid (SA) accumulation by increasing ethylene production and reducing auxin production (Uppalapati *et al.* 2005; Gimenez-Ibanez *et al.* 2014; Lee *et al.* 2015). This shifts the plant's metabolism by preventing various SA-signalling dependent defence genes from being upregulated such as: *PATTERN RECEPTORS (PR) PROTEINS, FLAGELLIN-SENSITIVE-2 (FLS2), ETHYLENE RESPONSE FACTOR (ERF), CHITIN ELICITOR RECEPTOR KINASE 1 (CERK1), SUPPRESSOR OF BIR 1-1 (SOBIR1), MITOGEN-ACTIVATED PROTEIN KINASE (MAPK)* enzymes*, CALCIUM-DEPENDENT KINASE* enzymes*,* and *RESPIRATORY BURST OXIDASE HOMOLOG PROTEIN-D (RBOHD)* (Zhang *et al.* 2025). Coronatine secretion also causes the leaf chlorosis, by activating the chlorophyllase coronatine-induced protein-1 (*COR1*) gene in *Arabidopsis thaliana* leading to chlorophyll degradation (Benedetti *et al.* 2002), inhibition of stomatal

closure (Uppalapati *et al.* 2005; Ichinose, Taguchi and Mukaihara, 2013), along with inhibition of root elongation (Bender, Alarcón-Chaidez and Gross, 1999).

Because of *P. syringae's* significance as a widespread plant pathogen with a broad variety of hosts, it has become an excellent model for studying plant defence processes and plant-pathogen interactions (Tarkowski *et al.* 2014).

2.5 The vector species: *Agrobacterium tumefaciens*

Agrobacterium tumefaciens is a gram-negative, tumour-inducing bacterium which infects plants through horizontal gene transfer as its primary pathogenicity pathway. *A. tumefaciens* transfers tumour-inducing (Ti) plasmids to its hosts' cells, which encode oncogenic genes to be expressed by the invaded tissue (Das *et al.* 2020, 8). Wild-type *A. tumefaciens* causes crown-gall disease by transforming plants with Ti plasmids carrying a 30 kb virulence (*vir*) region carrying genes that are essential for plant cell transformation (*virA, virB, virD,* and *virG*), along with accessory genes which enhance the efficiency of Ti-plasmid transfer (*virC* and *vifE*) (Zambryski, Tempe and Schell, 1989). Ti-plasmids also carry genes that promote the upregulation of phytohormones such as auxin and cytokinin, which accumulate and cause tumour formation by inducing uncontrolled cell proliferation (Suzuki *et al.* 2009).

A. tumefaciens was first established as a method of stable gene introduction in the 1980s, when Lloyd *et al.* (1986) Published a protocol using a modified *A. tumefaciens* strain carrying a chimeric hygromycin phosphotransferase (*hph*) gene. This gene conferred hygromycin-B resistance to recipient leaf discs suspended in culture with *A. tumefaciens*. Leaf discs were then grown in media containing hygromycin-B to select for transformants that were positive for the *hph* insert. The discs that survived were regenerated into explants, which were then transferred to soil (Lloyd *et al.* 1986). While this approach is suitable for agriculturally significant crops, it is time consuming, requires skilled labour and specialist equipment and laboratory facilities (Zhang *et al.* 2006). Furthermore, the regeneration step for this method can result in unintentional DNA modifications and somaclonal variation in the progeny plants (Chang *et al.* 1994; Clough *et al.* 1998; Zhang *et al.* 2006).

The lack of simplified transformation methods for model plants species, drove the development of new techniques. One such approach was targeting embryonic plant tissue (Kaur *et al.* 2019). Feldmann *et al.* (1987), first reported stable transformation in *A. thaliana* seeds that had been cultivated in liquid media for 24 hours with *A. tumefaciens*

carrying the *neomycin phosphotransferase II gene* (*nptII*), which confers resistance to kanamycin and G418 . They identified 200+ transgenic progeny from the transformed seeds by growing them on selective media containing kanamycin, and using southern blot analysis, they discovered that all resistant seedlings had at least one T-DNA insert, with many having several inserts, present in their nuclear DNA (Feldmann *et al.* 1987).

Eventually, Clough *et al.* (1998), developed a protocol for floral dipping: a stable transformation which produces in genetically-modified seeds. This method is widely used for *A. thaliana*, although its transformation rate is relatively low (Zhang *et al.* 2006). However, unlike for other model species, floral dipping is more suited for *A. thaliana* due to its high seed production and because it goes through the appropriate developmental stage to allow for transformation (Nagle *et al.* 2018). Different methods vary in transformation yield (Martinez-Trujillo *et al.* 2004; Wang *et al.* 2020), although incorporation of techniques such as subjecting transformant plants to drought stress (Ali *et al.* 2022) or applying resuspended *A. tumefaciens* drop-by-drop to developing buds of *A. thaliana* (Martinez-Trujillo *et al.* 2004) can improve the yield of transformed seeds.

Other methods of stable transformation includes vacuum infiltration, developed in 1993, which involved placing recipient plants in a vacuum with *A. tumefaciens* inoculum. Vacuum infiltration draws the Ti-plasmid carrying *A. tumefaciens* into fully grown plant reproductive tissue, resulting in a yield of 1% of seeds being transgenic (Zhang *et al.* 2006; Kaur *et al.* 2019). This method targets *A. thaliana*'s ovule tissue, as demonstrated by Ye *et al.* (1999) when they took *A. thaliana* transformed via vaccum infiltration and crossed them with untransformed *A. thaliana*. The results showed that only seeds obtained from crosses where the transformed plants were the pollen recipient, were transgenic . Though it was developed after floral dipping, vacuum infiltration is often less preferred to floral dipping due to the need for specialist equipment (Clough *et al.* 1998).

To date, vacuum infiltration and floral dipping remain the two most widely used methods of transformation. Though some debate remains over which method is more efficient, both methods target female germline tissue (Ye *et al.* 1999; Desfeux *et al.* 2000) and comparisons of the two methods have shown that optimal transformant seed yield can be achieved if the plants are transformed between days 5 and 10, while floral buds are still immature and their pistils are still open, giving *A. tumefaciens* direct access to the ovule cells (Wiktorek-Smagur, Hnatuszko-Konka and Kononowicz, 2009; Khan *et al.* 2022; Qamar *et al.* 2022).

2.6 Transient transformation via infiltration

Syringe infiltration was subsequently developed as one of the first rapid transient transformation methods, which made use of Silwett L-77 to lower the surface tension of *Agrobacterium tumefaciens* resuspended in liquid, increasing the uptake of exogenous DNA and overcoming the need for vacuum equipment (Kapila *et al.* 1997; English *et al.* 1997; Kaur *et al.* 2019). The method runs on the same principle as vacuum infiltration: forcibly injecting *Agrobacterium tumefaciens* into plant tissue by creating a pressure gradient (Chincinska, 2021). The method was first developed to study plant-viral interactions, as an easier method to introduce the virus compared to using insect vectors (Grimsley *et al.* 1986). In their study, Grimsley *et al.* (1986) transformed *Agrobacterium tumefaciens* with Ti-plasmids carrying the genome for *Cauliflower Mosaic Virus* (*CaMV*), cultured and resuspended the transformed bacteria and infiltrated the leaves of 3-week-old turnip plants, which subsequently developed symptoms of *CaMV* infection.

Schöb *et al.* (1997) used syringe infiltration with *A. tumefaciens* carrying P35S-*CHN48* in a binary Ti-plasmid vector to transform the leaves of wild-type and transgenic *Nicotiana sylvestris* expressing *tobacco class I chitinase A gene*, to test if they could achieve *CHN48* gene silencing in the transgenic plants. Their results showed that leaves from the wild-type plants infiltrated with the P35S-*CHN48* vector showed *CHN48* expression, while *CHN48*-expressing plants infiltrated with the same vector showed signs of *CHN48*-silencing, something that was not observed when *CHN48*-expressing plants were infiltrated with an unrelated chimeric sequence (Schöb, Kunz and Meins Jr., 1997). Schöb *et al.* (1997)'s results indicated that the additional copies of *CHN48* infiltrated into the *CHN48*-expressing leaves were silenced by the resident copies of the gene.

The original syringe infiltration protocol was improved upon, and by 2018, it had become a preferred method of transient transformation, due to being quick and efficient (Norkunas *et al.* 2018). To date, several methods of syringe infiltration exist, each with differing methods of *A. tumefaciens* cultivation and resuspension, however the principle is the same for all: cultivate the vector carrying *A. tumefaciens* on solid media, transfer to liquid media, centrifuge the liquid cultures and resuspend the cells in resuspension buffer containing chemical additives to promote Ti Plasmid transfer (Leuzinger *et al.* 2013; Norkunas *et al.* 2018; Zhang *et al.* 2020). A widely used chemical additive in infiltration experiments is acetosyringone (Schott *et al.* 2011; Nosaki *et al.* 2021; Fernandez *et al.* 2023), which causes an upregulation of virulence genes in *A. tumefaciens* (Baker *et al.* 2005; Yoneyama *et*

al. 2010), promoting the transfer of Ti plasmids to recipient plant cells and improving efficiency of the transformation (Nakano, 2017).

2.7 Aims and Hypothesis

In this project we aimed to investigate whether transient expression of nonspecific, non-host derived RNA hairpins, specifically designed to target the Green Fluorescent Protein (GFP), introduced to the leaves of *Arabidopsis thaliana* conferred a protective effect against infection with *Pseudomonas syringae.* To investigate this, we set out to design a protocol that could be used to transiently transform *Arabidopsis thaliana* leaves with the non-host targeting GG-*egfp*^{hp}GUS hairpin T-DNA vector and then infect the transformed plants with *Pseudomonas syringae*. We hypothesised that introduction of the hairpin to the leaves of *A. thaliana* via agroinfiltration would reduce the development of disease symptoms when the plants were subsequently infected with *Pseudomonas syringae*, and lead to improved localised and systemic acquired resistance to the pathogen.

3. Methodology

Our hypothesis was that transiently transformed *Arabidopsis thaliana* expressing RNAi hairpins targeting nonself genes would show enhanced disease resistance to infection with *Pseudomonas syringae* compared to the uninfiltrated wild-type Col-0.

Agrobacterium tumefaciens carrying different RNAi-hairpin vector T-DNAs was infiltrated into the leaves of *A. thaliana* plants. This infiltration step was undertaken to transiently transform the leaves with the T-DNA hairpin insert carried by the *A. tumefaciens*. Next, *P. syringae* was infiltrated either in the same leaf that had received the *A. tumefaciens*, to test for an improved localised response, or the adjacent leaf to test for an improved systemic response to infection. This combined infiltration system was used to test whether the introduction of RNAi hairpins targeting the GFP gene led to improved localised and systemic acquired resistance to *Pseudomonas syringae* in Col-0.

Additionally, RNASeq read counts data from Walker *et al.* (2023) (available at: https://www.ncbi.nlm.nih.gov/geo/query/acc.cgi?acc=GSE217513) was downloaded and analysed for differentially expressed genes (DEGs), to test whether the HIGS-expressing group showed an upregulation of defence pathways pre-infection with the pathogen compared to the wild-type. We compared the expression profiles of both groups to see if the differences observed correlated with the improved disease response to *S. sclerotiorum* in the HIGS-expressing group reported in the original study.

3.1 Designing the Level II Golden Gate Cloning RNAi Hairpin Constructs

RNA interference hairpin vectors first needed to be constructed for transformation into EHA105 *Agrobacterium tumefaciens*. All hairpin vector T-DNAs were designed using Geneious Prime and constructed via Golden Gate Cloning. They were GG-*egfp*^{hp}GUS, GG-*wc1*^{hp}GUS and GG-Kan^{R}GUS the control vector (Figure 3). The following genetic elements were inserted into each vector in the 5′→3′ orientation using Golden Gate assembly (Table 1).

Table 1: Sequences, Promotors and Terminators used in Level 2 Golden Gate T-DNA vector plasmid construction

Position (5'-3')	Sequence	Species of origin	Function
1	*Nopaline synthase promoter* (*Nos^{prom}*)	*Agrobacterium tumefaciens*	Bacterial promoter
2	*Neomycin phosphotransferase type II* (*nptII*) *gene*	*Escherichia coli*	To confer Kanamycin resistance
3	*Octopine synthase terminator* (*OCS^{term}*)	*Agrobacterium tumefaciens*	Bacterial terminator
4	*Ubiquitin 10 promoter* (*AtUB10^{prom}*)	*Arabidopsis thaliana*	Plant promoter
5	One of two marker genes:		
	Green Fluorescent Protein (*eGFP*)	*Aequorea victoria*	Reporter Gene: produces the green fluorescent protein
	β-glucuronidase (GUS) exon	*Escherichia coli*	Reporter Gene: converts 5-bromo-4-chloro-3-indolyl β-D-glucuronide to 5-bromo-4-chloro-3-hydroxyindole Which oxidises to form 5,5′-dibromo-4,4′-dichloro-indigo producing a blue phenotype when oxidised
6	*Ribulose-1,5-bisphosphate carboxylase/oxygenase small subunit terminator* (*RBSC^{term}*)	*Arabidopsis thaliana*	Plant terminator
7	*35S promoter* (*35S^{prom}*)	Cauliflower mosaic virus (CaMV)	Plant promoter

8	One of three RNAi hairpins targeting the following genes:		
	sge1-targeting hairpin	*Verticillium dahliae.* *(targeting)*	Produce an RNA hairpin to knockdown the production of the complementary gene in its host organism.
	The *wc1*-targeting hairpin	*Verticillium dahliae.* *(targeting)*	
	The *egfp*-targeting hairpin	*Aequorea Victoria* *(targeting)*	
9	*Nopaline synthase terminator* (*Nos*^{term})	*Agrobacterium tumefaciens*	Plant terminator

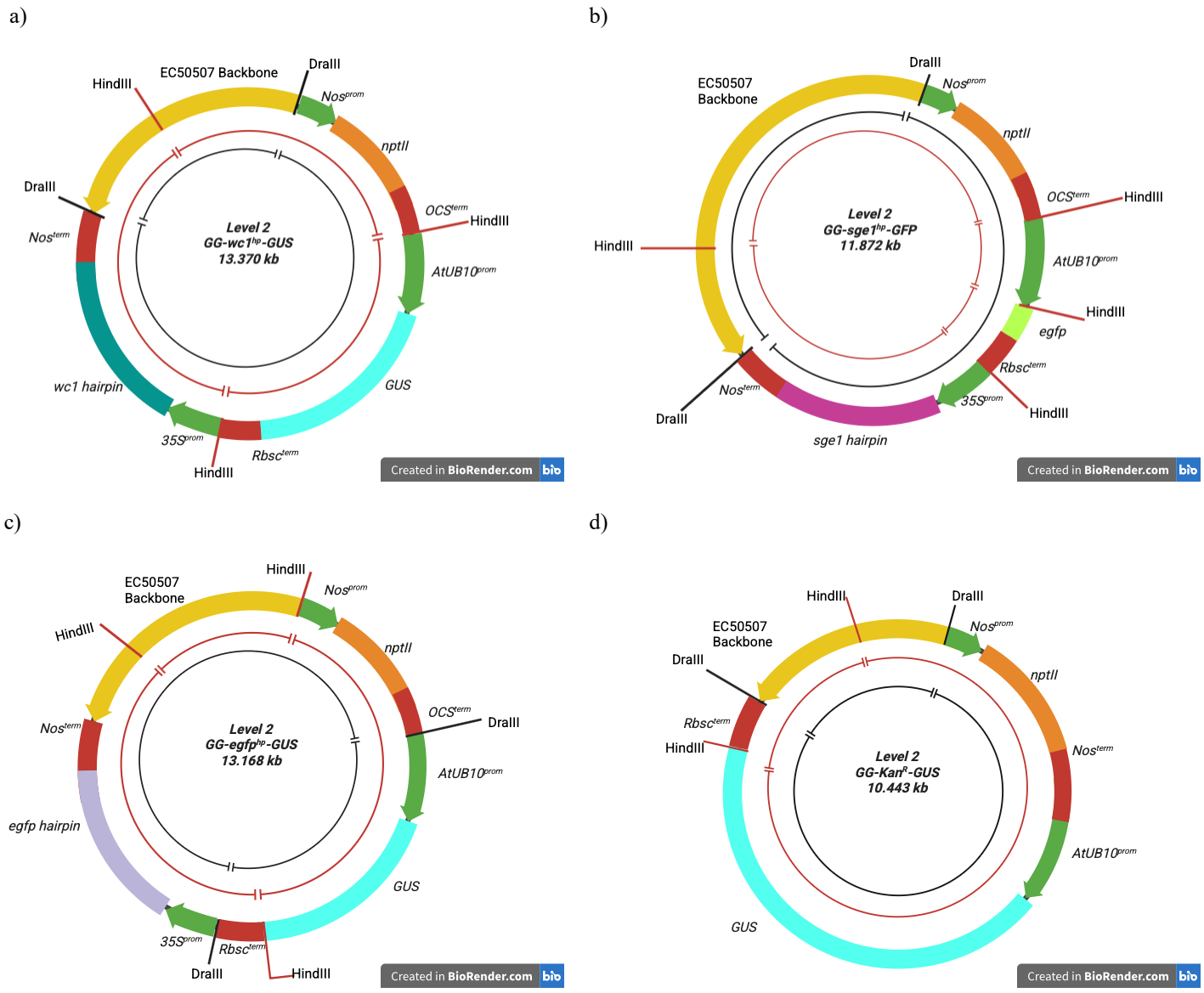

Figure 3: Plasmid maps of the Level 2 golden gate vectors: GG-*wc1*^{hp}GUS (a) GFP, GG-*sge1*^{hp}GFP (b), (c) and the control GG-Kan^{R}GUS (d), generated in Benchling. The 3'-5' strand is shown running clockwise, 5'-3' strand is shown running counterclockwise. All vectors were constructed via Golden Gate cloning, using *E. coli* 50507 (EC50507) backbone plasmid of 4,753 Kb.

The hairpins were designed to target the *V. dahliae* genes: *wc1* and *sge1* (from the *Verticillium dahliae* genome) and *egfp* (the Green fluorescent protein encoding gene). The sequence of each hairpin was then analysed *in silico*, using SiRNA Finder (SiFi) (Lück *et al.* 2019), to predict off-target matches to reference genomes for the plant host and fungal pathogen. Reference genomes for Col-0 (GCA_020911765.2 v2.0) and *V. dahliae* JR2 (GCA_000400815.2 v.4.0) were sourced from the NCBI database. Positive and negative control sequences were

generated by extracting the first 500 bp from Chromosome 2 from the *V. dahliae* JR2 genome and the first 500 bp of the Col-0 ABF gene. These sequences served as the positive control in their native genomes and negative controls in the reciprocal genome. Each hairpin was analysed for off-target and efficient matches in both the Col-0 and *V. dahliae* genomes. As SiFi cannot differentiate between coding and non-coding DNA in the reference genomes, hairpins that had efficient off-target hits (those with ahigh likelihood of binding) were mapped to the same reference genome in BLAST (Altschul *et al.* 1990). Alignment in BLAST determined whether any predicted efficient off-target matches were in coding or noncoding regions of the genome and if these off-target matches were likely to disrupt the plant/pathogen's gene expression.

3.2 Transformation of *Agrobacterium tumefaciens*

The GG-Kan^{R}GUS (the control vector) and GG-*sge1*^{hp}GFP hairpin vectors were transformed into EHA105 *Agrobacterium tumefaciens*. EHA105 *Agrobacterium tumefaciens* were transformed with the constructs GG-Kan^{R}GUS (the control vector) and GG-*sge1*^{hp}GFP, following the standard protocol outlined by Hofgen et al (1988). Transformed bacteria was plated at 50 µl and another at 100 µl to allow single colonies to be selected for analysis. As a negative control, untransformed bacteria were spread onto plates, 1x 50 µl and 1x 100 µl, and incubated alongside the transformed bacteria at 28ºC for 48 hours.

3.3 Single colony selection and preparation of feeder cultures

After incubation for 48 hours, single colonies of transformed *Agrobacterium tumefaciens* were selected to produce feeder cultures, following the standard protocol outlined by Zhang *et al.* (2006). Feeder cultures were incubated at 28ºC and 180 RPM for 48 hours.

3.4 Confirming the presence of the hairpin in transformed *Agrobacterium tumefaciens*

3.4.1 MiniPrep of Control Hairpin and Spectrophotometry

To ensure the transformation was successful, 3.5 ml of *Agrobacterium tumefaciens* culture samples were centrifuged at 4000 RPM for 10 minutes at room temperature. The MiniPrep was then carried out using Qiagen® Spin MiniPrep Kit according to the standard protocol. Once extracted and purified, 1 µl of DNA was loaded onto a BMG-Labtech 16-well LVis microplate and analysed using a FLUOstar Omega spectrophotometer, which measured the 260:280 nm ratio to determine the quality of the samples and calculate the concentration of the DNA

in ng/µl. A 260:280 nm ratio reading of 1.8-2 nm was considered evidence for uncontaminated purified bacterial DNA.

3.4.2 Gel Electrophoresis of Restriction Digest and PCR Products

All agarose gels were prepared for electrophoresis by adding 0.6 g of Melford Agarose powder to 60 ml of 1X Tris-Acetate-EDTA (TAE) buffer to produce a 1% electrophoresis gel. Then, 1.6 µl of New England Biolabs (NEB) GelRed® DNA stain was added to the gel before it was poured into a gel electrophoresis frame to set. Once set, the gel was placed into an electrophoresis cradle, filled with 1X TAE buffer.

All restriction digest and PCR samples were run on the gel for 30 minutes at 150 mV. After which, all gels were loaded into the Syngene G:Box visualiser and visualised using the Syngene software. The NEB 100kB DNA ladder was loaded into the gel into the leftmost and rightmost wells of the gel and used to measure the size of the bands produced for each sample.

3.4.2.2 Digestion with *DraIII*

For digestion with *DraIII*, 2 µl of DNA each sample was added to 10X rCutSmart Buffer, 20,000 units/ml *DraIII* (NEB®) and MiliQ water to get a final concentration of 20,000 units/µl of restriction enzyme in each PCR tube. Tubes were placed in a PCR machine (Bio-Rad T100^{TM} thermal cycler) and left to digest at 37ºC for 1 hour. Once the digest was completed, 1.6 µl of 6X Purple Loading Dye was added to the digest samples. Then 10 µl of each sample was loaded into the wells of the gel, one well per sample. Gel electrophoresis was then used as specified above (Section 3.4.2).

3.4.2.3 Digestion with *HindIII*

For digestion with *HindIII*, a master mix was prepared with the following reagents: MiliQ Water, Promega 10X Multicore Buffer E, 10 µg/µl Acetylated Bovine Serum Albumin (BSA) and 10 units/µl *HindIII* to produce a total volume of 120 µl. 19 µl of Master Mix was aliquoted into PCR tubes and 1 µl of DNA elution was added to each tube, making a total volume of 20 µl of restriction digest mix. For controls, 1 µl of the 50507-backbone plasmid was added the Master Mix. MiliQ was used as a negative control. Tubes were run for 2 hours at 37ºC, followed by heat deactivation at 65ºC for 15 minutes. Once the digest was complete, the samples were loaded onto the gel

and electrophoresis was then used to produce and the samples' banding patterns. The gels were then visualise as specified above (Section 3.4.2).

3.4.2.4 PCR of Diluted Control Hairpin DNA

As a final test for the presence of the hairpin vector T-DNA in transformed *Agrobacterium tumefaciens*, diluted GG-Kan^{R}GUS vector (G1.2) and GG-Kan^{R}GUS vector (G2.2) samples were amplified using PCR.

Primers for forward and reverse amplification of a 212 bp region between the pNOS promotor and the Kan-R cassette in the control hairpin vector T-DNA were designed using Geneious Prime and ordered from Integrated DNA Technologies LTD Inc©. The dry stock primers were then dissolved in the appropriate amount of nuclease-free water, as lined out by their individual IDT Preparation Instructions, to a concentration of 100 mM. Working stocks of the primers with a final concentration of 10 mM were then prepared by performing a 10-fold dilution with nuclease-free water. The Primer dilutions were then used in the PCR Master Mix.

PCR Master Mix was prepared by adding the following reagents: NEB Quick-Load® Taq 2X Master Mix, Forward Primer 10mM, Reverse Primer 10mM and Nuclease free water making a total volume of 253 µL. For each sample 23 µl of PCR mix was added to 2 µl of sample. GG-Kan^{R}GUS vector (G1.2) and GG-Kan^{R}GUS vector (G2.2) were added to the Master Mix at 1x and 10x dilution. Additionally, 100 ng/µl 50507-backbone was added to PCR Master Mix in one PCR tube and Nuclease-free water was added to PCR Master Mix in another as negative controls.

Samples were placed into the PCR machine (Bio-Rad T100^{TM} thermal cycler) and cycled through the following conditions: 95ºC denaturation for 30 seconds, 54°C annealing for 1 minute, 68°C elongation for 8 minutes and 30 seconds, 95°C denaturation; repeat 30x, 68°C final elongation 5 minutes and followed by an infinite hold stage, holding at 12ºC until samples were removed. PCR product for each sample was then analysed by gel electrophoresis, loading 5 µl from each sample, as stated above (Section 3.4.2).

3.5 Transforming *Arabidopsis thaliana* via floral dipping

Using the transformed *Agrobacterium tumefaciens* lines, *Arabidopsis thaliana* plants were transformed with the RNAi hairpins via the floral dipping method, following the protocol outlined by Zhang *et al.* (2006).

3.5.1 Growing *Arabidopsis thaliana* plants for transformation

Ecotype Col-0 *A. thaliana* plants were grown in growth cabinets (PHCbi MLR-352H Climate Chamber) at 22ºC with a light/dark cycle of 16/8 hours and a relative humidity of 65 %, following the cold stratification in 0.05 % agarose at 4ºC for 24 hours as specified by Zhang *et al.* (2006). Col-0 was planted in 7 cm diameter pots filled with Growmoor Multipurpose soil. Seeds suspended in agarose were planted 3 ml per pot and allowed to grow until their true leaves had emerged. After approximately 2 weeks post-sewing, the young plants were re-potted to 4 plants per pot. Plants were grown for 3-4 weeks until their floral shoots emerged.

3.5.2 Floral dipping with *Arabidopsis thaliana*

Plates of transformed bacteria were incubated at 28ºC for 48 hours. After single colony selection, low salt Luria Broth (LB) Agar (LBA) plates containing the antibiotics rifampicin and kanamycin were stored at 5ºC for 5 days. Feeder cultures for each hairpin group were incubated in low salt LB broth at 28ºC and spun at 220 RPM and left for 48 hours. After incubation, feeder cultures were placed in the fridge for 1-2 days before use.

Floral dip cultures of *Agrobacterium tumefaciens* were prepared for a maximum of two hairpin groups at a time over the space of 3-weeks. For each floral dip culture, the total 5 ml of the respective feeder culture was pipetted into a 1000 ml conical flask containing 500 ml of Low Salt LB Broth (LBB) and 500 µl of Kanamycin. Once inoculated the cultures were sealed with foam stoppers, covered with foil and placed in the incubator at 28ºC at 220 RPM for 48 hours.

After incubation, floral dip cultures were then centrifuged for 10 minutes at 4000 RPM, using a JA10 Rotor, to sediment the *A. tumefaciens*. The supernatant was discarded, and the bacterial pellet resuspended in a solution of 5 % sucrose and 0.02 % Silwett and transferred to a sterile beaker. Three Col-0 pots were selected for dipping. Col-0 pots were inverted, and the floral bolts dipped into the bacterial resuspension for 3-5 seconds, while swirling the beaker, to allow the floral buds to be heavily coated in bacterial suspension. Pots were laid on their side on a tray. The tray was placed inside a large biohazard bag, to retain humidity for 24 hours after the floral dip.

Once transformed, plants returned to growth conditions mentioned above. After 24 hours, plants were removed from the biohazard bags, and the pots were stood upright. Plants were left to grow at 20ºC with a light/dark cycle

of 16/8 hours for several weeks until senescence. Plants were watered until their siliques senesced, at which point watering was halted, to cause drought stress which induced seed maturation.

3.5.3 Seed collection

Once the transformant plants had senesced, the siliques were collected in 1.5 ml Eppendorf tubes. To extract the seeds, siliques were transferred from the Eppendorf tubes to a piece of A4 paper and manually broken open by hand. Seeds were then separated from the debris and poured into fresh Eppendorf tubes. Tubes were transferred to dry storage in falcon tubes filled with silica and stored in dark conditions for two weeks.

3.5.4 Screening primary transformants

3.5.4.1 Preparing Murashige and Skoog selective media plates

Murashige and Skoog selective growth media was prepared by mixing: 650 ml of water, 4.3 g of Murashige and Skoog, 10 g sucrose and 0.5 g of anhydrous 2-Morpholineethanesulfonic acid (MES). The pH of the mixture was adjusted using 1M NaOH or 1M HCl to 5.7 pH. Next, 5.2 g of agar was added to the mixture, and the media was autoclaved. Once autoclaved, the media was opened in laminar flow hood (Air Science® USA LLC PurAir LF Series HLF-72 Model), and 50 mg/µl kanamycin and 100 mg/µL of carbenicillin were added to the media. Then, 25 petri dishes were pipetted with 20 ml of the solution each, using an e-Pipette before being left to set for 30 minutes under sterile conditions.

3.5.4.2 Seed sterilisation

Cleaning solution was prepared by adding 50% water with 50% bleach and 0.05% Tween. Individual Eppendorf tubes of seed were sterilized by adding 70% ethanol for 1 minute. Afterwards, ethanol was pipetted from the tubes, then seeds were resuspended in cleaning solution and vortexed every 2 minutes for 10 minutes. Tubes were then centrifuged to pull seeds to the bottom of the tube, and the cleaning solution was pipetted off. To remove any remaining cleaning solution, seeds were washed three times, or until clear of any yellow colour by adding 0.5 ml of MiliQ and vortexing. After a third wash, seeds were transferred into falcon tubes, and remaining excess water was removed.

Once the seeds were sterilised, 0.05% agarose was added to each falcon tube. The contents of each falcon tube was pipetted onto MS plates, one plate per tube. Plates were then sealed with parafilm and placed at 5ºC for 3-day cold stratification.

Selected seeds were plated onto selective media to select seeds carrying the plant-compatible Kan^R cassette present in the vector T-DNA backbone. After 7 days of growth, surviving seedlings (T1 plants) were transferred to soil, and screened for the hairpin marker gene phenotype (Section 3.5.4.6).

3.5.4.3 Growing Primary Transformants

T1 seeds on media were moved into a growth cabinet for 7 days at 20ºC, with a light/dark period of 16/8 hours. At the end of 7 days, viable plantlets were replated on to fresh MS plates until their true leaves emerged.

3.5.4.4 Transferring viable transformants to soil

Once the transformant plants' true leaves had emerged, they were transferred to 5 cm wide pots of Growmoor Multipurpose soil. The pots were kept in propagator trays to maintain humidity. Once the plants showed signs of bolting, they were placed into plastic ARA system tubes. The ARA system kept the *Arabidopsis thaliana* floral bolts reproductively isolated to prevent cross-pollination and induce self-pollination. This ensured that any second generation (T2 seeds) were homozygous for the hairpin insert.

3.5.4.5 Using PCR to screen transformants for hairpin vector T-DNA

T1 plants were screened for the presence of the hairpin using the PHIRE Plant Direct PCR Kit. DNA was extracted from Col-0 (negative control) and T1 plants by taking a 0.5 mm of leaf disc sample from each of the plants and suspending them in PHIRE Dilution Buffer, according to the manufacturer's instructions. Next, 10 mM of forward-reverse primer pairs amplifying the plant-compatible Kan^R cassette, present in all our Golden Gate Level 2 constructs, was added to 2X PHIRE buffer and Nuclease-free water. A control master mix was prepared and run as a separate PCR, using ACT2 primers, targeting the Col-0 ACT2 gene, to confirm the presence of plant DNA in the samples (Table 2). The recommended cycling protocol was used, as per the manufacturer's instructions. The initial denaturation step was for 5 minutes at 98°C, followed by 40 repetitive cycles of: denaturation for 5 seconds at 98°C, annealing for 5 seconds (temperature dependent on the primer pair used), extension for 20 seconds at 72ºC, followed by a final extension step for 1 minute. The annealing temperatures set to 64.7ºC when using Kan-R primers and 60.1ºC using ACT2 primers.

Table 2: Primer Sequences

Primer Name	Sequence	Expected Product Size in bp
HS-P-Kan-F	GAGTACGTCCTCGCTCGATG	632 bp
HS-P-Kan-R	ACGTTGAAGGAGCCACTCAG	
ACT2-F	ATGGCTGAGGCTGATGAT	495 bp
ACT2-R	CTAACCGGTTGTACGACC	

Gel electrophoresis was used to analyse PCR products, using tenfold-diluted purified vector plasmid as a positive control, with an expected band size of 495 bp, for the Kan^R-targeting primer master mix and Col-0 DNA as a positive control, with an expected band size of 632 bp, when using ACT2 primers. Nuclease free water was used as a negative control for both master mixes.

3.5.4.6 GUS staining of transformant leaves

The GUS exon encodes for the β-glucuronidase enzyme which converts 5-bromo-4-chloro-3-indolyl-β-D-glucuronide to 5-bromo-4-chloro-3-hydroxyindole. 5-bromo-4-chloro-3-hydroxyindole is white in colour, but when oxidised, it forms 5,5′-dibromo-4,4′-dichloro-indigo which produces the characteristic blue pigment phenotype in the leaves. To visualise this marker phenotype, leaves were bleached of chlorophyll, then treated with oxidising agents outlined in the Sigma-Aldrich GUS kit (Sigma-Aldrich Co.LLC, 2016). Leaf samples from T1 replicates, the progeny of T0 floral bolts transformed via floral dipping, and leaf samples from wild-type Col-0 transformed with the Level 2 vector plasmid via syringe infiltration, were destained as per the Sigma-Aldrich GUS kit protocol after their respective transformation and growth periods. Col-0 was used as a negative control and *A. thaliana* genetically modified with P35S::UidA, to stably express the GUS exon, were destained as a positive control.

Once treated the leaves were left for 7 days in 100 % ethanol at room temperature, before visualisation by light microscopy.

3.5.4.7 Light Microscopy of transformant leaves

After 7 days, transformant leaves were removed from 100 % ethanol and placed on glass slides with 50 % glycerol. Slides were mounted onto a Lecia Microsystems DM Series R digital widefield dissection light microscope, and the field of view was adjusted between 10x to 40x to search the leaves for signs of GUS expression. Images of the whole leaf were captured using a 200 CR light microscope camera.

3.6 Disease assay with *Pseudomonas syringae*

3.6.1 Growing *Arabidopsis thaliana* for infiltration

Arabidopsis thaliana Col-0 ecotype seeds were cold stratified (Section 3.5.1). Following cold stratification, 1 ml of Col-0 seeds in agarose were spread on soil in 7 cm pots. Col-0 was grown at 22ºC on a 16/8-hour photoperiod, either in a growth room using a climate computer to control the light intensity ratios (µmol/m2/s) and photoperiods (hours) (see Table 3) or in PHCbi MLR-352H Climate Chamber growth cabinets (Section 3.5.1).

Table 3: Light Wavelengths and intensities used to cultivate *Arabidopsis thaliana*

Wavelength (nm)	Blue light (450-495 nm)	Green light (495-570 nm)	Red light (620-750 nm)	Far red (700-800 nm)
Intensity (µmol/m^2/s)	36	45	35	30

After 1-week of growth, seedlings were separated into their own individual pots, 1 per plant and were grown for an additional 2 weeks.

3.6.2 Infiltration with *Agrobacterium tumefaciens* for transient hairpin expression

To transiently transform Col-0 leaf tissue with the GG-*egfp*^{hp}GUS and GG-Kan^{R}GUS vector plasmids, leaves were infiltrated with *Agrobacterium tumefaciens* by syringe infiltration following the protocol outlined in Zhang *et al.* (2020). *A. tumefaciens* was grown for 48 hours at 28ºC on Yeast Extract Broth (YEB)-induced media, then resuspended in wash solution prepared by combining MiliQ with $MgCl_2$ and 20 mM acetosyringone. Resuspended bacteria were then diluted to an OD_{600} of 0.5 using infiltration solution prepared with filter sterilised 1% sucrose,

Silwett-L77 and 20 mM acetosyringone. The following adjustments to the original protocol were made: the Col-0 plants were grown under a 16/8-hour light/dark cycle at 22ºC in propagator trays and the infiltration step was carried out in a CAT2 hood.

Col-0 leaves were infiltrated with EHA105 *A. tumefaciens* that were either wild-type (as a negative control) or carrying the GG-*egfp*^{hp}GUS or GG-Kan^{R}GUS vector plasmids. Mock infiltrations were performed with sterile infiltration solution with added sterile MiliQ water in place of bacterial resuspension.

3.6.3 Screening infiltrated Col-0 leaves for transient hairpin expression using PCR

After 5 days post-infiltration, leaf samples were taken and analysed with the PHIRE Plant Direct PCR Kit as outlined above (Section 3.5.4.5).

3.6.4 Infiltration with *Pseudomonas syringae*

Col-0 was infected with the bacteria following the protocol specified by Yao *et al.* (2013). Col-0 plants were grown under a 16/8-hour light/dark cycle at 22ºC in propagator trays. *P. syringae* plates grown on Luria Broth Agar (LBA) plates containing 50 µg/ml of rifampicin for 48 hours at 28ºC, after which single colonies were selected for culture in LB Broth (LBB) containing 50 µg/ml of rifampicin. Liquid cultures were incubated for 24 hours at 28ºC and 180 RPM. Liquid cultures were then centrifuged, and the pellet resuspended in MiliQ. The resuspended bacteria was diluted to an OD_{600} of 0.02 and introduced to 3-4 randomly selected Col-0 leaves via syringe infiltration. Infiltrations were carried out in a CAT2 hood and mock infiltrations were performed with sterile MiliQ. After infiltration, a randomized block design was implemented so the trays were a mix of different treatments, to control for environmental variation in the growth cabinets.

3.6.5 Visual assessment of *Pseudomonas syringae* disease symptoms

Plant disease symptoms were scored 5 days post-infection with *Pseudomonas syringae*. Col-0 plants were photographed with a Canon EOS 2000 camera mounted to a stand using a plain background.

Photographs of each plant were taken 1 d.p.i and 5 d.p.i, and disease severity was visually assessed based on two symptoms: the level of chlorosis and physical leaf damage. Symptoms were scored on a scale of 1 to 10 (1- little to no symptoms, 10 - most of or the entire leaf area affected). For each replicate, fixed effects such as whether the

leaves had been infiltrated with *P. syringae*, and confounding variables, such as perforation damage from the syringe or visual matches to bite marks from fungus gnat larvae, were recorded.

For the *P. syringae*-only infiltrations (Section 3.6.4), mock and infiltrated plants were photographed 1 d.p.i and 5 d.p.i and their chlorosis levels were visually scored on day 5 as described above. Infiltrated leaves were then removed and photographed as described above. The photos were then analysed in ImageJ, to calculate the % of chlorotic-to-healthy tissue as outlined in Pride *et al.* (2020). Visual scores were then correlated with the % chlorosis measurements, by calculating the range and average % chlorosis seen for visual scores 1-10, to test whether visual assessment can provide an accurate a measurement of disease symptoms comparable to the measurements calculated in ImageJ.

3.6.6 Combined infiltrations

Once the infiltration protocols for *Agrobacterium tumefaciens* (Section 3.6.2) and *Pseudomonas syringae* DC300 (Section 3.6.4) were established, the two assays were combined into a single experiment through transforming *Arabidopsis thaliana* with the GG-*egfp*^{hp}GUS and GG-Kan^{R}GUS hairpins and then infecting the plants with *P. syringae* (Figure 4).

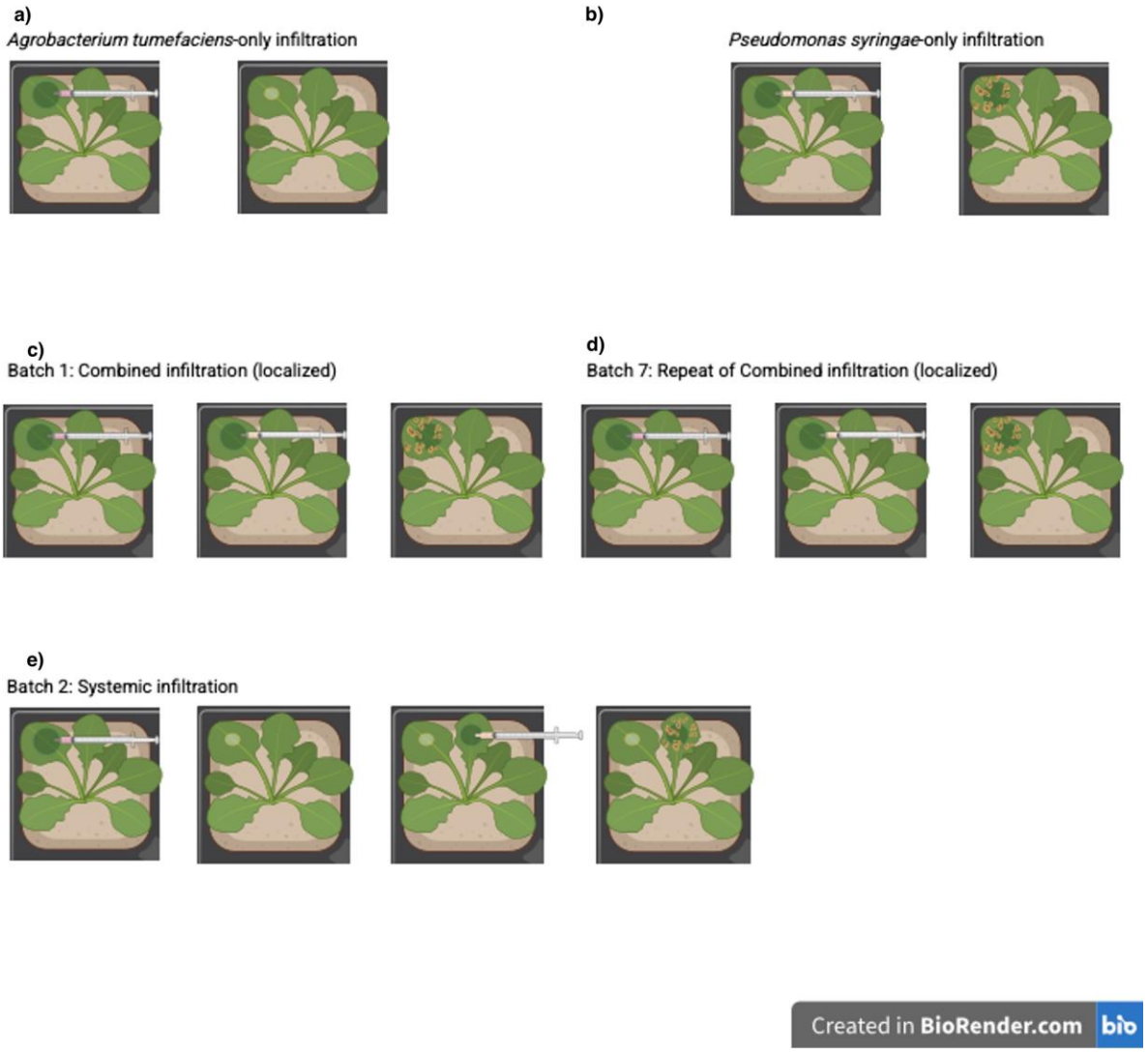

Figure 4: The five different infiltration experiments performed in this project. *Arabidopsis thaliana* was infiltrated with: (a) *Agrobacterium tumefaciens*-only (transient transformation), *Pseudomonas syringae* infiltration (infection assay) (b), *A. tumefaciens* and *P. syringae* in the same leaf (initial localised assay) (c), *P. syringae* infiltrated in the adjacent leaf to the leaf infiltrated with *A. tumefaciens* (initial systemic assay) (d), *A. tumefaciens* and *P. syringae* in the same leaf (repeat localised assay) (e).

For the initial localized and systemic infiltration experiments *A. thaliana* plants were grown in a growth room (Section 3.6.1) and, due to limited capacity, *A.thaliana* plants for the technical replicate of the localized infiltration had to be grown in PHCbi MLR-352H Climate Chamber growth cabinets (Section 3.5.1). *A.thaliana* plants grown in the growth room grew at a faster rate than those grown in the growth cabinets, so the age at which the plants were infiltrated varied between 3-5 weeks. Additionally, there was variation in growth rates for plants grown in the growth room, resulting in visible disparities in leaf size. To account for this, plants were selected for infiltration

on the basis of their physiological age: their leaves had to be visibly large enough to cover the entire head of a needless syringe, with some room left around the edges.

Between 3-4 leaves of recipient Col-0 plants were infiltrated with one of three *Agrobacterium tumefaciens* strains: untransformed wild-type (EHA105), transformed to carry the GG-*egfp*^{hp}GUS hairpin vector T-DNA (GFP) or transformed to carry the GG-Kan^{R}GUS control vector T-DNA (Ctrl.HP). A group of Col-0 plants were infiltrated with sterile infiltration solution mixed with MiliQ as a negative control (Water.I) for the transformation step. These treatments were designed was to test whether transient expression of the GG-*egfp*^{hp}GUS hairpin upregulated baseline immunity by measuring if there was a significant difference between symptoms in the hairpin compared to the water infiltrated plants.

After 5 days, leaves were then infected with *P. syringae*, returned to the growth cabinets under a randomised block design to avoid symptom scoring bias. Col-0 was left to grow for an additional 5-day post-infection and assessed for disease symptoms (Section 3.6.7).

During the initial localized infiltration, 5 biological replicates for each treatment were used, and the leaves were infiltrated as specified above with resuspended *A. tumefaciens* diluted to an OD_{600} of 0.5. During the technical repeat of the localized infiltration, to improve the statistical power of the data, the number of biological replicates was raised from 5 plants to 10 per treatment. Additionally, adjustments were made to reduce the instance of confounding variables such as rot and fungus gnats. Trays were dried after soaking for 30 minutes to 1 hour in water. Additionally, a higher OD_{600} of *A. tumefaciens* appeared to be correlated with an early hypersensitive response in the leaves before *P. syringae* infection during the initial localized infiltration, which confounded the subsequent assessment symptom severity after infection with *P. syringae*. Therefore to reduce the effect of this confounding variable on the results, *A. tumefaciens* was diluted to a lower OD_{600} of 0.025 before being applied to *A. thaliana* during the agroinfiltration step.

During the initial (and only) systemic infiltration, 10 biological replicates were used for each treatment group to ensure the results had strong statistical power, and the leaves were infiltrated as specified above with resuspended *A. tumefaciens* diluted to an OD_{600} of 0.5.

3.6.7 Statistical analysis of disease scores for combined infiltrations

Visual Scores for chlorosis and leaf damage for each assay was modelled using mixed model analysis in R using the lme4 package (Version: 1.1-37) (Bates, 2025). Analysis of Variance (ANOVA) tests were used to compare models, to determine which factors they differed on significantly, and the simplest model was obtained via process of elimination. The model of best fit was then assessed with a post-hoc Tukey test, and a clustered letter display was obtained for each treatment group illustrating any significant differences between them. If mixed model analysis showed that plant scores were not significantly impacted by random factors, and where the data was not normally distributed, a Kruskal-Wallis test was performed, followed by a post-hoc Dunn-test with an adjusted *p*-value of 0.05.

The average leaf damage and/or chlorosis scores were calculated for each group and plotted on a box plot with standard error bars and the clustered letter display for each group included using the ggplot2 package (Version 3.5.2) (Wickham, 2016).

There were a few instances where the leaves had been heavily damaged from factors such as repeated physical strain, rot due to excessive moisture or damage from fungus gnat larvae to the point where symptoms were completely obscured. In these instances, replicates were excluded from the data set as there was no way to accurately score their symptoms.

In the case of early disease symptoms caused by *Agrobacterium tumefaciens* infiltration, pre-infection with *Pseudomonas syringae*, the scores for leaf damage and chlorosis 5 d.p.i for *A. tumefaciens* were subtracted from the scores for leaf damage and chlorosis 5 d.p.i for *P. syringae* producing an overall score for each individual replicate. Model of best fit for the overall scores for leaf damage and chlorosis was calculated in the same way described above. The average result for each treatment group was calculated for each treatment group from these overall score values.

3.6.8 Differentially Expressed Genes (DEGs) Analysis

Using the RNASeq data from Walker *et al.* (2023) a study that compared the different responses to infection with *Sclerotinia sclerotiorum* in wild-type (Col-0) and a HIGS-expressing line (*AT1703*) of *Arabidopsis thaliana* (2023) was analysed using iDEP 2.0 (found at: http://bioinformatics.sdstate.edu/idep/) to extract differentially

expressed genes and identify upregulated/downregulated pathways, followed by the GO.db() Bioconductor package (Version: 3.20.0) (Marc Carlson, 2024) in R to link the extracted genes to the specific pathways identified in iDEP 2.0.

3.6.8.1 iDEP 2.0

The RNASeq expression matrix data Walker *et al.* (2023) was pre-processed by retaining genes that had a minimal Counts Per Million value of 0.5, in at least 2 libraries. Data was automatically normalised at the sample-level in iDEP, and the normalised dataset was quality checked to ensure there were no sample level-biases that would cause the data to not reflect the biological variation across replicates in the dataset.

The normalised data was then transformed using Variance Stabilizing Transformation (VST), as there were >10 samples to analyse. VST is a more aggressive filtering method allowing for the removal of lowly expressed genes to reduce the possibility of noise in the processed data. The algorithm was set to substitute missing expression values by calculating the median expression value of any affected genes across the entire dataset

The transformed expression matrix data was then analysed for DEGs using the DEG1 and DEG2 tabs. For DEG1 analysis, DESeq2 was used with a standard False Discovery Rate (FDR) cutoff value of 0.01 and minimum fold change filter value set to 2. The experimental design was set as follows (See Table 4):

Table 4: Experimental Design for Differentially Expressed Genes Analysis in iDEP 2.0

Comparison	Time point
Wild-type only	0d.p.i-2d.p.i
	2d.p.i-3d.p.i
	0d.p.i-3d.p.i
AT1703 only	0d.p.i-2d.p.i
	2d.p.i-3d.p.i
	0d.p.i-3d.p.i
Wild-type vs *AT1703*	0d.p.i
	2d.p.i
	3d.p.i

Gene Set Enrichment Analysis (GSEA) of Gene Ontology (GO) terms was performed, using the fully ranked expression matrix for each comparison at time points 0 d.p.i, 2 d.p.i and 3 d.p.i. This design allowed us to follow the disease response over time for the two *A. thaliana* lines, comparing the two lines at each time point and highlighting which pathways were being differentially up- and downregulated in the *AT1703* plants compared to Col-0.

For DEG2 analysis, DEGs for each comparison were sorted by fold-change. For the wild-type vs *AT1703* at 0 d.p.i comparison group, the top 25 DEGs with the most significant p-adjusted values (transformed using the negative base-10 logarithm ($-\log_{10}$)) were labelled using the set FDR cut-off value of 0.01. This allowed visualisation of the DEGs that showed the most statistically significant increase or decrease in expression. Where potential outlier DEGs were seen in the data, the labelling threshold in iDEP for the volcano plots was increased to 50, these labelling genes for further functional analysis.

The enriched genes set, containing the genes' ENSEMBL IDs, for each comparison group was downloaded. R was then used to compare the enriched DEGs set identified for *AT1703* vs WT at time points 0 and 2 d.p.i, plotting Venn diagrams to display the number of genes being consistently up/downregulated across both time points. The intercept() function from the dplyr() package was then used to extract the genes consistently up/downregulated and the list was used to filter these genes out of the enriched genes list, leaving only the genes that were differentially regulated on 0 d.p.i or 2 d.p.i, not both.

3.6.8.2 Ontology of enriched genes

Once the enriched gene lists were filtered, they were further analysed to identify their pathway ontology using the GO.db() (Version: 3.20.0) package in R. Once ontology was identified, the enrichplot() library was used to produce dot plots showing the ratio of the total genes, with a P-adjusted value of ≤ 0.05, belonging to each of the identified pathways.

4. Results

4.1 Predicting off-target matches to the hairpin sequences in the genomes of *Arabidopsis thaliana* and *Verticillium dahliae*

Off-target matches in this context, referred to sequences within the host or pathogen's genomes, other than the intended target of siRNAs produced from these hairpin sequences could potentially bind to. Efficient hits were predicated off target matches which siRNAs had a high-probability of binding to. This could have potentially led to RISC-mediated degradation of non-target mRNAs, if the matches occurred within coding regions of the genome. Furthermore, if off-target matches occur in genes within the host or the pathogen that affect their viability, it could negatively impact the results of a pathogenicity assay. To mitigate this risk, the sequence of each hairpin was compared against the reference genomes for the Col-0 ecotype of *Arabidopsis thaliana* (GCA_020911765.2 v2.0) and *Verticillium dahliae* JR2 (GCA_000400815.2 v.4.0), using siRNA Finder (Figure 5).

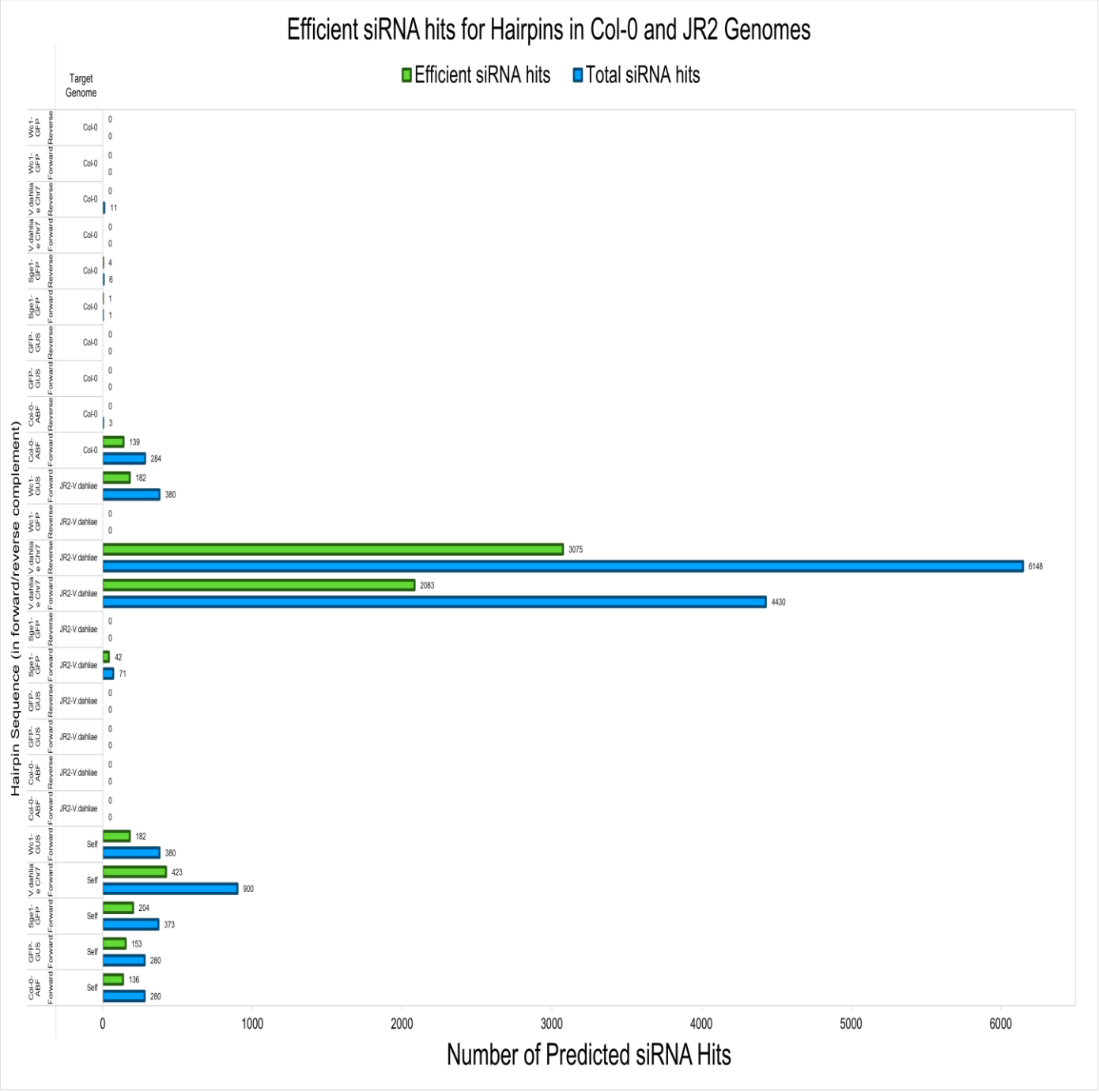

Figure 5: Total number of potential non-target siRNA-binding loci (blue) and the number of potential non-target siRNA-binding loci (green) as predicted by siRNA finder in the reference genomes Col-0 ecotype of *Arabidopsis thaliana* (GCA_020911765.2 v2.0) and *Verticillium dahliae* JR2 (GCA_000400815.2 v.4.0) for the hairpin sequences of GG-*wc1*^{hp}-GUS, GG-*sge1*^{hp}GFP and GG-*egfp*^{hp}GUS,). Control sequences of the first 500 bp from Chromosome 2 of the *V. dahliae* JR2 genome and the first 500 bp of the Col-0 ABF gene were used. All hairpins have been compared to themselves in the forward complement to ensure the program was working.

As shown in Figure 5, the hairpin sequences of GG-*wc1*^{hp}GUS and GG-e*gfp*^{hp}GUS had no predicted off-target hits in the Col-0 or *V. dahliae* genomes. However, the hairpin sequence of GG-*sge1*^{hp}GFP showed 71 total off-target hits to the *V. dahliae* genome, 42 of which were predicted to be efficient. For the Col-0 genome there was 1 efficient off-target hit for the hairpin sequence of GG-*sge1*^{hp}GFP in its forward complement and an additional 6 total off-target hits for the hairpin it its reverse complement, 4 of which were efficient hits. Efficient hits from the GG-sge1^{hp}GFP hairpin to the *A. thaliana* and *V. dahliae* genomes were analysed in BLAST. The results for BLAST comparison to the Col-0 and the *V. dahliae* genomes illustrated that the predicted efficient hits were not in the sequences of any known genes and therefore would not lead to off target post-transcriptional gene silencing in either the host plants or the invading pathogen.

4.2 Infiltration with *Agrobacterium tumefaciens*

4.2.1 Validating the presence of hairpin vector T-DNAs in *Agrobacterium tumefaciens*

Agrobacterium tumefaciens was transformed with: GG-*egfp*^{hp}GUS, GG-*wc1*^{hp}GUS or GG-Kan^{R}GUS (control vector) vector T-DNAs. To confirm transformation single colonies of *A. tumefaciens* carrying each hairpin group had their DNA extracted. DNA samples were then amplified using the primers HS-KANR-F and -R, which amplified a 632-bp region of the KanR cassette present in each of the Level 2 Golden Gate vectors. Purified GG-*egfp*^{hp}GUS, GG-*wc1*^{hp}GUS or GG-Kan^{R}GUS (control vector) plasmids were amplified alongside the single colony extracts as a positive control. After the reaction, PCR products' banding pattern were visualised using gel electrophoresis.

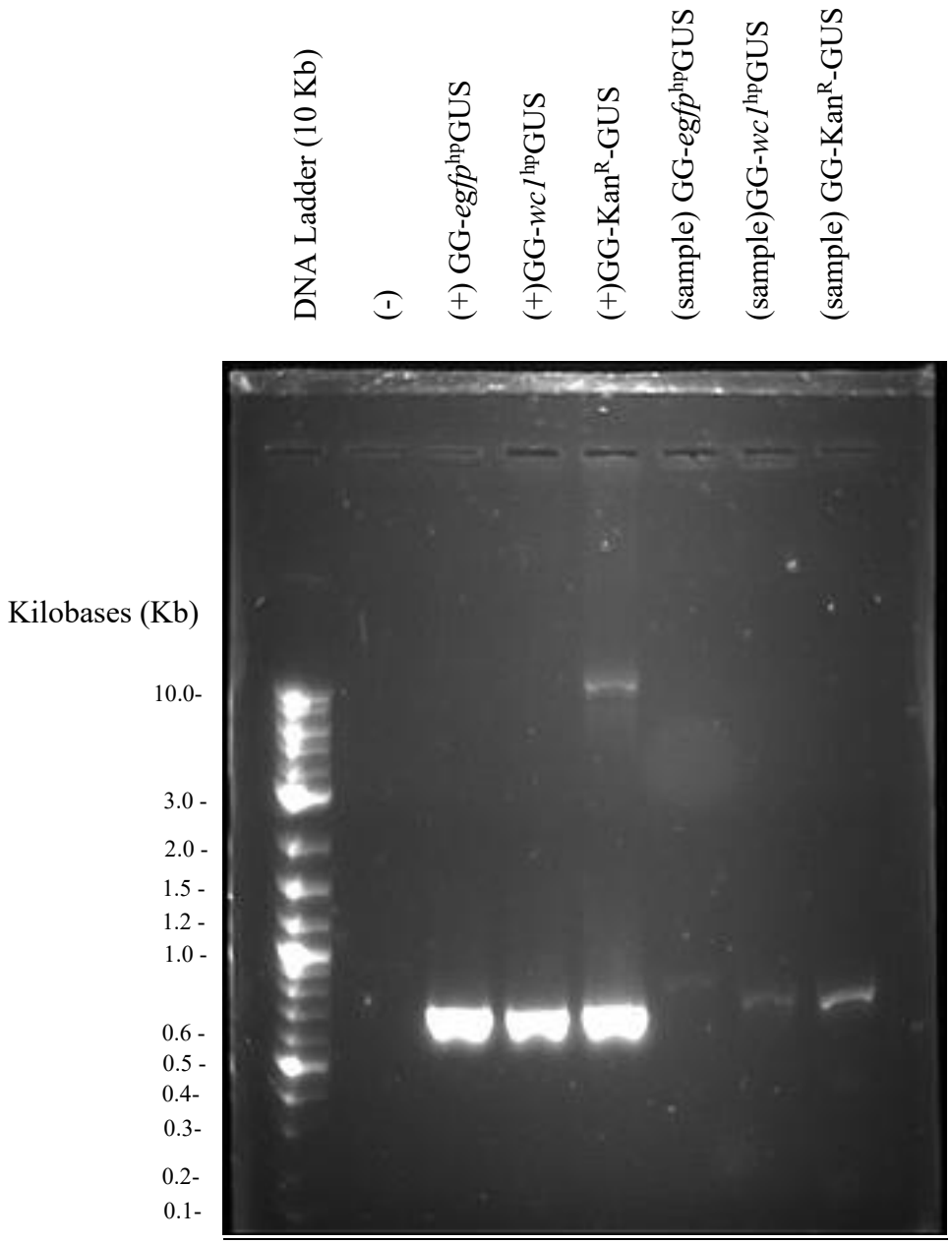

Figure 6: Gel electrophoresis of single colony PCR amplified samples from transformed *A. tumefaciens* colonies. Each sampled colony had been carrying one of the Level 2 Golden gate vector plasmids: GG-*egfp*^{hp}GUS, GG-*wc1*^{hp}GUS or GG-Kan^{R}GUS (control vector). Nuclease free water was used as a negative (-) control. Purified vector plasmids (GG-*egfp*^{hp}GUS, GG-*wc1*^{hp}GUS or GG-Kan^{R}GUS) of known concentrations extracted from *E.coli* were used as positive (+) controls for each colony sample. (n samples = 3). Ladder size: 10 Kb.

As shown in Figure 6, each single colony of *A. tumefaciens* DNA sample showed a band at 632-bp for the amplified region of the Kan^{R} cassette present in each of the Level 2 Golden Gate vector T-DNAs, matching the

band shown for the purified vectors in the positive controls. The nuclease-free water showed no band. The results of this PCR reaction indicated that the glycerol stocks of *A. tumefaciens* each hairpin group used for transformation of *A. thaliana*, were carrying the T-DNA vectors for each hairpin.

4.2.2 Screening for hairpin vector T-DNAs in infiltrated leaves

Col-0 leaves were transformed with *Agrobacterium tumefaciens* carrying the GG-*egfp*^{hp}GUS hairpin vector T-DNA, via syringe infiltration. To assess if the hairpin vector T-DNA was present in the infiltrated leaves, leaf DNA extracts were amplified using PCR, with the same HS-KAN-R primers used to confirm the hairpin's presence as used in the single *A. tumefaciens* colonies (Section 4.2.1). Nuclease-free water and extracted DNA from one of the mock-infiltrated plants were used as negative controls and purified GG-*egfp*^{hp}GUS hairpin vector T-DNA was diluted 10-fold and used as a positive control.

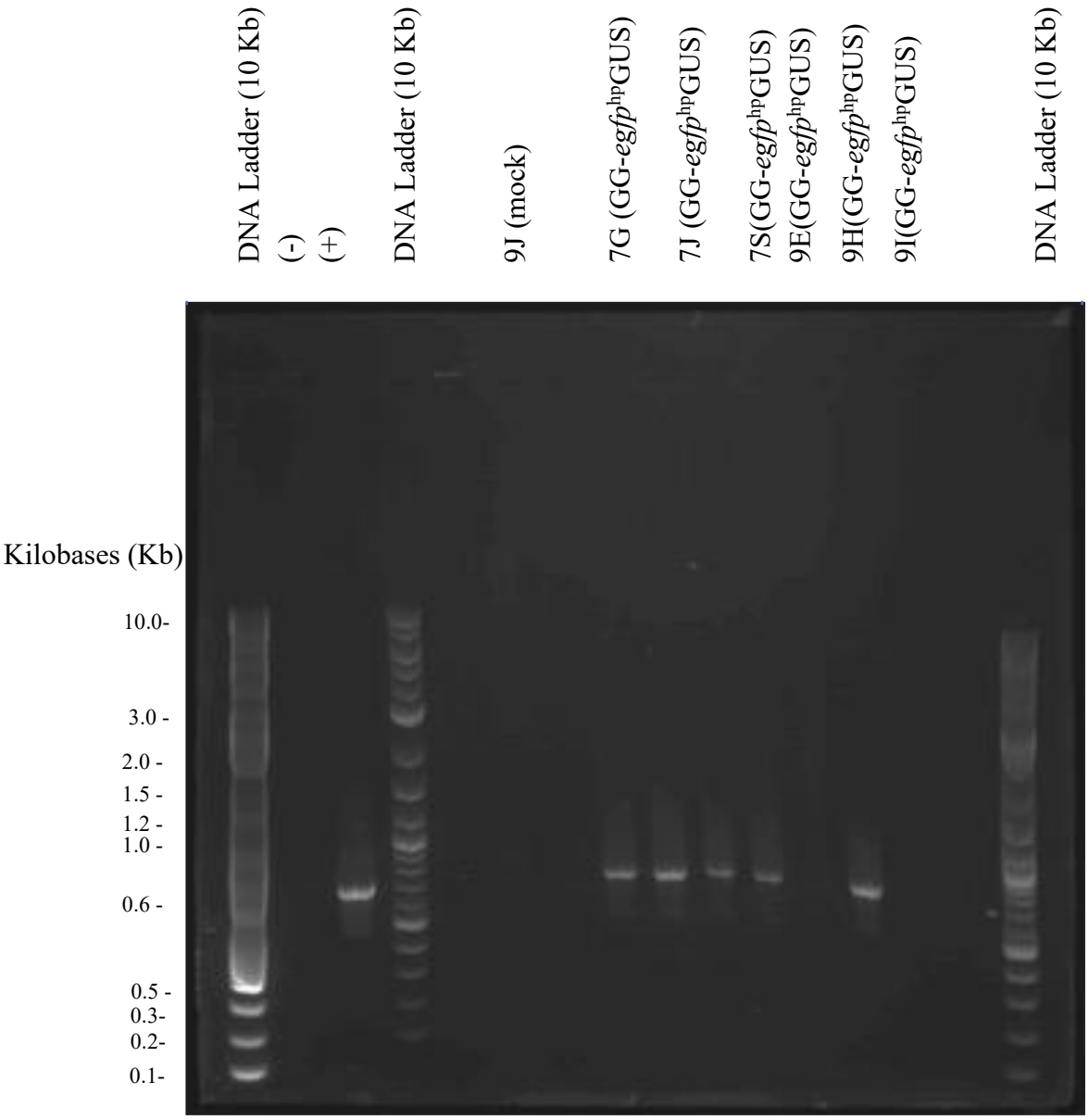

Figure 7: Gel electrophoresis of *Agrobacterium tumefaciens* infiltrated leaves. A negative (-) control sample (nuclease-free water), and positive (+) control samples of purified vector plasmid (1/10x GG-*egfp*^{hp}GUS) and 9J (mock- infiltrated leaf), were compared to Col-0 replicates 7G, 7J, 7S, 9E, 9H, 9I infiltrated with *A. tumefaciens* carrying GG-*egfp*^{hp}GUS plasmid. (n samples = 6). Ladder size: 10 Kb.

As shown in Figure 7, amplification of leaf DNA extracts from infiltrated Col-0 plants using the HS-KAN-R primers, produced a band of 632 bp for replicates 7G, 7J, 7S, 9E, and 9I, indicating that the GG-*egfp*^{hp}GUS hairpin vector T-DNA was present in the infiltrated leaves. This indicates that the infiltration process was successful in introducing *A. tumefaciens* into the apoplast of the leaf tissue 5 days post-infiltration.

4.3 Using PCR to screen T1 transformants for the GG-egfp^{hp}GUS vector

Arabidopsis thaliana floral bolts were transformed using *Agrobacterium tumefaciens* to contain the GG-*egfp*^{hp}GUS vector. The progeny seeds (T1) from these transformed plants were initially grown on selective media before transfer on to soil. To confirm transformation of surviving T1 plants, DNA samples were taken and amplified using PCR primers: JH-GFP which amplified a 1.2 kb region of the hairpin and ACT2 primers which amplified a 465 bp fragment of the Col-0 ACT2 gene (Figure 8).

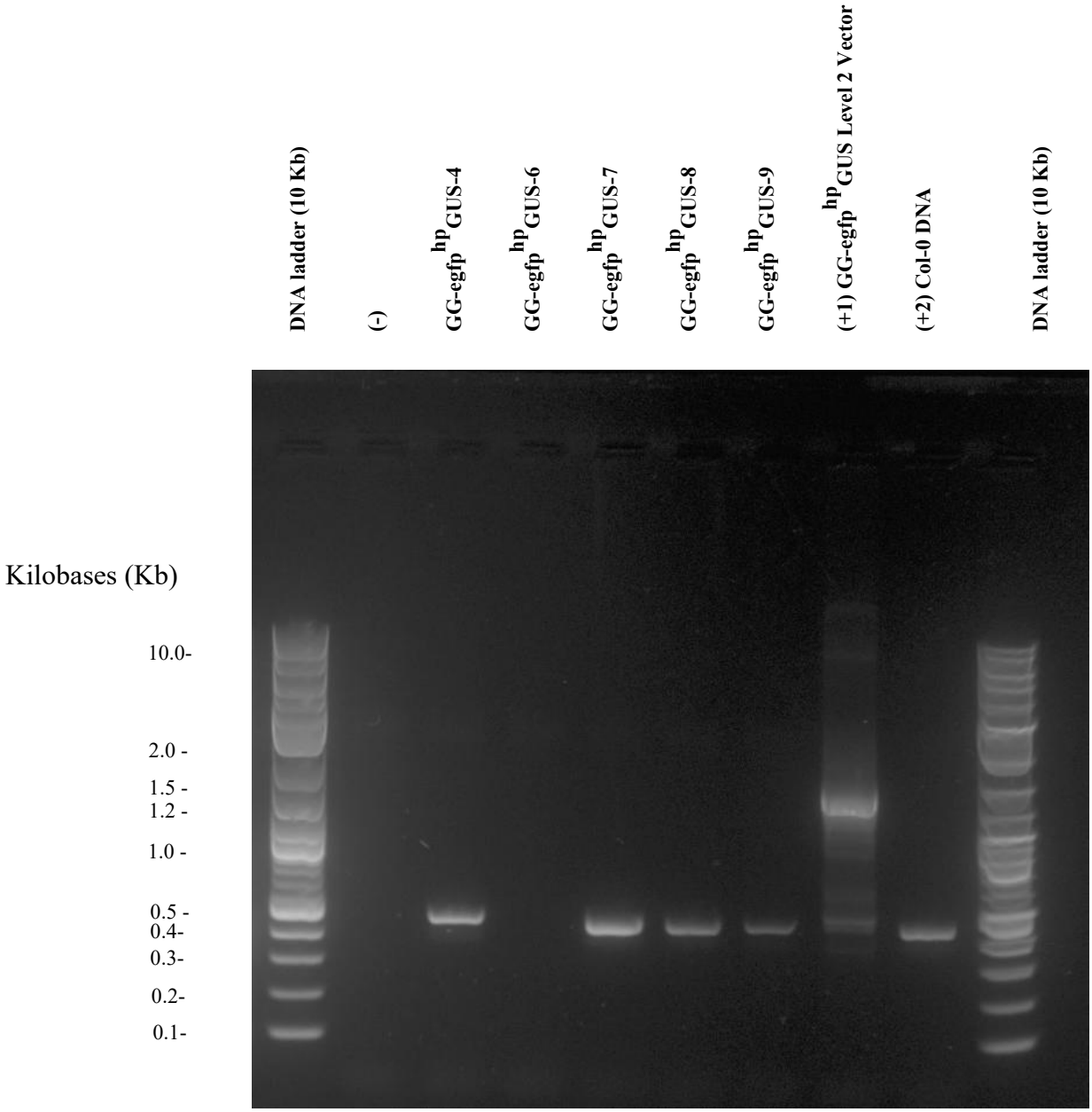

Figure 8: Gel electrophoresis screening of DNA samples from leaves of *A. thaliana* transformed with the GG-egfp^{hp}GUS insert. Controls were nuclease-free water (negative control), GG-egfp^{hp}GUS level 2 vector (positive control for JH-GFP primers), Col-0 DNA (positive control for ACT2 primers). Leaf samples were taken from biological replicate first generation transformant (T1) *A. thaliana* plants : -4, -6, -7, -8, -9. (n samples = 5). Ladder size: 10 Kb. PCR bands using GFP-specific Primers and ACT2 primers (control).

As shown in Figure 8, there were bands present at 465 bp for all T1 DNA samples, except for the GG-*egfp*^{hp}GUS-6 sample which showed no bands, indicating that the actin gene and that there was good quality plant DNA present in four out of the five T1 leaf samples and in the positive control. The Level 2 vector positive control showed a

band for the JH-GFP primers at 1.2 kb, indicating that the vector was present in the control sample and that the vector specific PCR reaction worked. However, in each T1 plant leaf DNA sample there was no band at 1.2 kb, indicating that the vector could not be detected in the T1 plants.

4.4 Light Microscopy of T1 transformant leaves

The GUS marker gene carried on the vectors used in this project, produces a β-glucuronidase enzyme which converts 5-bromo-4-chloro-3-indolyl-β-D-glucuronide to 5-bromo-4-chloro-3-hydroxyindole which forms the blue coloured compound 5,5′-dibromo-4,4′-dichloro-indigo when oxidised through GUS staining. T1 plants that had successfully been transformed with the GG-*egfp*^{hp}GUS hairpin vector T-DNA, would have contained the GUS gene, which would have acted as a marker to distinguish transformed plants from untransformed plants.

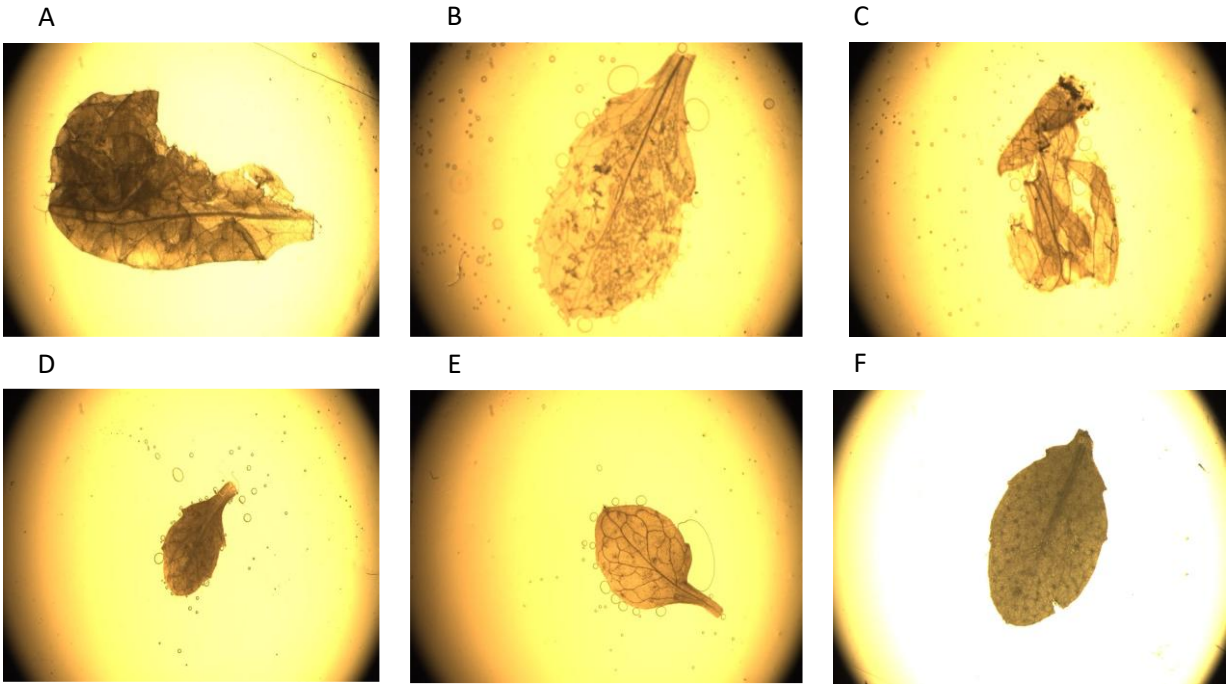

Figure 9: Light microscopy of GUS stained first-generation transformant (T1) GG-*egfp*^{hp}GUS *Arabidopsis thaliana* leaves. Col-0 was used as a negative (-) control) (a), and the following T1 biological replicates were screened: -4 (b), -6 (c), -7 (d), -8 (e), -9 (f). (n samples = 5).

As seen in Figure 9, none of the T1 *Arabidopsis thaliana* leaves (b-f) showed oxidised 5,5′-dibromo-4,4′-dichloro-indigo after GUS staining and did not differ in colour from the untransformed Col-0 control leaves (a). This indicated that the original T1 plants (GG-*egfp*^{hp}GUS-4, GG-*egfp*^{hp}GUS-6, GG-*egfp*^{hp}GUS-7, GG-*egfp*^{hp}GUS-8,

and GG-*egfp*^{hp}GUS-9) were not transformed with the GG-*egfp*^{hp}GUS hairpin vector T-DNA. This was consistent with the PCR results observed for the same plants (Figure 8).

As there were no GG-*egfp*^{hp}GUS lines generated via stable transformation, further work exploring the protective effect of the GG-*egfp*^{hp}GUS T-DNA vector in *A. thaliana* against pathogen infection was, instead, investigated via transient transformation of the hairpin into Col-0.

4.5 Light Microscopy of syringe infiltrated leaves

As a positive control transgenic P35S::UidA *Arabidopsis thaliana* leaves were destained and oxidised. P35S::UidA is genetically modified to ubiquitously express the GUS exon, controlled by a 35S promotor, leading to consistent production of the β-glucuronidase enzyme in the leaf tissue.

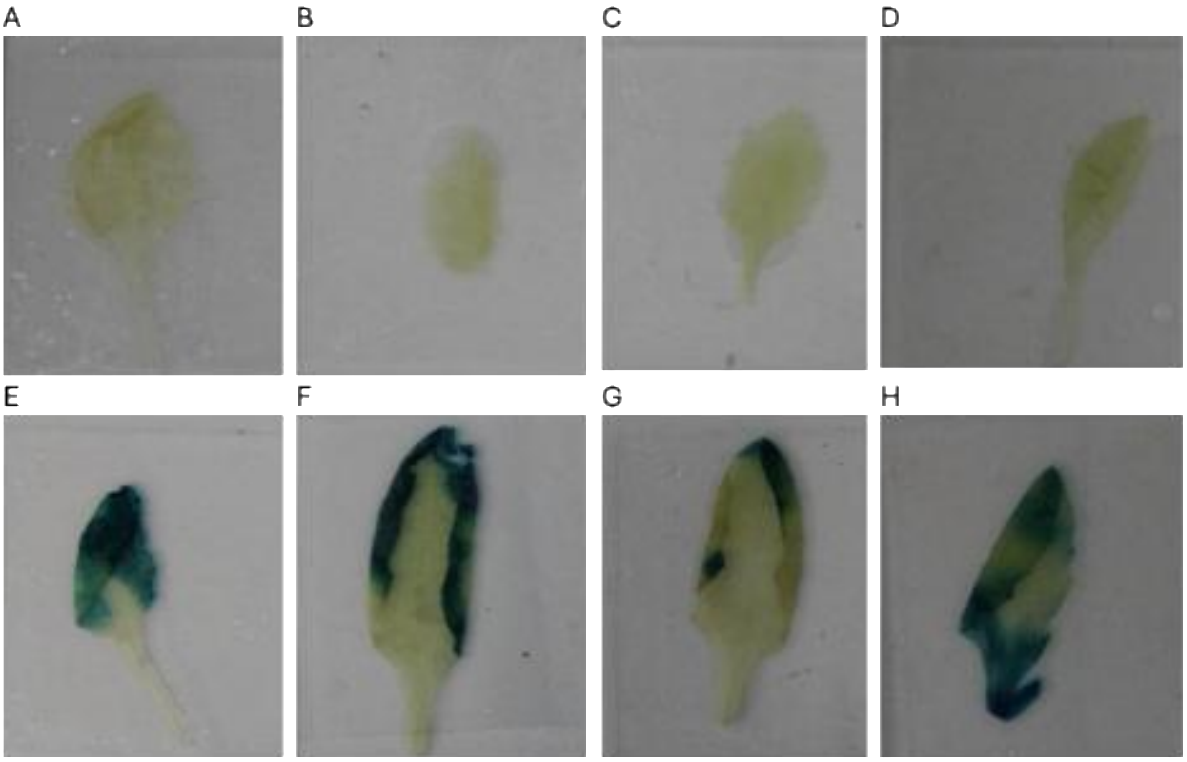

Figure 10: GUS-stained *Arabidopsis thaliana* leaves from wild-type (Col-0) compared to a transgenic GUS expressing line (P35S::UidA). Samples included biological replicates from plants: Col-0 1.2 (a), Col-0 1F.2 (b), Col-0 2 (c) and Col-0 2.1 (d) and P35S::UidA 1(e), P35S::UidA-A(f), P35S::UidA-B (g), P35S::UidA-C (h).

As shown in Figure 10 the P35S::UidA leaves had strong blue pigment, which was visible to the naked eye, indicating the presence of the marker phenotype, compared to control wild-type Col-0 which showed no pigment.

To determine if the GUS marker phenotype was expressed after transient transformation, leaves transformed via syringe infiltration with GG-*egfp*^{hp}GUS were screened using GUS staining, 5 days post-infiltration.

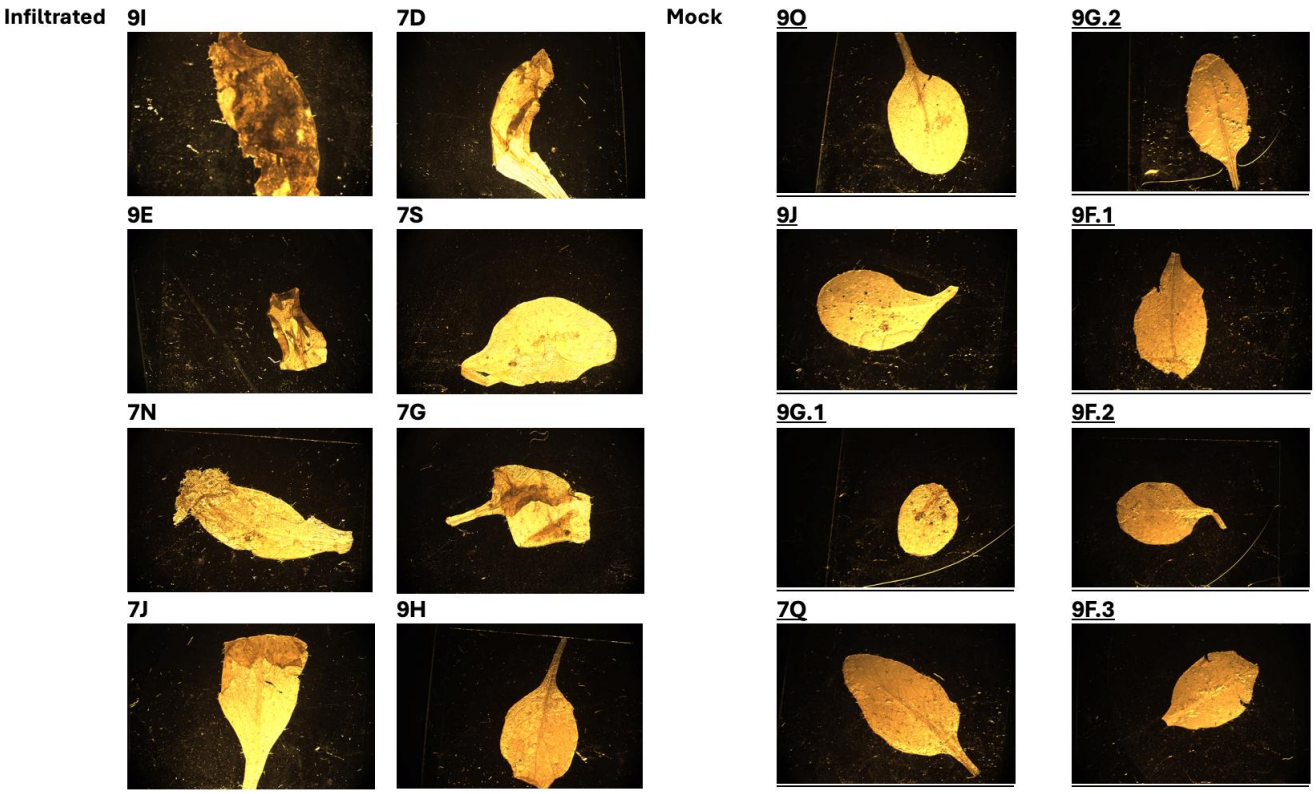

Figure 11: Light microscopy of *Arabidopsis thaliana* leaves from biological replicates syringe infiltrated with GG-*egfp*^{hp}GUS (7D, 7G, 7J, 7N, 7S, 9E, 9H and 9I) or mock infiltration solution (7Q, 9F.1, 9F.2, 9F.3, 9G.1, 9G.2, 9J and 9O).

As shown in Figure 11, leaves in the syringe infiltrated group showed no visual difference to the mock group, indicating that 5,5′-dibromo-4,4′-dichloro-indigo may not have been present in the leaves. This could indicate that the hairpin has not been introduced, however this contradicts the PCR results for these same infiltrated plants which indicate the presence of the hairpin in the leaves (Figure 6). Alternatively, it is possible that the β-glucuronidase enzyme was not expressed at a sufficient level, therefore GUS staining produced no discernible blue pigment phenotype.

4.6 Infiltration with *Pseudomonas syringae*

Infection of *Arabidopsis thaliana* with *Pseudomonas syringae* was undertaken via syringe infiltration of leaves. This experiment was conducted to test whether infiltration could successfully introduce *P. syringae* into the leaves of *Arabidopsis thaliana* and cause symptoms of chlorosis and leaf damage. This experiment also served to test visual and computerised scoring methods to see if the two produced comparable results.

The syringe infiltration method proved to be highly effective at achieving disease symptoms of *P. syringae* in the leaves (Figure 12).

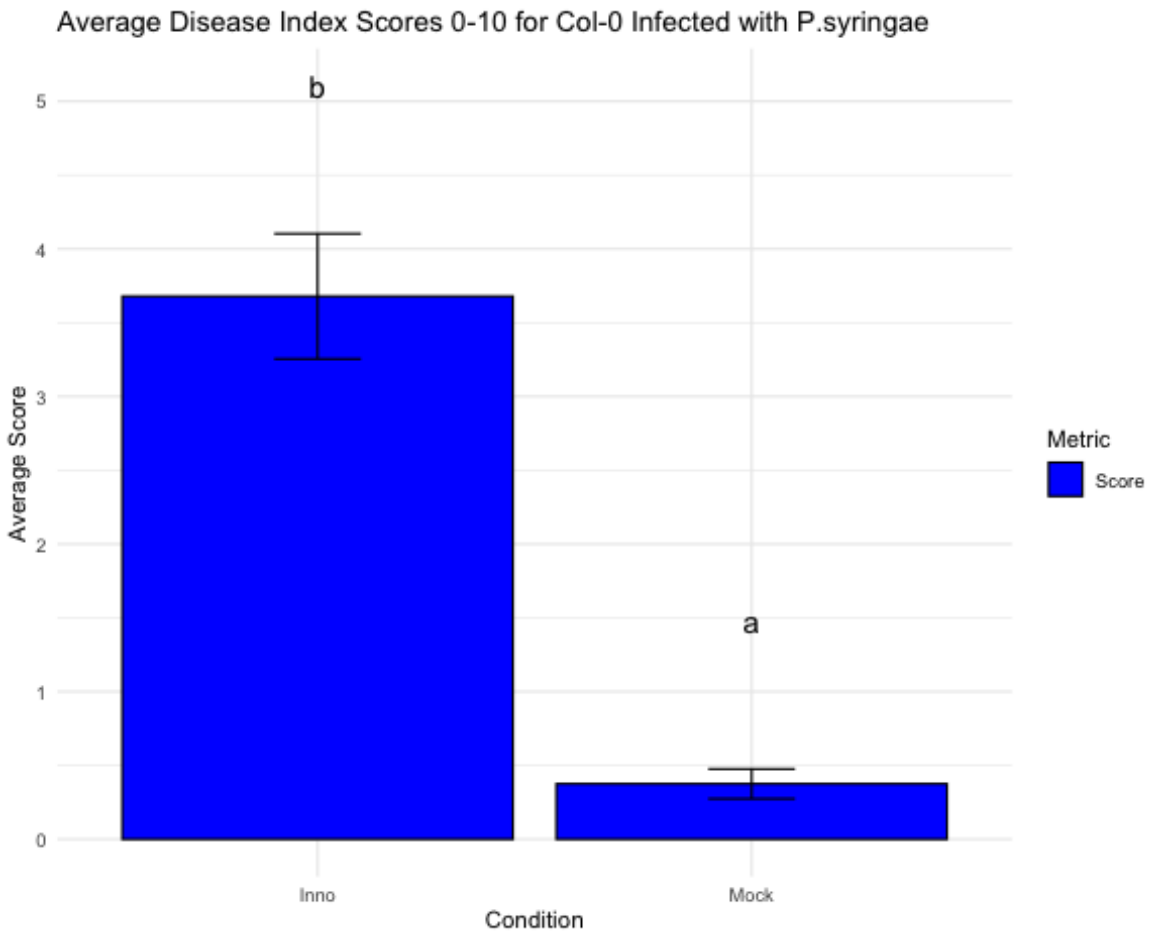

a)

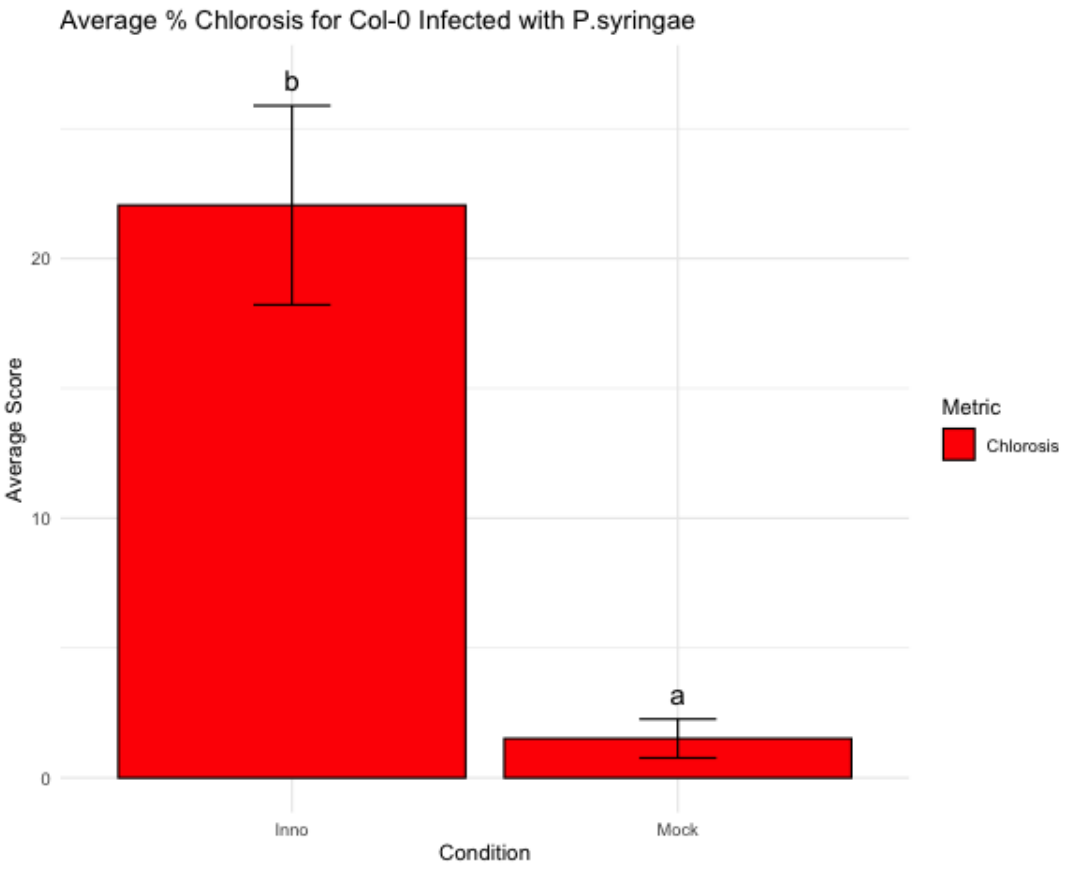

b)

Figure 12: Average visual symptom scores (1-10) (a) compared to average % chlorosis calculated in ImageJ (b) for *Arabidopsis thaliana* infected with *Pseudomonas syringae* (Inno) compared to water infiltrations (Mock).

The results from the statistical analysis (Figure 12a-b) show that average disease index scores and average chlorosis levels (as a % of total leaf area) measured using ImageJ showed a significantly higher level of chlorosis in infected plants than mock plants. The higher level of chlorosis in the infected plants compared to the mocks demonstrated that the infiltration with *P. syringae* achieved disease symptoms in the leaves of Col-0.

4.7 Combined disease assay

4.7.1 Localized co-infiltrations

Local co-infiltrations involved infiltrating 3-4 leaves of a Col-0 plant with one of three *Agrobacterium tumefaciens* strains and then, after 5 days, infecting the same leaves with *P. syringae* before monitoring the plants for disease

symptoms for an additional 5 days (10 days in total). The aim was to test whether transient transformation with the hairpin had any impact on the plants' localised response to the pathogen.

In the first local infiltration experiment, Col-0 plants in treatment groups: GFP.I, EHA105.I and Water.I, showed a significant amount of leaf damage at the end of the experiment in comparison to the uninfected control group (GFP.M). The group infiltrated with the GG-Kan^{R}GUS (control vector) was excluded as only two replicates survived the infiltration process. Statistical analysis of the data for the remaining groups was used to determine any significant variation in leaf damage scores between treatments (Figure 13). The results for average leaf damage assessment, show that GFP.M (which received the hairpin vector T-DNA but not the *P. syringae*) showed significantly lower average leaf damage scores compared to the groups that were infiltrated with *A. tumefaciens* (EHA105.I and GFP.I) and *P. syringae*, indicating that inoculation with the pathogen produced significant disease symptoms. However, GFP.I did not differ significantly from EHA105.I and Water.I treatments, which had received untransformed *A. tumefaciens* or the sterile infiltration solution, before being infected with *P. syringae* (Table 5). This indicates that the presence of GG-*egfp*^{hp}GUS vector T-DNA in the leaf tissue did not confer protection against *P. syringae* infection.

Table 5: Disease Index scores for the initial localised infiltration

Summary of leaf damage scores for Col-0 Batch 1					
Treatment	Average	SE	Maximal bound	Minimal Bound	CLD
EHA105.I	6.250	0.750	8	5	a
GFP.I	6.000	0.707	7	4	a
GFP.M	2.800	1.020	6	0	b
Water.I	5.800	0.374	7	5	a
Summary of chlorosis scores for Col-0 Batch 1					
EHA105.I	5.000	0.408	6	4	a
GFP.I	2.500	1.040	5	0	ab
GFP.M	1.400	0.980	5	0	b
Water.I	4.000	0.548	6	3	ab

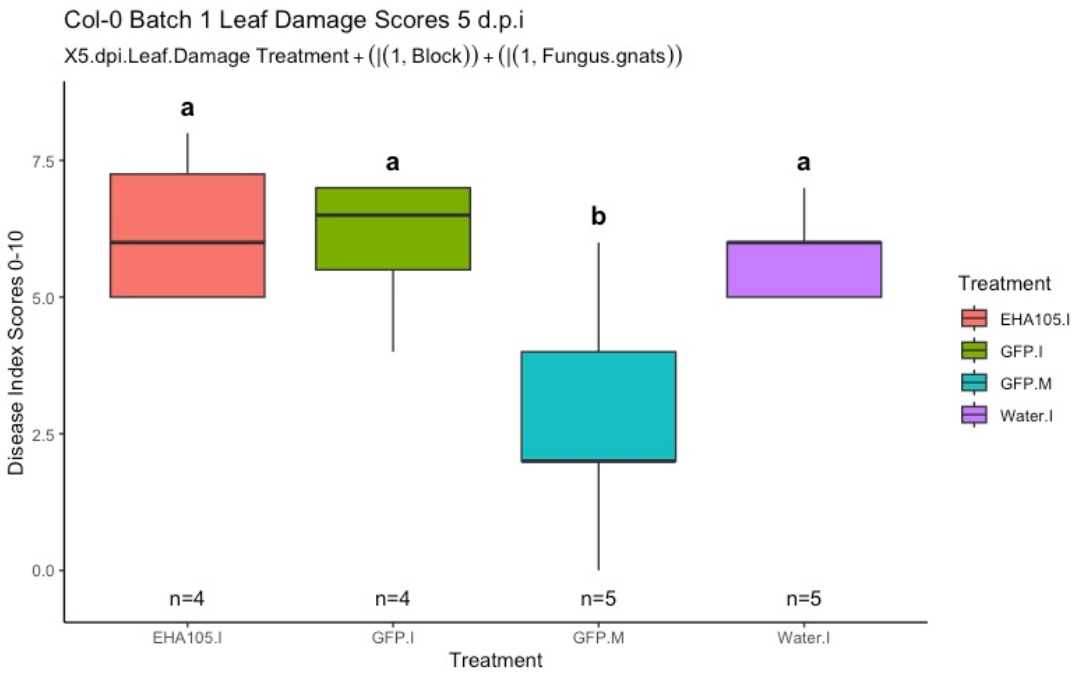

a)

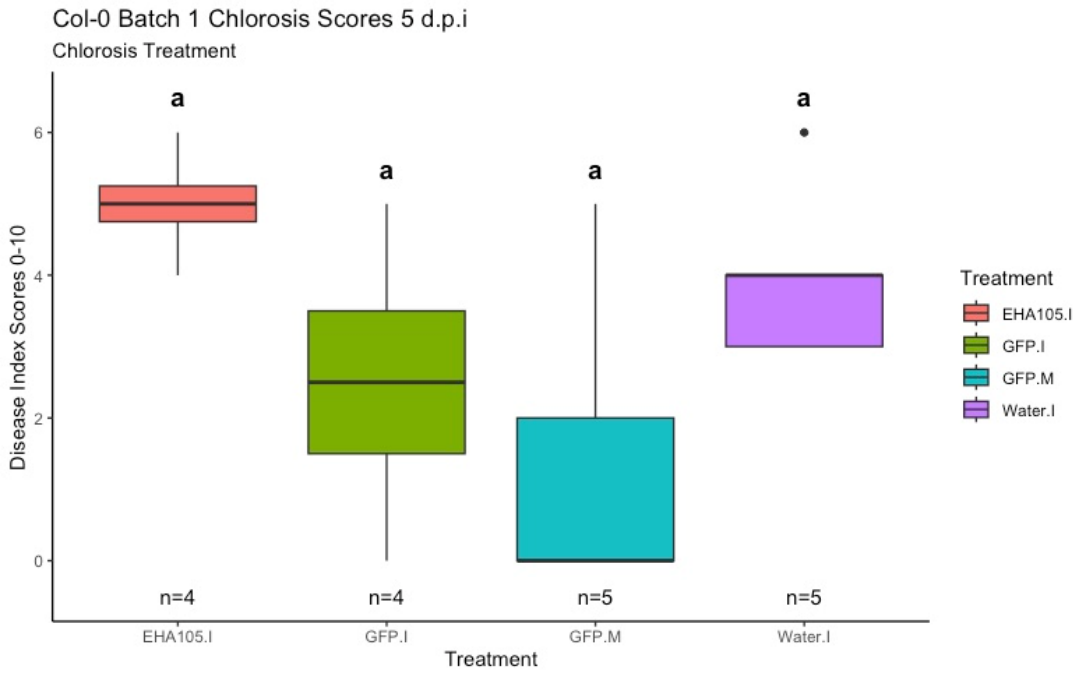

b)

Figure 13: Average visual leaf damage (a) and chlorosis (b) scores (1-10) for the first round of Col-0 combined local infiltrations, 5-d.p.i with *P. syringae*.

As shown in Figure 13, despite the trend seen for leaf damage, the average chlorosis levels observed did not differ significantly for the GFP.I, EHA105.I and Water.I groups (which were infected with *P. syringae*) compared to the GFP.M group (which was not infected with *P. syringae*) (Figure 13b). This indicates that similar disease symptoms were observed for the uninfected control group compared to the infected groups. The two control treatments, Water.I and GFP.M did not show significantly different chlorosis from one another, even though Water.I only received *P. syringae* and GFP.M only received GG-*egfp*^{hp}GUS carrying *A. tumefaciens*. This indicated that our focal treatment could not be tested for significant differences in chlorosis levels in this experiment.

In conclusion, the results show that there was no significant difference between the positive and negative control groups for chlorosis. However, the results from the leaf damage assay indicates that introduction of the GG-*egfp*^{hp}GUS T-DNA vector does not provide protection from *P. syringae* induced leaf damage. Overall, the matter of whether the introduction of the hairpin provides protection against *P. syringae* was inconclusive from the results of this test.

A repeat experiment was conducted for the localised infiltration assay. Early leaf damage and chlorosis symptoms after infiltration with *A. tumefaciens* were observed and were scored using the same visual scoring method used

for the *P. syringae* disease assay (Figure 13a-b), with the sterile infiltration solution treatment (Water.I) group serving as a negative control.

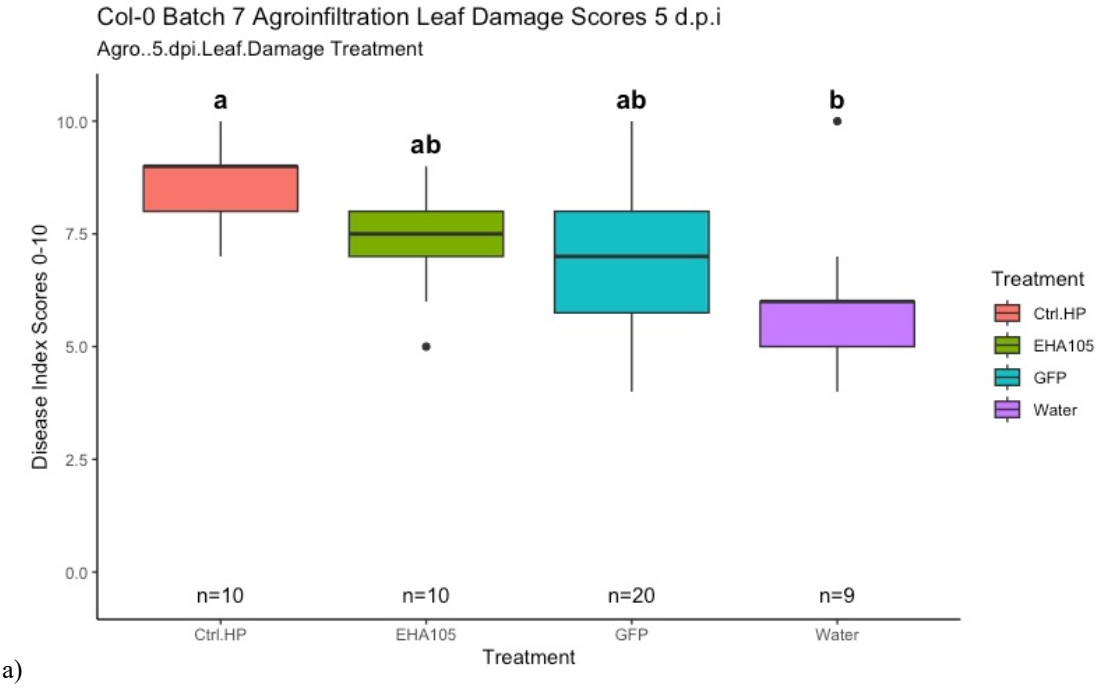

a)

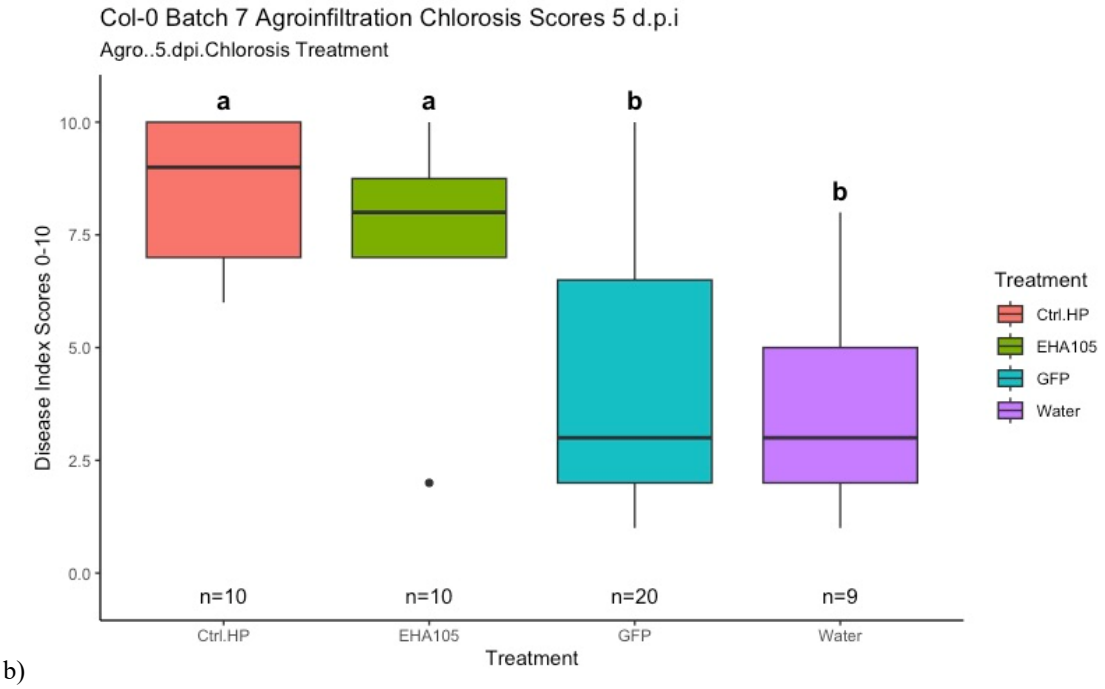

b)

Figure 14: Average visual leaf damage (a) and chlorosis (b) scores (1-10) for *Arabidopsis thaliana* plants 5 d.p.i with *Agrobacterium tumefaciens*

As shown in Figure 14a-b introduction of *A. tumefaciens*, prior to *P. syringae* infection, appeared to elicit disease-associated symptoms. Leaf damage (Figure 14a) was consistently high across all treatment groups (Ctrl.HP, EHA105, GFP and Water). Mixed model analysis, followed by a post-hoc Tukey-test, revealed that infiltration

with sterile infiltration solution (Water.I), showed the lowest average leaf damage scores and this was significantly lower than the average leaf damage observed in leaves infiltrated with GG-Kan^{R}GUS (Ctrl.HP). However, both the Ctrl.HP and Water.I groups did not differ significantly from infiltration with untransformed *A. tumefaciens* (EHA105) or *A. tumefaciens* carrying GG-*egfp*^{hp}GUS (GFP). The average leaf damage scores for these groups overlapped with that of the control hairpin and sterile infiltration solution and with one another. The results show that the Ctrl.HP treatment group had a significantly higher level of leaf damage compared to the Water treatment group but the EHA105 and GFP showed a similar level of damage to the Ctrl.HP and the Water group, not differing significantly from either. This indicates that *A. tumefaciens* caused leaf damage in Col-0, regardless of whether it was untransformed or carrying one of the hairpin T-DNA inserts.

Chlorosis showed a different trend (Figure 14b), with the Ctrl.HP and EHA105 treatment groups showing a similarly higher level of chlorosis compared to each other. Additionally, the GFP and Water treatment groups showed significantly less chlorosis than the Ctrl.HP and EHA105 treatment groups. This indicates that the Ctrl.HP and EHA105 treatments induced significantly higher level of chlorosis than the Water or GFP treatments. The fact that the GFP treatment showed similar levels of chlorosis to the Water treatment and significantly lower chlorosis level compared to the Ctrl.HP and the EHA105 treatments indicates that the *A. tumefaciens* carrying GG-*egfp*^{hp}GUS was less prone to eliciting plant defence pathways than untransformed *A. tumefaciens* and the strain carrying GG-Kan^{R}GUS.

The early emergence of symptoms was accounted for by analysing disease severity as difference scores, calculated by subtracting leaf damage and chlorosis scores obtained 5 d.p.i with *A. tumefaciens* from the corresponding scores obtained 5 d.p.i with *P. syringae* infection (Table 6). These difference scores were then modelled with linear mixed-effects models, taking the symptom scores from *A. tumefaciens* infiltration at 5 d.p.i into consideration as covariates during model selection. The models of best-fit for leaf damage and chlorosis were subsequently analysed using a post-hoc Tukey test. The Ctrl.HP group was excluded, as leaves infiltrated with *A. tumefaciens* carrying GG-Kan^{R}GUS died after agroinfiltration and were unusable for subsequent *P. syringae* infection.

Table 6: Disease Index scores for the technical repeat of localised infiltration

Summary of average differential leaf scores (scores post-*Pseudomonas syringae* infiltration – scores post-*Agrobacterium* tumefaciens) for Col-0 Batch 7

Summary of leaf damage scores for Col-0 Batch 7

Treatment	Average	SE	Maximal bound	Minimal Bound	CLD
EHA105.I	1.000	0.309	2	0	a
GFP.I	1.500	0.289	2	1	a
GFP.M	1.380	0.183	2	1	a
Water.I	1.500	0.428	3	0	a
Summary of chlorosis scores for Col-0 Batch 7					
EHA105.I	1.140	0.261	2	0	a
GFP.I	1.500	0.645	3	0	a
GFP.M	0.875	0.611	5	0	a
Water.I	4.670	1.12	9	1	a

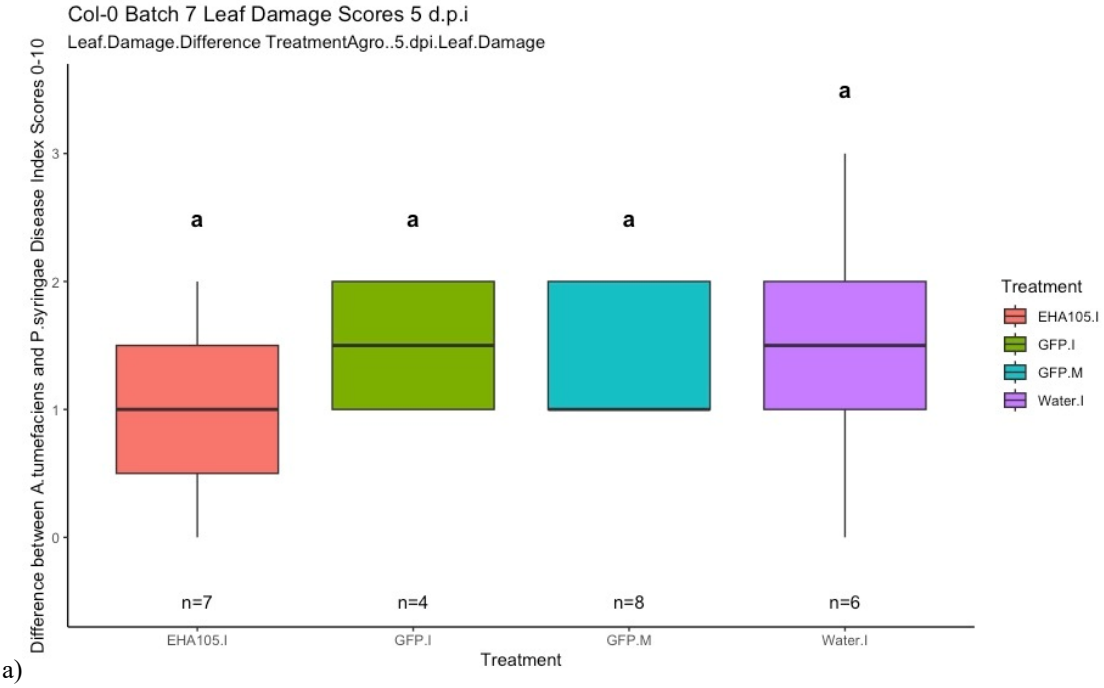

a)

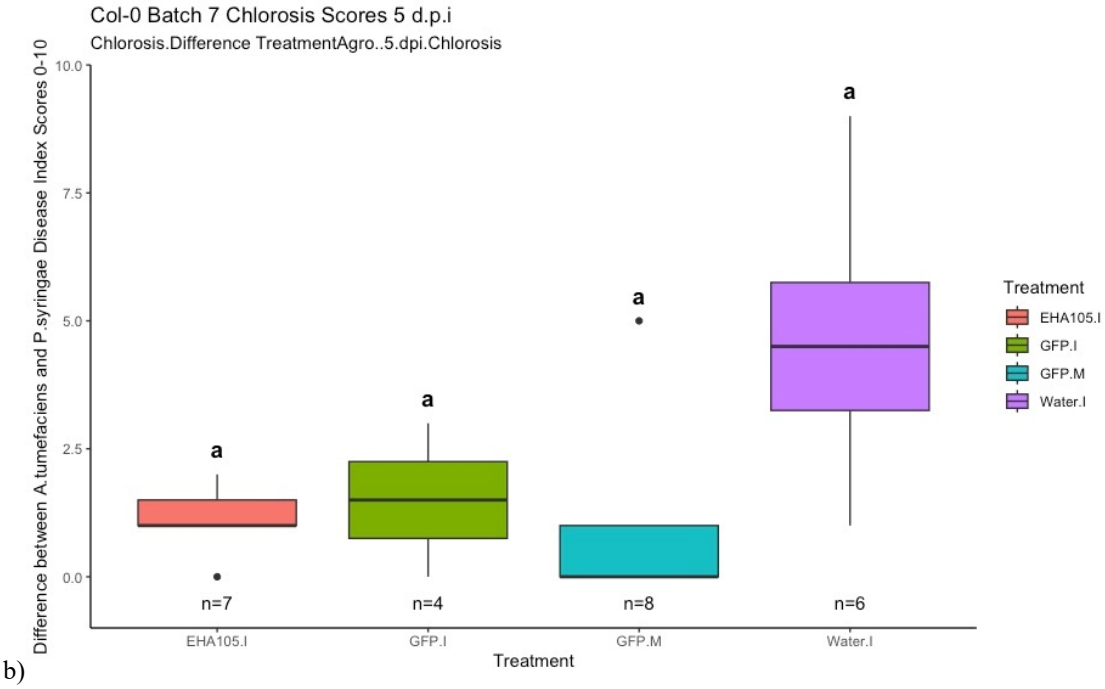

b)

Figure 15: Average visual leaf damage (a) and chlorosis (b) scores (1-10) for the repeat of Col-0 combined local infiltrations, 5-d.p.i with *P. syringae*.

Leaf damage symptoms were observed after agroinfiltration prior to infiltration with *P. syringae* (Figure 14a) and mixed model analysis revealed that the leaf damage observed 5 d.p.i with *A. tumefaciens* had a significant impact on the variation observed in the leaf damage scores 5 d.p.i with *P. syringae* (Figure 15a). The results of the post-

hoc Tukey test revealed that the average leaf damage scores did not differ significantly across any of the treatment groups.

Chlorosis symptoms were observed after agroinfiltration prior to infiltration with *P. syringae* (Figure 14b) and mixed model analysis revealed that the chlorosis observed 5 d.p.i with *A. tumefaciens* had a significant impact on the variation observed in the chlorosis scores 5 d.p.i with *P. syringae* (Figure 15b). Like the leaf damage results, the results of the post-hoc Tukey test revealed that the average chlorosis scores did not differ significantly across any of the treatment groups.

The GFP.M and Water.I groups did not differ significantly from one another in terms of leaf damage or chlorosis. The results do not prove, nor do they disprove that the introduction of *A. tumefaciens* or the GG-*egfp*^{hp}GUS or GG-Kan^{R}GUS hairpins provided any localised protective effect against *P. syringae* infection, as the results were likely confounded by the leaf damage and chlorosis symptoms caused by infiltration with *A. tumefaciens.*

4.7.2 Systemic infiltration

To test whether the introduction of GG-*egfp*^{hp}GUS conferred systemic resistance to *P. syringae,* Col-0 plants were syringe infiltrated with *Agrobacterium tumefaciens* and *Pseudomonas syringae*. Unlike the local infiltration experiments detailed above (Section 4.7.1), the *Pseudomonas syringae* was introduced into the leaves adjacent to the leaves that had been infiltrated with *A. tumefaciens*. As before, leaves were agroinfiltrated and left for 5 days. Plants were then infected with *P. syringae* in the adjacent leaves, before being left an additional 5 days. Leaf damage and leaf chlorosis was visually scored as a measurement of disease progression.

Table 7: Disease Index scores for the initial systemic infiltration

Summary of leaf damage scores for Col-0 Batch 2					
Treatment	Average	SE	Maximal bound	Minimal Bound	CLD
Ctrl.HP.I	1.820	0.698	7	0	a
EHA105.I	1.360	0.491	5	0	a
GFP.I	2.600	0.777	8	0	a
GFP.M	1.550	0.455	4	0	a
Water.I	1.000	0.539	6	0	a
Summary of chlorosis scores for Col-0 Batch 2					
Ctrl.HP.I	1.180	0.423	4	0	a
EHA105.I	2.000	0.426	5	0	a
GFP.I	1.700	0.731	7	0	a
GFP.M	1.360	0.364	4	0	a
Water.I	0.545	0.157	1	0	a

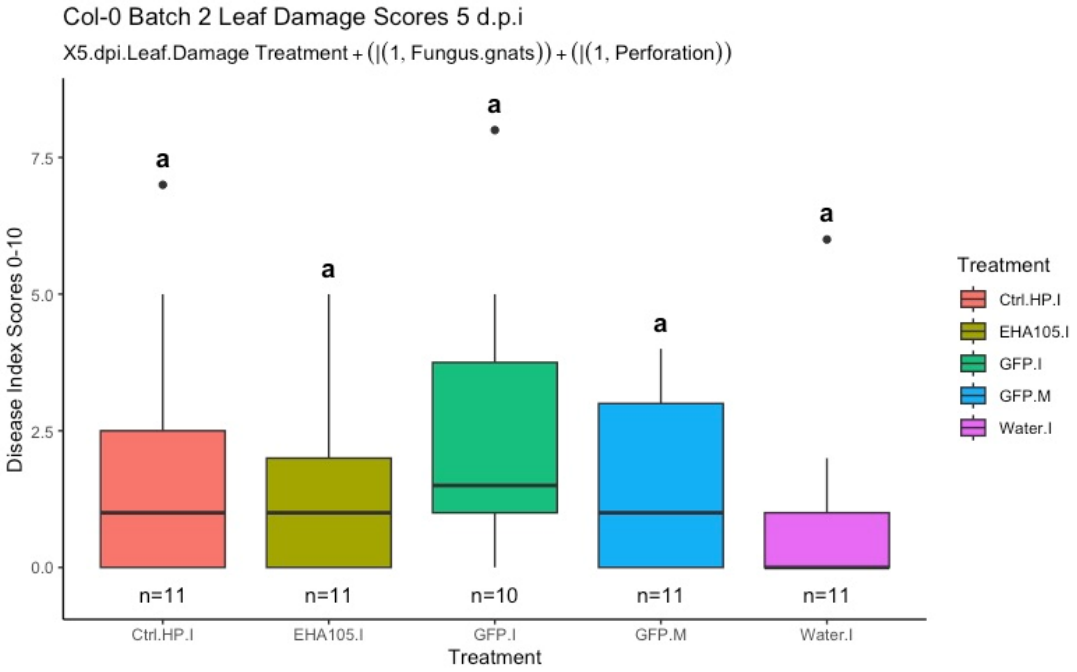

a)

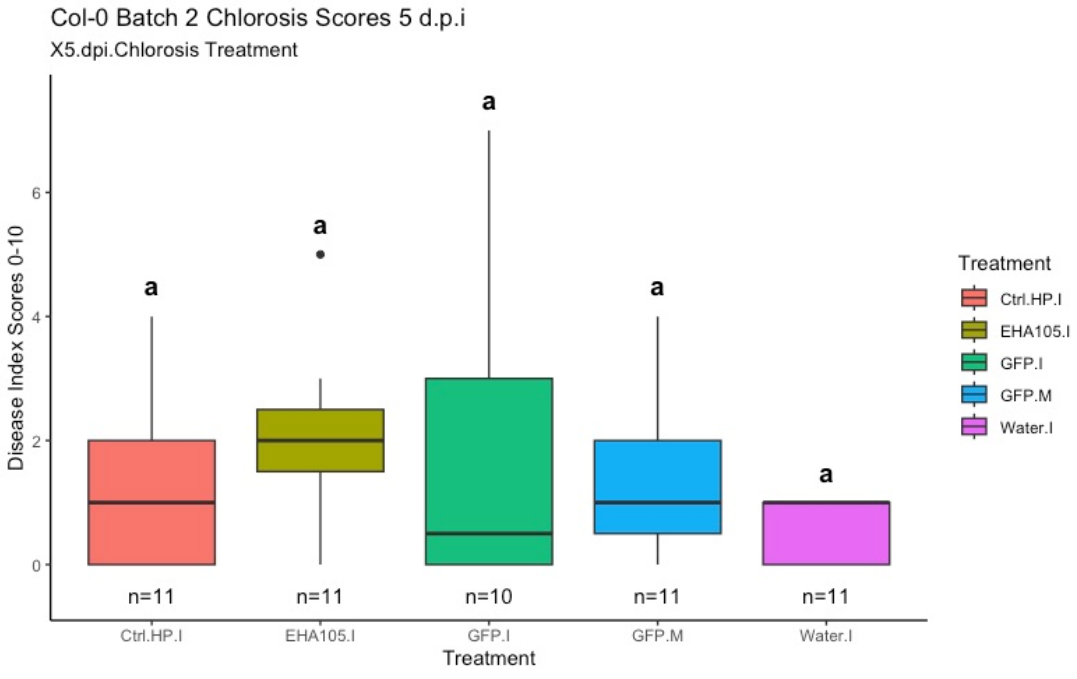

b)

Figure 16: Average visual leaf damage (a) and chlorosis (b) scores (1-10) for the first round of Col-0 combined systemic infiltrations, 5-d.p.i with *P. syringae*.

Col-0 showed low level signs of both leaf damage and chlorosis (Figure 16a-b). However, statistical analysis revealed that there was no significant difference between the average leaf damage or chlorosis scores between

mock and inoculated plants. Therefore, the results did not prove or disprove that the introduction of GG-*egfp*^{hp}GUS hairpin via agroinfiltration confers systemic protection from infection with *P. syringae*.

4.8 Differentially Expressed Genes analysis of published genomes

The original premise of this project was to investigate whether resistance to *Verticillium dahliae* could be achieved in *Arabidopsis thaliana* using Host-Induced Gene Silencing to target the genes for: the transcription factor *sge1* and the blue-light sensing complex component *wc1*. Additionally, this project aimed to test whether HIGS using GG-*egfp*^{hp}GUS (containing a non-specific hairpin), could improve baseline immunity in *A. thaliana*, providing enhanced resistance to *V. dahliae*. Floral dipping was used to try and create hairpin expressing lines of *A. thaliana* seeds carrying the hairpins GG-*egfp*^{hp}GUS, GG-Kan^{R}GUS, GG-*sge1*^{hp}GFP and GG-*wc1*^{hp}GUS, with the intention of running a disease assay with *V. dahliae*, followed by an RNASeq analysis and a Differentially Expressed Genes (DEGs) analysis to identify the genes active in the hairpin-expressing lines and compare them to wild-type Col-0 during infection. Once the DEGs were obtained, the intention was to analyse the DEGs and characterise the functions and the pathways they were part of, to better understand how the introduction of a hairpin altered and potentially improved the plants' response to infection with *V. dahliae*.

Transformant seeds were not obtained after floral dipping (Sections 4.3 and 4.4), however a similar study by Walker *et al.* (2023) published the read counts data from RNASeq analysis that they carried out when investigating the use of HIGS to improve *A. thaliana* resistance to *Sclerotina sclerotiorum*.

Walker *et al.* (2023) published read counts data containing the expression profile for the two *A. thaliana* lines, representing the genes being expressed at three time points during an infection assay with the white mould fungus *S. sclerotiorum*. These lines were Col-0, a wild-type strain, and *AT1703*, a hairpin-expressing line that produced an RNAi hairpin targeting the *Anhydrolase-3* gene, a key pathogenicity factor in *S. sclerotiorum*. We aimed to test whether, in line with previous literature, if the *AT1703* lines showed signs of downregulation for photosynthesis and growth-related pathways in favour of an upregulation of stress response genes before inoculation with the pathogen.

DEGs were calculated for each comparison group (Table 4) across 0-3 d.p.i (Table 8)

Table 8: Total number of up/downregulated DEGs for the Wild-type and *AT1703* across 0-3 d.p.i, individually and compared to each other

Comparisons	Up	Down
Wild-type only		
0 d.p.i to 2 d.p.i	2629	2790
2 d.p.i to 3 d.p.i	555	1001
0 d.p.i to 3 d.p.i	1759	2308
***AT1703*-only**		
0 d.p.i to 2 d.p.i	2586	2636
2 d.p.i to 3 d.p.i	57	169
0 d.p.i to 3 d.p.i	1992	2440
***AT1703* vs.. wild-type**		
0 d.p.i	1761	835
2 d.p.i	1861	1261
3 d.p.i	904	346

iDEP utilizes the DESeq2's size-factor normalisation when pre-processing data. This method is a sample-level normalisation and scales each sample so that the relative median ratio of counts equals ~1, making the read counts data comparable across samples regardless of sequencing depth or library size. This removes sample level biases in the biological replicates from factors such as library size or sequence depth and ensures the normalised data set reflects true biological variation. Quality control was performed on the normalised RNASeq dataset, to ensure the

% read counts and normalised expression were across each chromosome was consistent across each individual replicates in the original data (Figure 17).

If individual replicates showed an inconsistent % of reads aligned to each chromosome this would have indicated mapping bias or sample contamination. Additionally, if individual replicates showed an inconsistent 75th percentile of normalised expression for each chromosome this would have also indicated possible mapping or gene annotation bias. Furthermore, if there was a variably inconsistent % of reads or 75th percentile of normalised expression, being aligned to mitochondrial or plastid DNA this would have indicated contamination from a high count of organelle RNA reads.

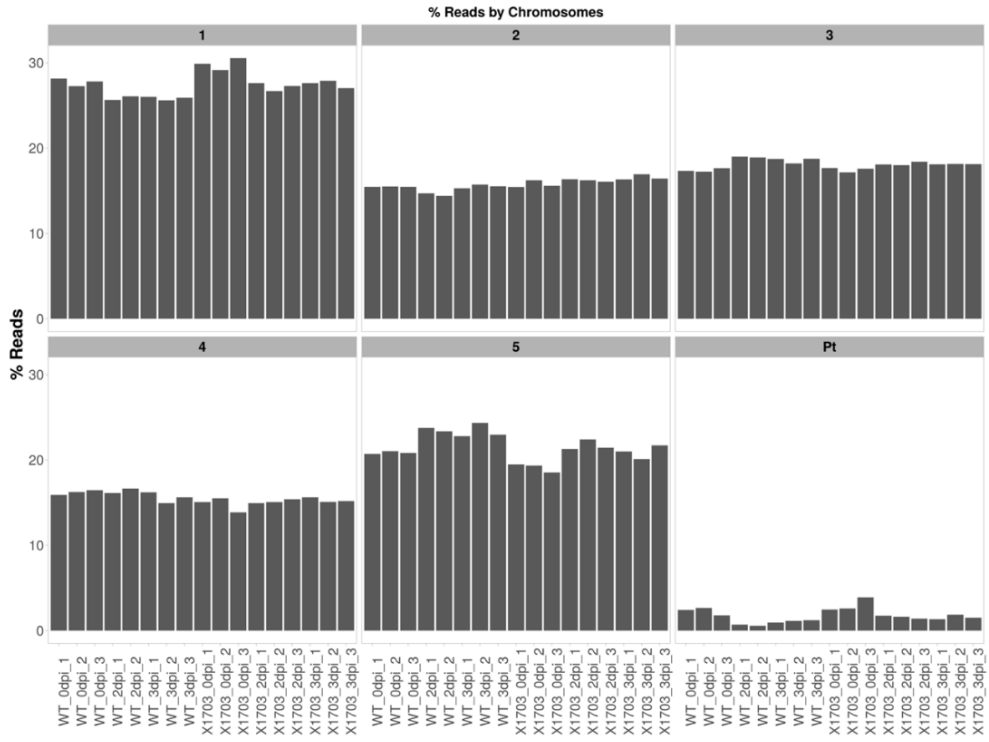

a)

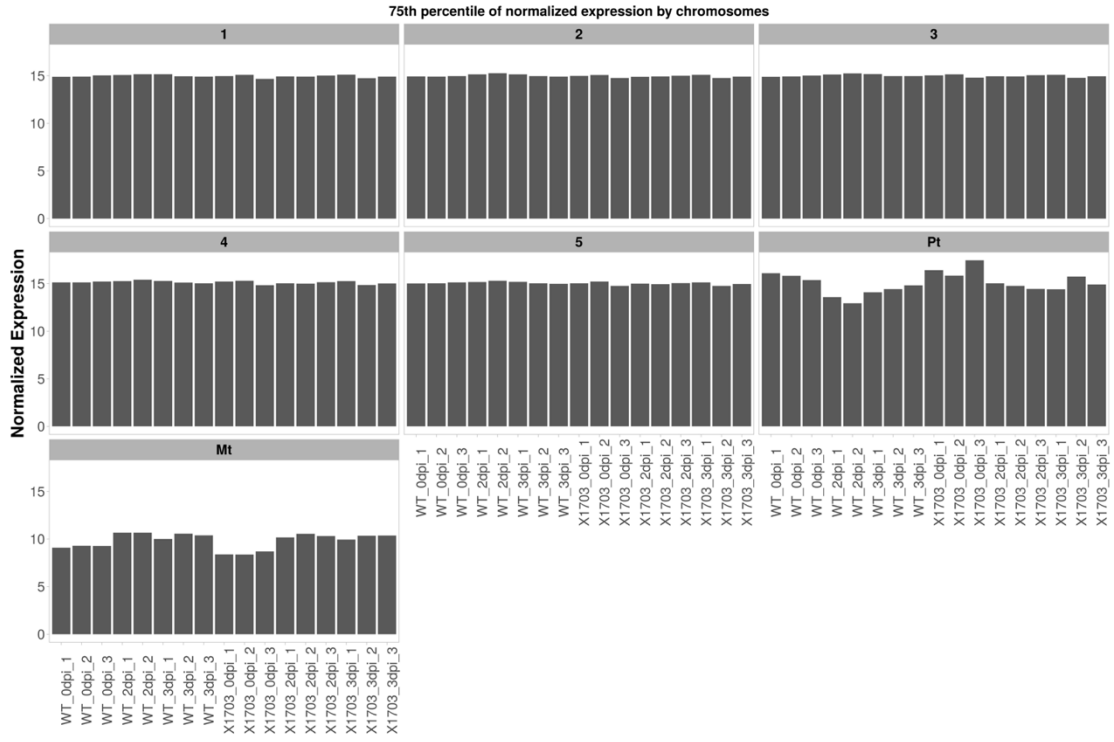

b)

Figure 17: The percentage (%) of total read counts (wild-type and *AT1703*) per chromosome (including mitochondrial and chloroplastic DNA) in the *Arabidopsis thaliana* TAIR10 genome (a) and the disruption of expression across the *Arabidopsis thaliana* TAIR10 genome after normalisation (b). Mitochondrial RNA is given as Mt and Chloroplastic RNA is given as Pt.

As shown in Figure 17, both the percentage of read counts per chromosome and 75th percentile of normalized expression suggested that the read counts were consistently distributed across the *A. thaliana* TAIR10 reference genome for each sample, indicating the data was of good quality.

The read counts data was then enriched in iDEP. Analysis of read counts data for in the wild-type (Col-0) showed that several pathways were up- and downregulated group across the different time points of the 3-day infection assay with *S. sclerotiorum* (Figure 16a-c).

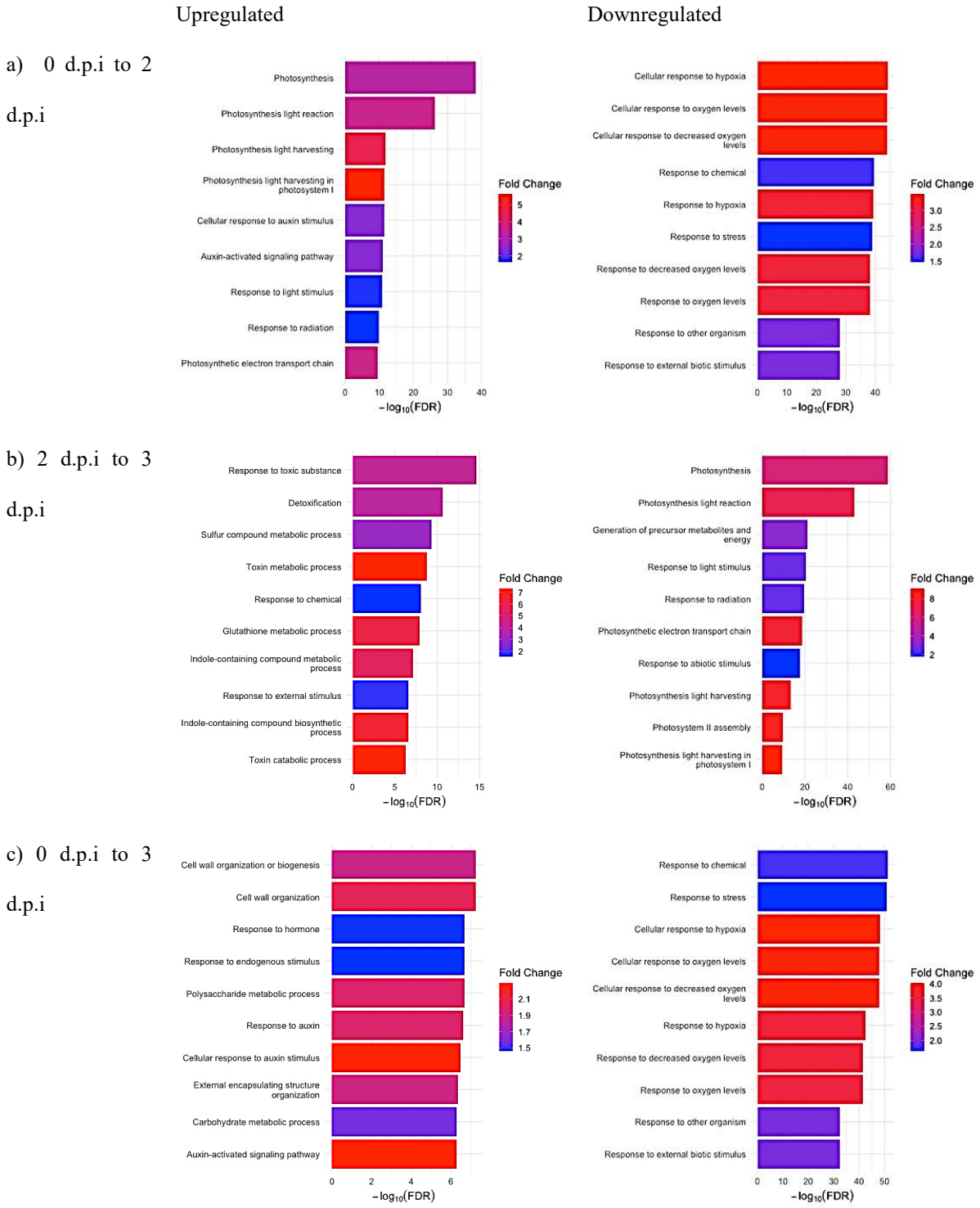

Figure 18: Gene Set Enrichment Analysis (GSEA) of GO terms using the fully ranked expression matrix for Col-0 at time points: 0-2 d.p.i (a), 2-3 d.p.i (b), 0-3 d.p.i (c). Upregulated pathways (left) and downregulated pathways (right). False Discovery Rate (FDR) of $\leq$ 0.01.

S. sclerotiorum supresses the plant's immune response by secreting virulence factors such as oxalic acid which downregulates salicylic acid (SA) production in the infected tissue (Walker *et al.* 2023). This leads to an upregulation of auxin due to the antagonistic relationship between auxin and SA. Col-0 is susceptible to *S. sclerotiorum* and, as shown in Figure 18, the response from Col-0 begins between 0 d.p.i and 2 d.p.i, where the plant's photosynthesis-related pathways were upregulated, while its stress response pathways to foreign organisms and hypoxia, were downregulated (Figure 18a). From 2 d.p.i onwards, the plant appeared to detect the pathogen (Figure 18b) causing the plants' response to light stimuli and photosynthesis related genes to be heavily downregulated, and chemical detoxification pathways to be heavily upregulated, as well as the indole-biosynthesis pathways, likely to activate the jasmonate-mediated pathways. Finally, by 3 d.p.i, it appears that the plant was being overwhelmed by the pathogen. As shown in Figure 18c, there was a sharp downregulation in biotic and abiotic stress pathways, as well as a sharp upregulation of cell wall biosynthesis pathways but also auxin-signalling related pathways, indicating the pathogen has transitioned to its necrotrophic phase and begun secreting cell-wall lytic enzymes as well as oxalic acid. This will have likely inhibited salicylic acid production causing an upregulation of auxin, leading to the plants' metabolism to switch back to auxin-related growth pathways, as well as causing the plants to upregulate cell-wall biosynthesis genes in response to the breakdown of their cell walls at the site of infection.

In contrast, *AT1703* plants, exhibited a greater resistance phenotype to the pathogen (Figure 19a-c).

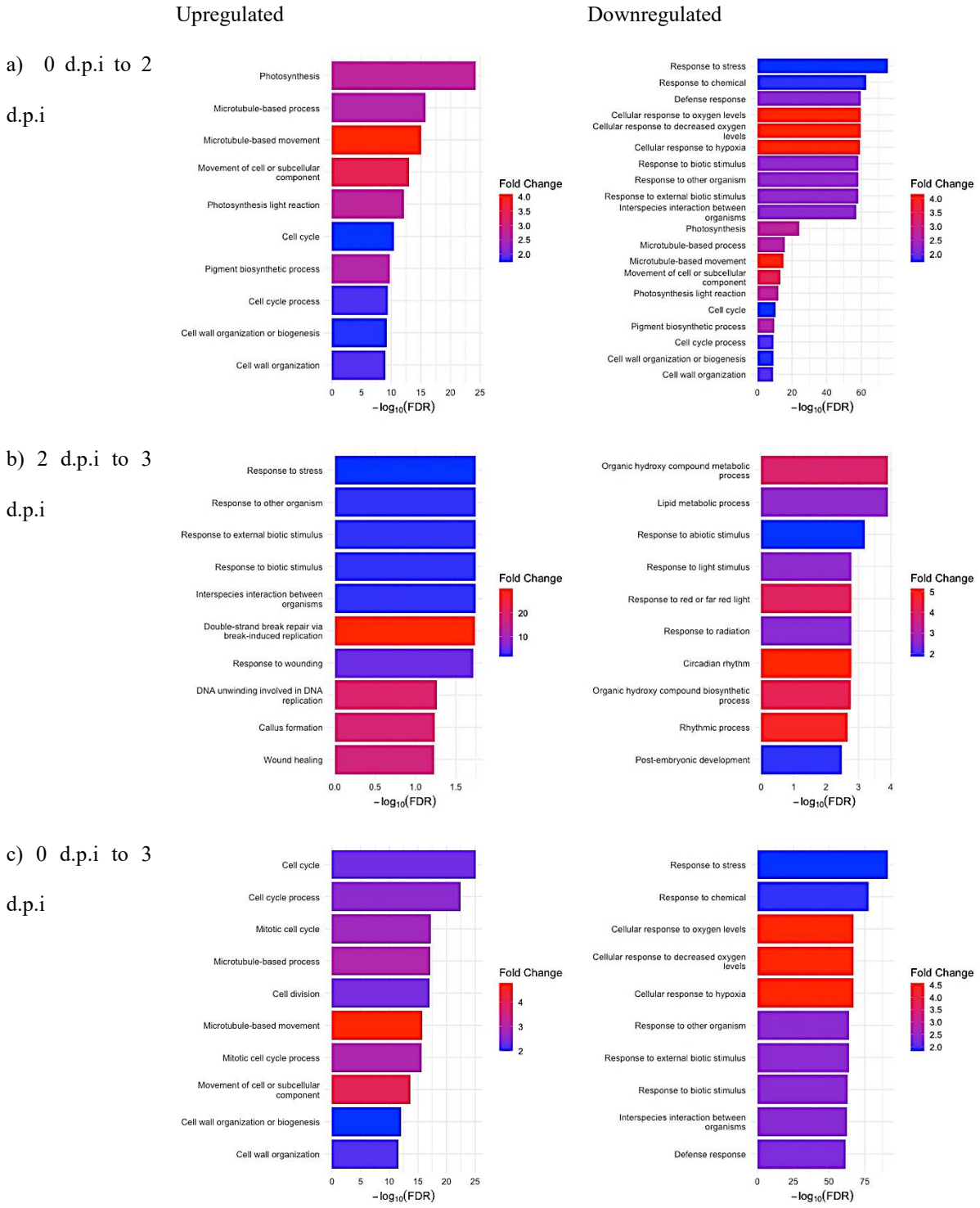

Figure 19: Gene Set Enrichment Analysis (GSEA) of GO terms using the fully ranked expression matrix for *AT1703* at time points: 0-2 d.p.i (a), 2-3 d.p.i (b), 0-3 d.p.i (c). Upregulated pathways (left) and downregulated pathways (right). False Discovery Rate (FDR) of ≤ 0.01.

As shown in Figure 19, *AT1703* shows an upregulation of photosynthesis and cell-cycle related pathways and a downregulation of abiotic and biotic stress related pathways during the 0-2 d.p.i period, just like Col-0. At this point in the infection, stress-related pathways were downregulated on a similar scale in *AT1703* (Log_2 Fold Change of 2-4) compared to Col-0 (Log_2 Fold Change of 2-5). Additionally, the growth and photosynthesis pathways were being upregulated in *AT1703* (Log_2 Fold Change of 2-4) to a similar level to Col-0 (Log_2 Fold Change of 2-5), during this time, indicating a similar base level of normal plant growth metabolism during this time frame. Over the 2 d.p.i to 3 d.p.i period, unlike Col-0, the *AT1703* plants began to upregulate immunity related pathways, rather than just responding to the chemical stimuli from the pathogen. The plant upregulated biotic stress response pathways, specifically pathways relating to infection from a pathogen, as well as callus formation and wound healing, likely at the site of infection to repair the leaf lesions induced by the infection process and contain the pathogen within the callused tissue. By 3 d.p.i, like Col-0, the plant upregulated cell wall biosynthesis, likely to repair damage induced by the pathogen, but by this time, it also appears to have resumed normal growth metabolism.

Walker *et al.* (2023) reports a visible reduction in the lesion size induced by *S. sclerotorioum* infection in *AT1703* compared to Col-0 (Figure 20). Therefore, a comparison of the pathways regulated differently in *AT1703* compared to Col-0, across the three time points, was conducted to highlight how the two lines responsed differently to *S. sclerotiorum* infection (Figure 21a-c).

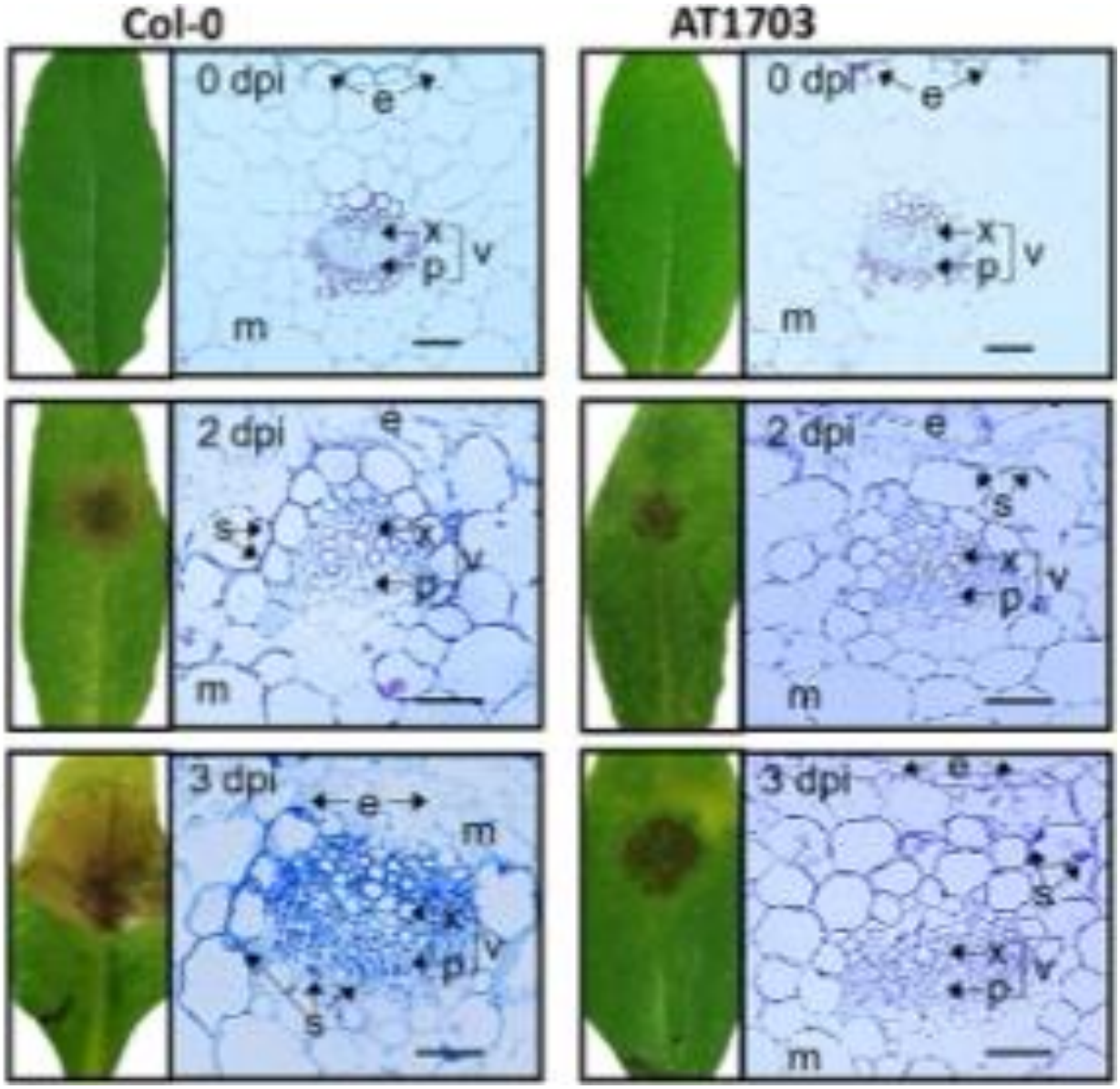

Figure 20: Lesion size for Col-0 compared to *AT1703* infected with *S. sclerotiorum* at: 0 d.p.i (a), 2 d.p.i (b), 3 d.p.i (c)(Walker *et al.* 2023).

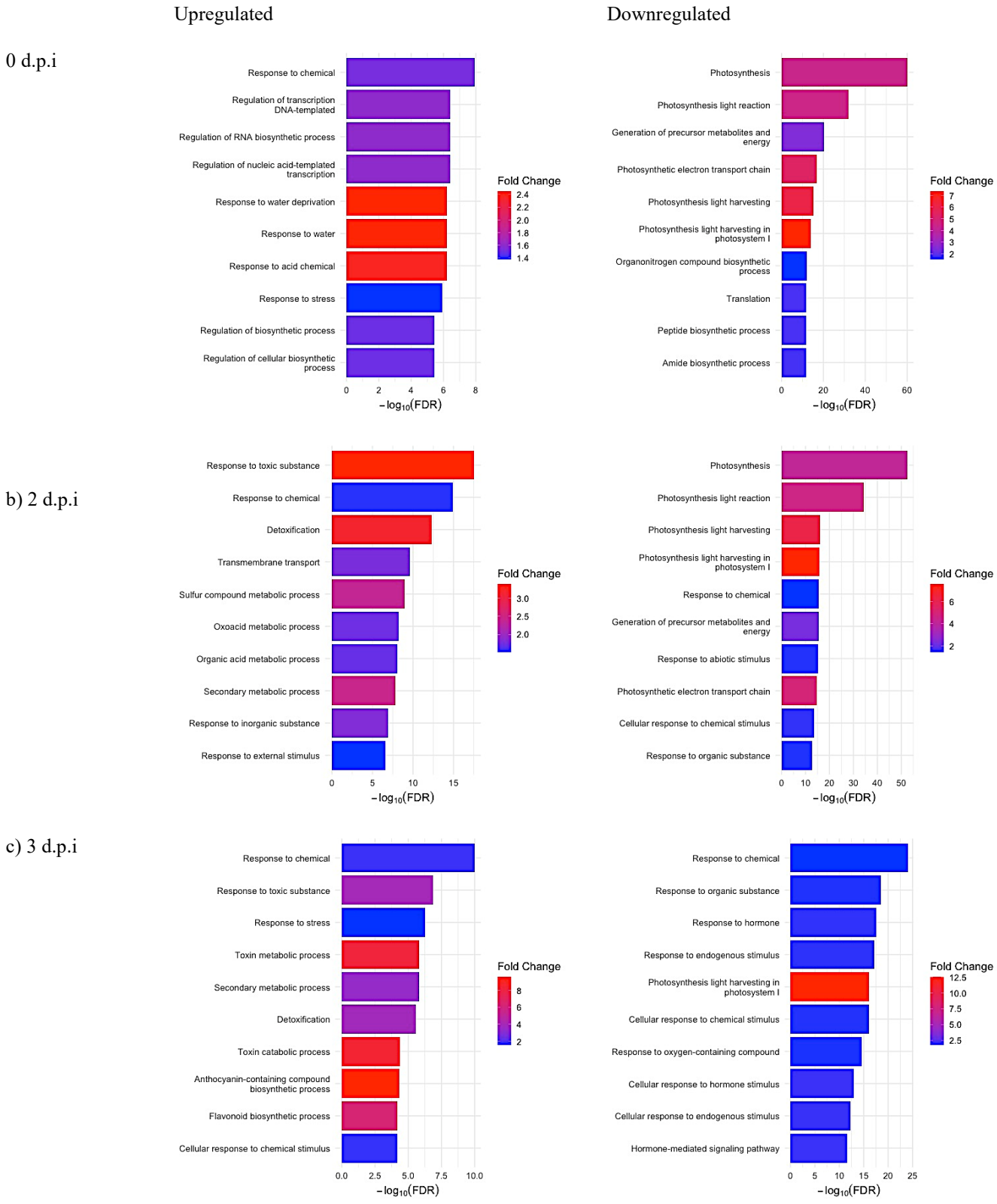

Figure 21: Gene Set Enrichment Analysis (GSEA) of GO terms using the full ranked expression matrix for *AT1703* compared to Col-0 at time points: 0-2 d.p.i (a), 2-3 d.p.i (b), 0-3 d.p.i (c). Upregulated pathways (left) and downregulated pathways (right). False Discovery Rate (FDR) of ≤ 0.01.

As shown in Figure 21a-b, *AT1703* plants show a sharp upregulation of chemical response and detoxification pathways 0-2 d.p.i and a sharp downregulation of photosynthesis related pathways in comparison to Col-0. Upregulation of detoxification and downregulation of photosynthesis was not something that was observed in the susceptible Col-0 until 2-3 d.p.i (Figure 18). Thus, the response from *AT1703* differs at first, as photosynthesis was downregulated and stress and immunity related pathways are upregulated 0 d.p.i (before inoculation) rather than at 2 d.p.i like in the response observed in Col-0. The upregulation of RNA metabolism in *AT1703* 0 d.p.i indicates that the expression of the *Anhydrolase-3* targeting hairpin coincides with this upregulation of baseline immunity pathways, therefore there may be a link between the expression of the hairpin and improved resistance, even before the plant is infected with the pathogen.

Based on the results GSEA analysis, Col-0 was unable to maintain a prolonged detoxification response, which was only triggered 2-3 d.p.i. By 3 d.p.i, the detoxification response in Col-0 had been surpassed by the auxin-signalling and cell wall regeneration pathways, indicating a failed detoxification response. Unlike Col-0, the *AT1703* plants appeared to maintain a prolonged detoxification response throughout the 2-3 d.p.i. period (Figure 19b-c), and their photosynthesis and growth-related pathways remain significantly downregulated across the 3-day period. This indicates a more efficient and prolonged response to *S. sclerotiorum*, as observed by Walker *et al.* (2023) in their original pathogenicity assay.

To further analyse the difference in responses between Col-0 and *AT1703* to *S. sclerotiorum*, the top DEGs from time points 0 d.p.i and 2 d.p.i were investigated (Figure 22).

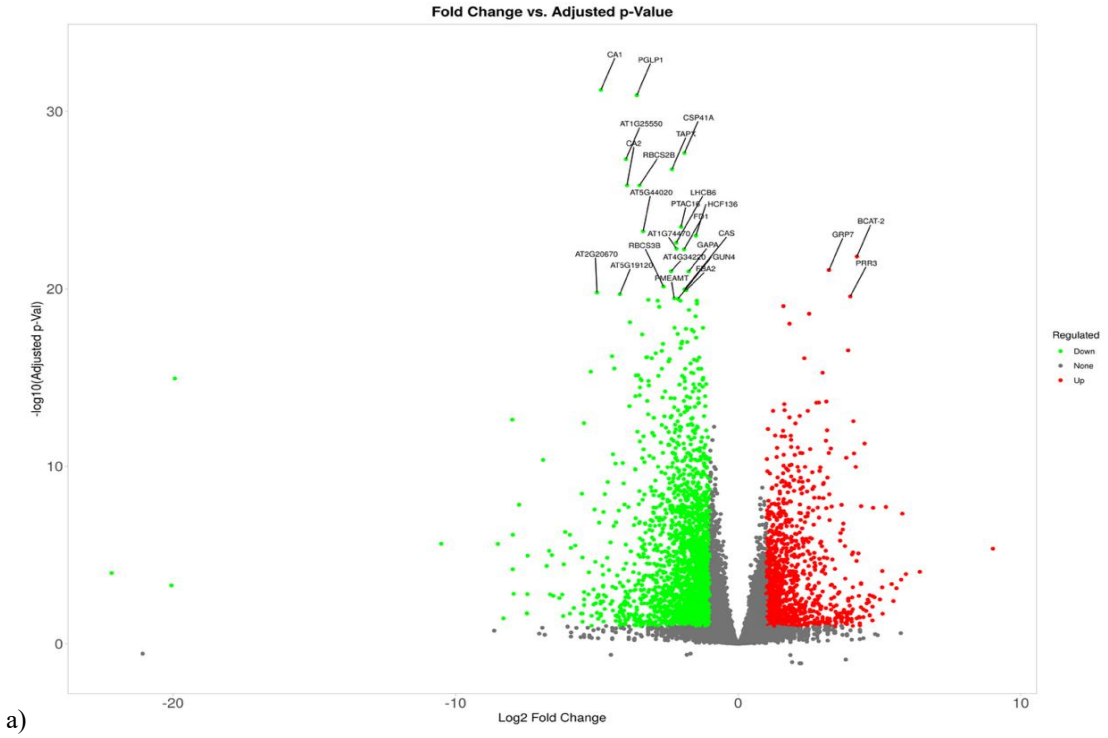

a)

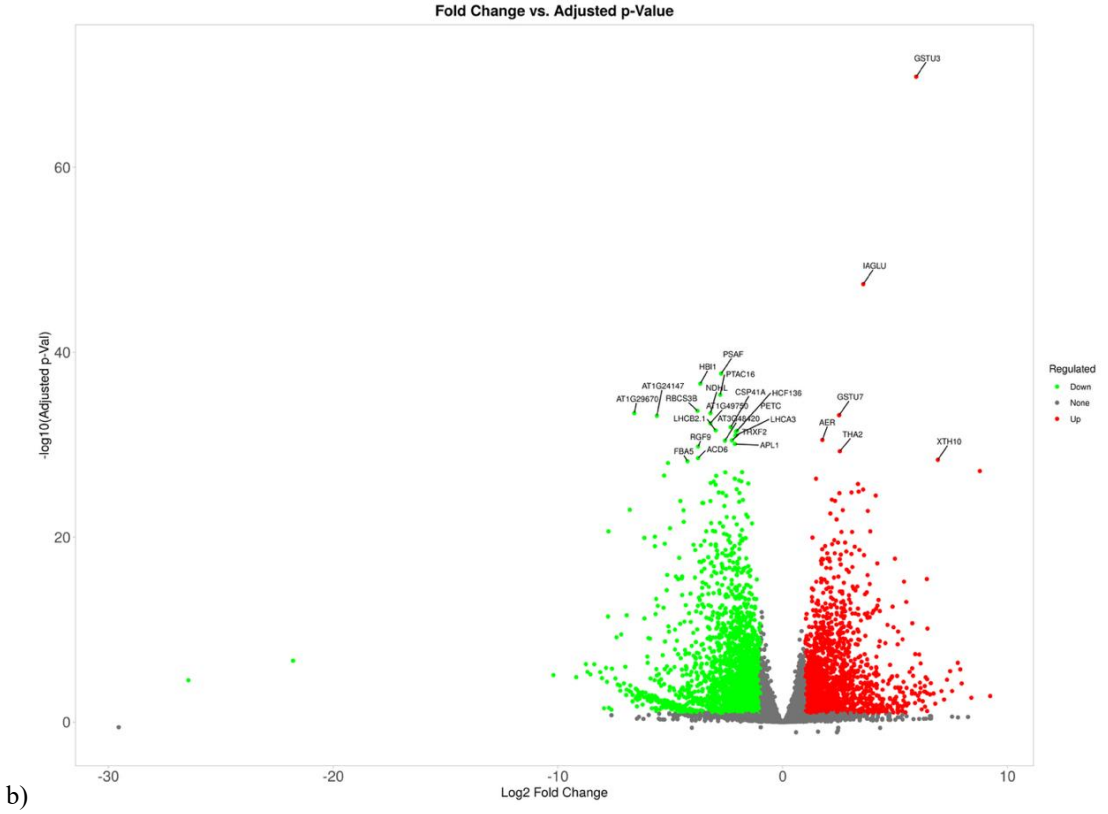

b)

Figure 22: A volcano Plot of the Top 25 Differentially Expressed Genes of Col-0 vs *AT1703* on 0 d.p.i. (a) and 2 d.p.i (b) with an False Discovery Rate (FDR) of $\leq$ 0.01.

The volcano plots in Figure 22 allowed the most significantly upregulated DEGs to be visualised by their adjusted *p*-value (p.adj), allowing the top 25 most significantly up/downregulated DEGs to be displayed. When comparing *AT1703* to Col-0 across the two time points, five DEGs were identified that are linked to functions in plant immunity: *PSEUDORESPONSE REGULATOR-3 (PRR3), ACCELERATED CELL DEATH-6 (ACD6)* and *GLUTATHIONE S-TRANSFERASES U3 AND - U7 (GSTU3* and *GSTU7)*.

Additionally, we noticed there were three highly downregulated outlier DEGs 0 d.p.i, with high log2 fold change but below the < -log10 (p.adj value: 25). These outlier DEGs were: *AT1G05333*, *AT3G44130* and *AT2G22121* (Appendix 7). *AT2G22121* was also highly downregulated 2 d.p.i, along with another outlier DEG *AT1G05523*. The function of these DEGs were investigated, however, apart from *AT3G22121*, *AT1G05523* and *AT3G44130*, most of these outlier genes do not have a characterised function in the *A. thaliana* genome. Furthermore, the functional annotations of *AT3G22121, AT1G05523* and *AT3G44130* were found to lack any established connections to the identified significantly downregulated pathways in *AT1703* 0 d.p.i and 2 d.p.i.

Some of the same DEGs for *AT1703* compared to Col-0 were recorded as being significantly up/downregulated both 0 d.p.i and 2 d.p.i. It was concluded that these genes were not truly being differentially expressed as they were expressed both before and during infection, indicating that they were not being expressed either as a result of transformation with the hairpin or due to infection with *S. sclerotiorum*. Therefore, the inclusion of these genes in further analysis of the identified DEGs would not have accurately represented the expressional differences between *AT1703* and Col-0 before and during infection. Venn diagrams were used to illustrate the number of overlapping DEGs identified for *AT1703* vs Col-0 at time points 0 and 2 (Figure 23), allowing the number genes being consistently up/downregulated across both time points to be visualised.

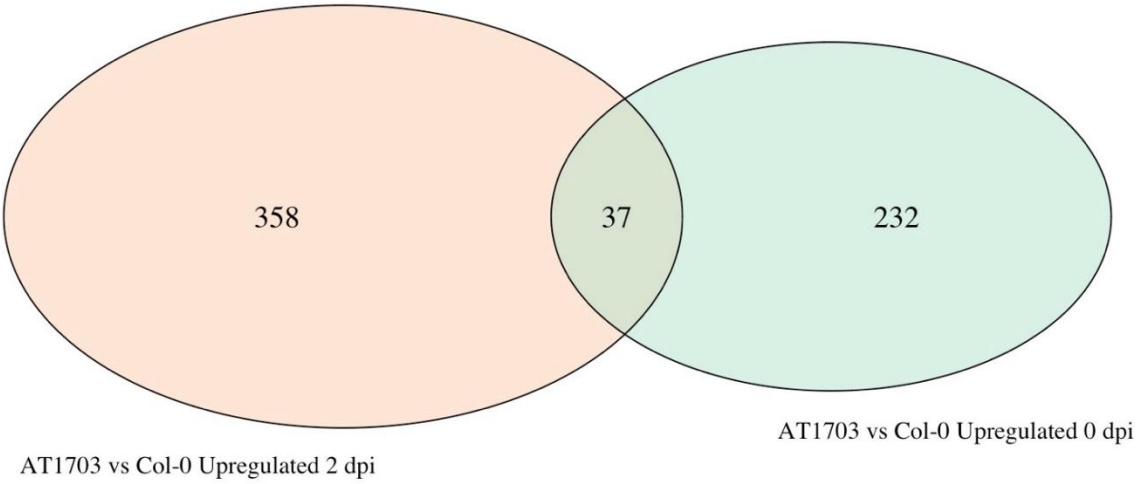

a)

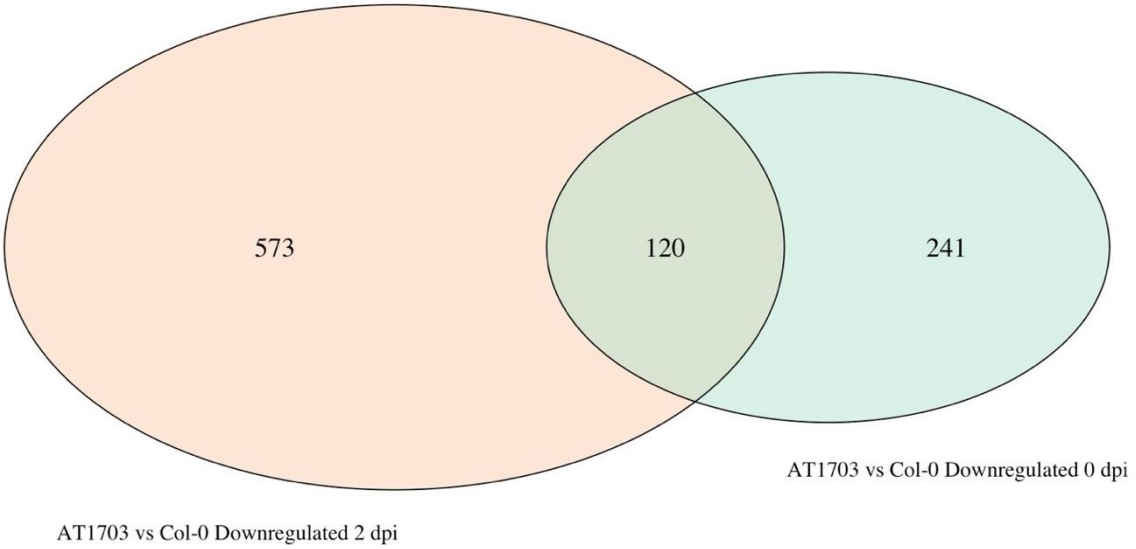

b)

Figure 23: Venn diagrams showing the number of genes being upregulated (a) and downregulated (b) on 0 d.p.i compared to 2 d.p.i. Overlapping regions indicates the number of genes up/downregulated across both time points, if any.

Across the 0-2 d.p.i period, 37 genes were consistently upregulated in *AT1703* compared to Col-0, while 120 genes were consistently downregulated. These genes were removed from the enriched gene list, allowing the genes

that were only differentially expressed at one of the two time points (pre- or post-infection) to be analysed. These remaining DEGs for each time point were counted and recorded (see Table 9).

Table 9: Number of differentially expressed genes (DEGs) being upregulated and downregulated in *AT1703* compared to Col-0, 0 and 2 d.p.i

Time point (d.p.i)	Upregulated	Downregulated
0	232	241
2	358	573

Once identified, the remaining DEGs were then analysed using Gene Ontology (GO) enrichment analysis allowing for the most significantly up/downregulated DEGs to be linked to the pathways shown in the pathways analysis (Figure 24). Combined with the pathways enrichment, GO enrichment analysis provided a multidimensional perspective of the data, by highlighting which genes were transcriptionally active and the specific metabolic pathways they belonged to.

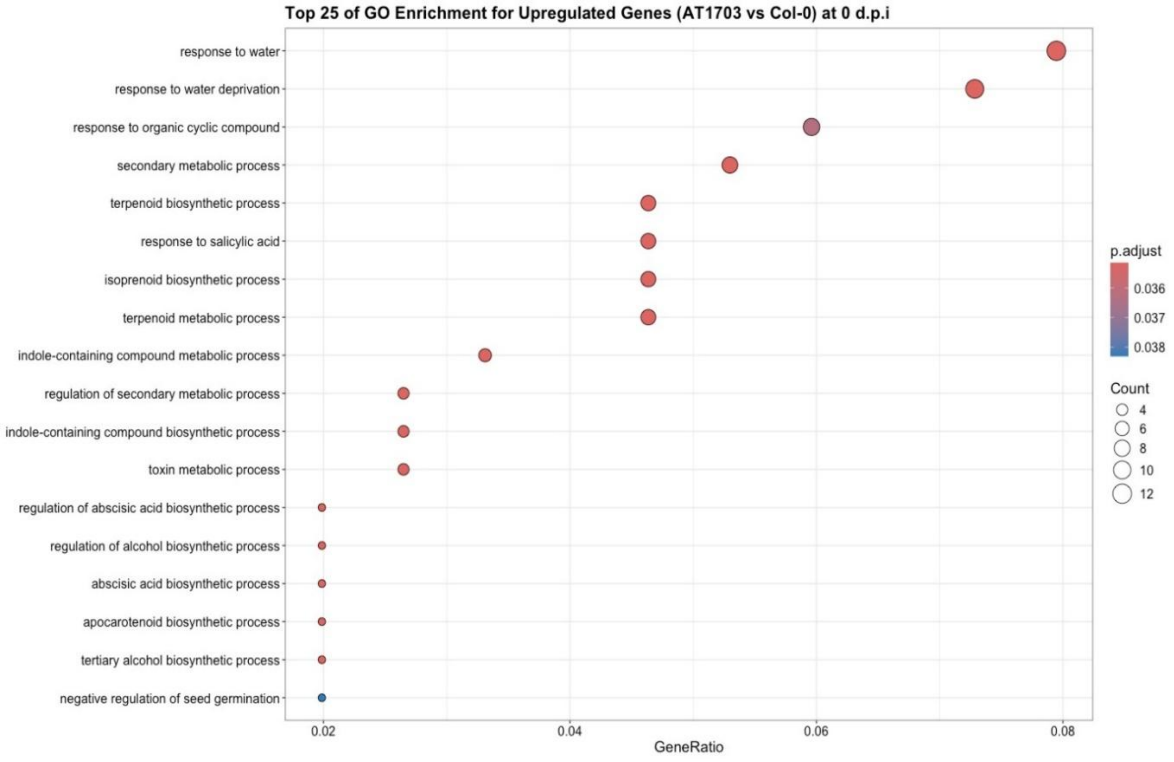
Top 25 of GO Enrichment for Upregulated Genes (AT1703 vs Col-0) at 0 d.p.i
response to water
response to water deprivation
response to organic cyclic compound
secondary metabolic process
terpenoid biosynthetic process
response to salicylic acid
isoprenoid biosynthetic process
terpenoid metabolic process
indole-containing compound metabolic process
regulation of secondary metabolic process
indole-containing compound biosynthetic process
toxin metabolic process
regulation of abscisic acid biosynthetic process
regulation of alcohol biosynthetic process
abscisic acid biosynthetic process
apocarotenoid biosynthetic process
tertiary alcohol biosynthetic process
negative regulation of seed germination
0.02
0.04
0.06
0.08
GeneRatio
p.adjust
0.036
0.037
0.038
Count
4
6
8
10
12

a)

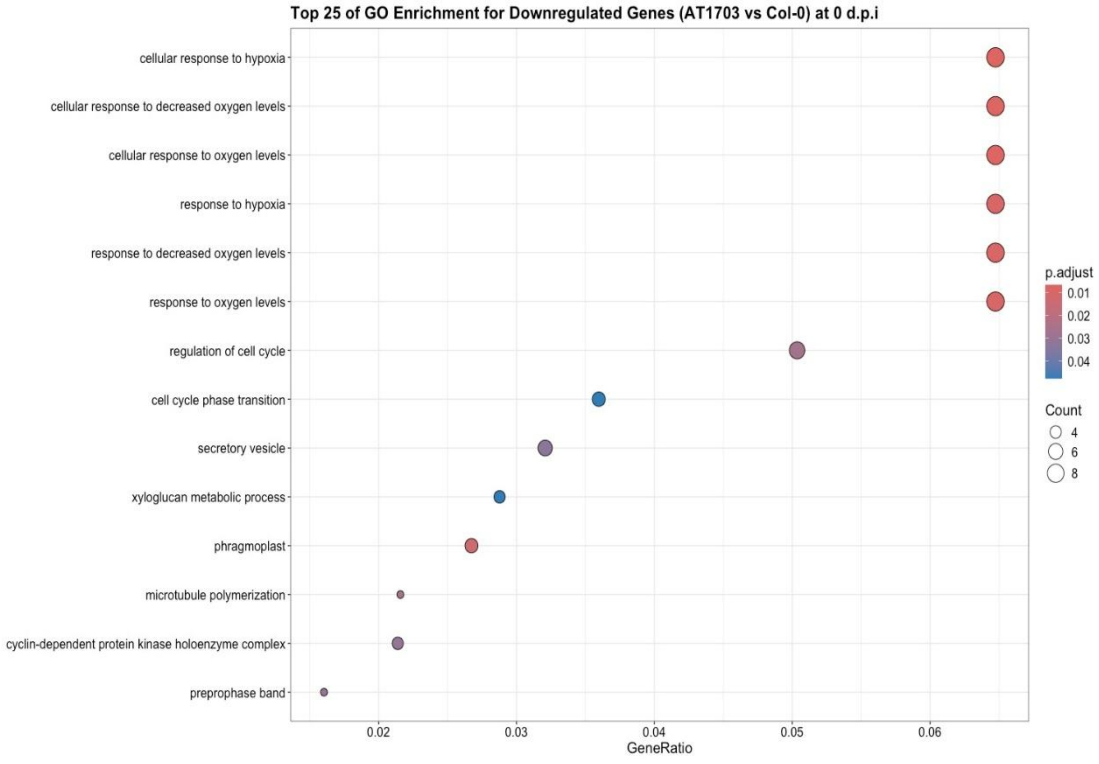
Top 25 of GO Enrichment for Downregulated Genes (AT1703 vs Col-0) at 0 d.p.i
cellular response to hypoxia
cellular response to decreased oxygen levels
cellular response to oxygen levels
response to hypoxia
response to decreased oxygen levels
response to oxygen levels
regulation of cell cycle
cell cycle phase transition
secretory vesicle
xyloglucan metabolic process
phragmoplast
microtubule polymerization
cyclin-dependent protein kinase holoenzyme complex
preprophase band
0.02
0.03
0.04
0.05
0.06
GeneRatio
p.adjust
0.01
0.02
0.03
0.04
Count
4
6
8

b)

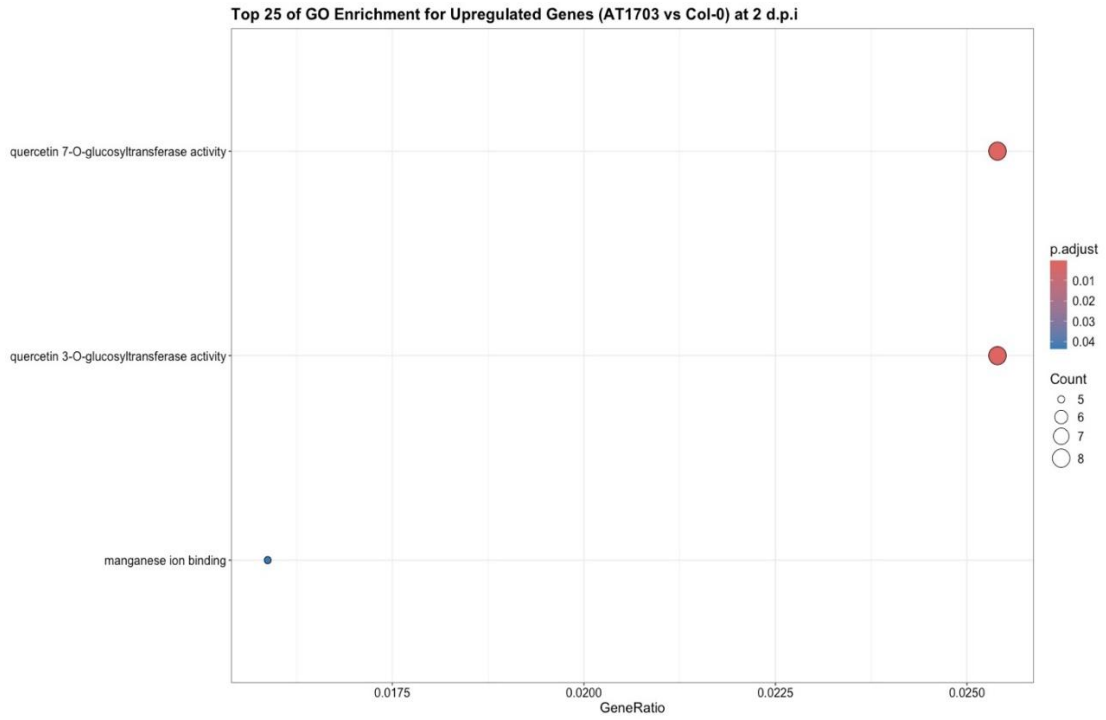

c)

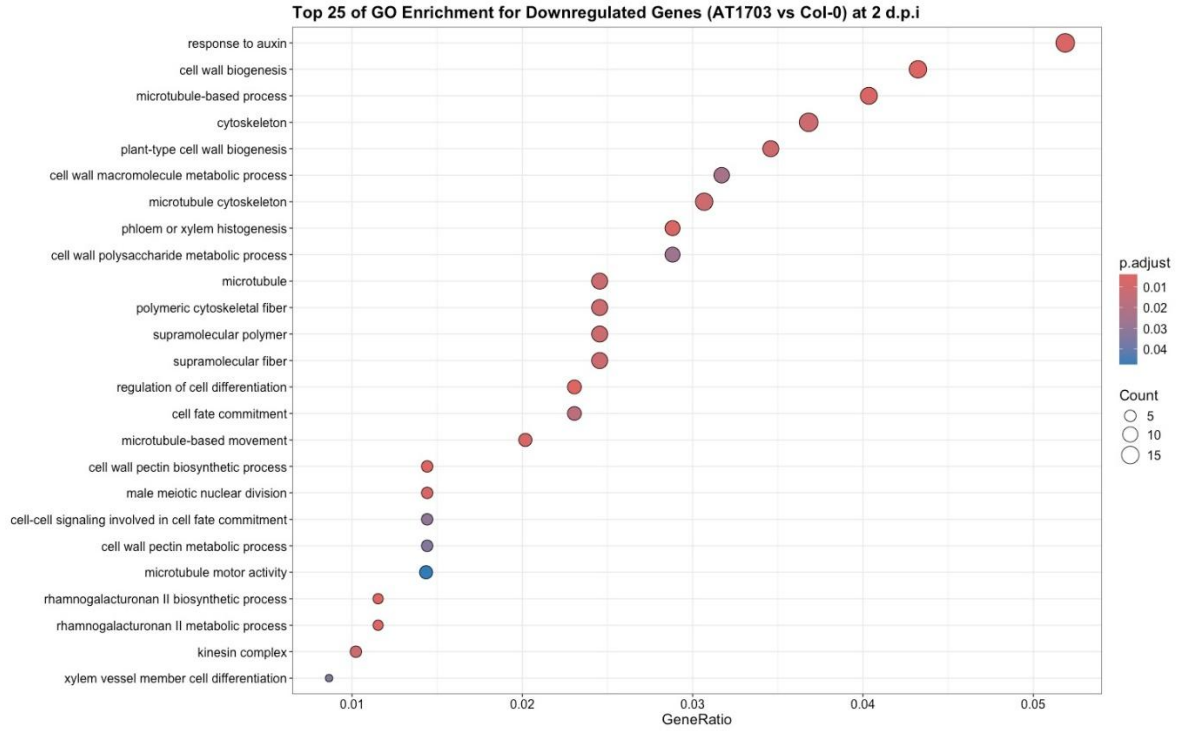

d)

Figure 24: Gene Ontology of the top 25 differentially expressed genes (DEGs) with an adjusted *p*-value of ≤ 0.05 that have been up/downregulated in *AT1703* compared to Col-0 on: 0 d.p.i (a-b) and 2d.p.i (c-d). Dot size corresponds to the gene ratio (number of genes associated with a certain GO term-total number of genes present) belonging to each identified functional category.

As with the pathway enrichment analysis, it appears that, compared to Col-0, *AT1703* significantly upregulated stress related genes even before infection with the fungus and significantly downregulated cell-cycle related genes, on 0 d.p.i. On 2 d.p.i, it appears that most upregulated genes appeared to be associated with one of three GO terms: *Quercetin 7-O-glucosyltransferase* activity, quercetin *3-O-glucosyltransferase* activity or manganese ion binding (Figure 24c). Additionally, large numbers of genes related to growth, auxin signalling, the cell cycle and cell wall biomolecule synthesis were significantly downregulated 2 d.p.i (Figure 24c-d), consistent with the observations made in the pathway enrichment analysis (Figure 21).

5. Discussion

It has been previously reported that nonself RNAs can have a priming effect on baseline immunity in plants (Whitehead *et al.* 2011) leading to improved systemic acquired resistance to invading pathogens (Serrano-Jamaica *et al.* 2021). Previous work in the lab has suggested that GG-*egfp*^{hp}GUS conferred a significant level of protection to infection with *Verticillium dahliae* when it has been stably transformed into *A. thaliana* via floral dipping.

The aim of this project was to design a protocol that could transiently transform *Arabidopsis thaliana* leaves with nonself RNA hairpins targeting the GFP gene and test whether the introduction of the GG-*egfp*^{hp}GUS hairpin could lead to improved local and systemic acquired resistance to the model plant pathogen *Pseudomonas syringae*.

5.1 Headline results

This project successfully achieved disease symptoms from *Pseudomonas syringae* in *Arabidopsis thaliana* in a pathogenicity assay for the first time in the lab. Agroinfiltration was achieved without triggering the plant's defence pathways and T-DNA was detected in recipient leaf tissue through PCR.

The combined infiltration assays, however, showed variable results. The first localised infiltration assay showed that agroinfiltration could be achieved without triggering a defence response, followed by infiltration with *P. syringae* which indicated that introduction of the GG-*egfp*^{hp}GUS does not reduce the amount of leaf damage caused by infection with *P. syringae*, however the results were inconclusive for chlorosis.

The second localised infiltration assay contradicted the findings of the first, as the controls for assaying leaf damage and chlorosis, exhibited disease symptoms after the agroinfiltration step. This confounded the results of the pathogenicity assay with *P. syringae*, as agroinfiltration triggered a hypersensitive response before the pathogen was introduced, demonstrating that even disarmed *Agrobacterium tumefaciens* strains can still elicit an immune response.

Finally, the systemic infiltration assay was inconclusive as disease symptoms were not achieved for *P. syringae* infection, demonstrating that infiltration with concentrated *P. syringae* (OD_{600}: 0.02) does not always lead to successful development of disease symptoms.

Table 10: Summary of the key findings in this project

Experiment	Plants had leaf damage after agroinfiltration?	Plants showed leaf chlorosis after agroinfiltration	Disease symptoms achieved?	Protection hypothesis can be tested?	Protection observed
Disease test	NA	NA	YES	NA	NA
Agroinfiltration test	NO	NO	NA	NA	NA
Localised 1	NO	NO	YES	YES	NO
Localised 2	YES	YES	YES	NO	NA
Systemic 1	NO	YES	NO	NA	NA

5.2 Agroinfiltration of hairpin-carrying *Agrobacterium tumefaciens* into the leaves of Col-0 leads to transient transformation

The results from the agroinfiltration test indicated that agroinfiltration can successfully transform leaves with GG-*egfp*^{hp}GUS. The PCR results showed amplified bands matching the hairpin T-DNA in the DNA extracts from Col-0 leaves that had been agroinfiltrated with the GG-*egfp*^{hp}GUS, GG-*wc1*^{hp}GUS and GG-Kan^{R}GUS hairpins. The results from agroinfiltration assays with hairpin-carrying *Agrobacterium tumefaciens* showed that infiltration can introduce the hairpin vector T-DNA to the recipient leaf tissue. This is in line with findings from previous studies using agroinfiltration methods in *Arabidopsis* and other model species: Wroblewski *et al.* (2005) demonstrated that agroinfiltration of lettuce leaves with suspensions of *A. tumefaciens*, carrying the GUS-exon, with an OD_{600} of 0.3 to 0.8 showed optimal levels of GUS-exon expression 4-10 days post-infiltration. They also noted that penetrability of the leaf tissue greatly impacted the success of agroinfiltration, with *A. thaliana* being easily penetrated by agroinfiltration, going on to demonstrated that Col-0 showed the highest level of transient expression out of all the *Arabidopsis* ecotypes they tested (Wroblewski, Tomczak and Michelmore, 2005). A similar study in *Solanum lycopersicum L.* used agroinfiltration to introduce a construct carrying the GUS exon conjoined to the promotor for the phosphate starvation gene *TRIOSEPHOSPHATE ISOMERASE 1* (TSPI1) to act as a diagnostic tool for phosphate starvation in the plants (Lin *et al.* 2016). Lin *et al.* reported that they successfully induced GUS expression in the leaves of *S. lypoersicum* and expression levels directly correlated with the time spent in phosphate-deficient conditions, making this system a useful diagnostic tool (2016). Additionally, recent

studies with *Tropaeolum majus*, another plant in the *Brassicales* order that is related to *A. thaliana*, demonstrated successful use of agroinfiltration to introduce marker genes such as the luciferase enzyme, the GUS exon and Yellow Fluorescent Protein (YFP) (Pitzschke, 2013b). They concluded that *T. majus* was highly compatible with screening methods for these common marker genes and may be useful in RNAi studies using *A. thaliana*-derived DNA constructs due to the high level of genetic conservation between the two species (Pitzschke, 2013b).

Our results show the hairpin vector T-DNA was present in DNA samples from the leaves, analysed with PCR. It is possible that the detection of the hairpin in the PCR gel was only indicative of the vector-carrying bacteria being present in the leaves. There are no studies that have tested for *Agrobacterium* persistence in the leaves of Col-0 after agroinfiltration, however one study reported that $2.3 \times 10^3 g^{-1}$(f.m.) colony forming units (CFU) of *A. tumefaciens* were isolated from the leaves of agroinfiltrated pakchoi even 9 d.p.i (Xu *et al.* 2008). Additionally, while the PHIRE Plant PCR Kit may not be designed to lyse bacteria, it does contain a dilution buffer designed to lyse plant cell walls, the protocol requires a denaturation step of 98ºC (Thermo Fisher Scientific, Inc, 2014), and the cell walls of bacteria are generally considered to be easier to lyse than those of plant cells. Therefore, as the leaves were taken 5 d.p.i, it is possible that hairpin carrying *A. tumefaciens* were still present when DNA was extracted from the leaves samples, leading to the banding pattern observed in the PCR gel.

The use of PCR to screen for the hairpin's presence in the leaf samples was limited in the sense that it only detected the hairpin's presence in DNA form – it does not indicate if the hairpin sequence has been integrated into the plant's genome or transcribed into dsRNA hairpins. Additionally, as discussed above, the appearance of bands for the hairpin in the PCR gel could have been from residual *A. tumefaciens* present in the leaf tissue. The hairpins were originally designed to be conjoined to marker genes (either the GUS exon or *egfp* gene) which would have provided visual indicators of transgene expression, had the plants been grown from seeds transformed via a stable method of transgene introduction such as floral dipping. The plants used in the combined infiltration assays, however, were wild-type Col-0 that had the hairpins introduced via a localised syringe infiltration method. Our attempts to use GUS-staining on leaves transformed with GG-*egfp*^{hp}GUS showed no signs of the GUS genotype being expressed. As transient expression leads comparatively lower yields of transgenic product in a restricted section of leaf tissue (Garabagi *et al.* 2012; Zhang *et al.* 2020), and it only lasts for 1-7 days in plants (Jones 2003), it is possible that the Col-0 transformed with this method did not express enough T-DNA to produce the levels of the Glucuronidase enzyme needed for the expected blue pigment marker phenotype after GUS staining. This is

consistent with previous literature because, while syringe infiltration can be used to introduce marker genes encoding fluorescent proteins to track different metabolic pathways in *Nicotina benthamiana* (Sparkes *et al.* 2006) Agroinfiltration has been deemed by some as an unsuitable method for species such as *A. thaliana* (Leuzinger *et al.* 2013) due to lower protein yields being expressed from inserted T-DNA (Zheng *et al.* 2021).

In conclusion, the hairpin vector T-DNAs can successfully be introduced into the plant via agroinfiltration and were confirmed to be present in DNA extracts from transformant leaves. Future work should aim to develop a more efficient screening method for hairpin expression and optimise the system to ensure maker gene expression is achieved.

5.3 Infection with *Pseudomonas syringae* via syringe infiltration

Col-0 plants infiltrated with *P. syringae* showed symptoms 5 d.p.i., with the infection originating and spreading from the leaf tissue that the bacteria was introduced into. Our observations are consistent with previous studies looking into *P. syringae-A. thaliana* interaction studies (Boch *et al.* 2002; Ishiga *et al.* 2011; Aung *et al.* 2020; Noh *et al.* 2021; Lee *et al.* 2022; Hu *et al.* 2024) where syringe infiltration was used to introduce the pathogen into the leaves, with the benefit of bypassing the epiphytic phase of *P. syringae*'s lifecycle and introducing the bacteria directly into the intracellular space (Katagiri, Thilmony and He, 2002). Infected Col-0 leaves all showed the characteristic formation of a water-soaked lesion (Katagiri, Thilmony and He, 2002; Munkvold *et al.* 2009) 1 d.p.i, followed by chlorosis of the surrounding tissue (Mittal *et al.* 1995) by 5 d.p.i. Furthermore, the disease symptoms (chlorosis) observed in the *P. syringae*-only disease assays showed that infected Col-0 exhibited significantly higher levels of chlorosis than the mock Col-0 which showed virtually none. This trend was observed both when measured using visual scoring and when measuring the ratio of healthy-to-chlorotic tissue using ImageJ.

The trend between visual scores and healthy-to-chlorotic ratio values indicates that the *P. syringae* infiltrations were successful and significant chlorosis was clearly observed in the infected plants.

5.4 Use of visual scoring compared to analysis with imaging software

The results from *P. syringae* infiltration assays demonstrate that both visual scoring and measuring the % chlorosis using ImageJ provides comparable results when used to measure disease progression in tandem. However, this

combined approach only works if the leaves remain intact by the end of the disease assays. In the combined infiltration assays a significant amount of leaf degradation occurred, so the possibility of using ImageJ to score leaf symptoms was unfeasible, as the leaves had to remain mostly intact to measure their total area. While subjective, on its own, visual scoring can still be a useful measurement: it was widely used in the decades before computational analysis (Whalen *et al.* 1991; Kunkel *et al.* 1993; Adam *et al.* 1996; Volko *et al.* 1998) and steps can be taken to reduce assessor bias and human error (El Jarroudi *et al.* 2015). However, visual assessments are still limited by factors such as: scientific transferability due to their subjectiveness (Mathieu *et al.* 2024), the amount experience and training an assessor has in evaluating disease symptoms (Barbedo 2013; El Jarroudi *et al.* 2015) and the process is still less accurate and prone to human error, even when using standardised scoring systems such as standard area diagrams improve the precision of the data (James 1971; Olmstead *et al.* 2001). The subjective nature of visual assessments means that having reliable computational methods to provide complementary measurements alongside them can be useful to validate subjective results and produce transferrable data. As we observed at the end of our combined infiltrations, visual scoring and computational methods cannot always be used to support the results of one another. Furthermore, our results from our *P. syringae*-only infiltrations demonstrate that a visual scoring system and a computerised image analysis method to compare disease symptoms can produce similar results, something that has been reported before in previous studies (Bock *et al.* 2008; Hernández *et al.* 2022). However, computational methods are not infallible. Digital assessment can be rendered unfeasible due to confounding variables such as leaf degradation, something that has previously been reported in studies using similar digital disease assessment methods (Marques *et al.* 2024). A common confounding variable with digital imaging is image colour and intensity, sometimes making it hard to distinguish infected tissue from healthy tissue, causing digital systems to fail to detect and accurately measure the area of infection (Blanchette, 1982). Later studies have also found that the disease symptoms themselves can confound the results of digital assessments. For instance, infected tissues can appear in various colours, while healthy plant organs naturally vary in colour, making it challenging for digital assessment methods to distinguish between healthy and infected tissue (Chungu *et al.* 1997).

In conclusion, digital and visual assessment methods both have their drawbacks, but when combined, they provided a reliable way to score disease progression in the *P. syringae*-only assays, by using digital assessment to validate the observations made using visual scoring. Had it been possible to visually and digitally assess disease symptoms for the combined infiltration experiments, the precision of the measurements made, and accuracy of

the results could have been improved. Future studies should aim to optimise a digital assessment method which complements visual assessment, while accounting for the confounding effect of factors such as leaf degradation.

5.5 Infiltration of hairpin-carrying *Agrobacterium tumefaciens* did not confer localised resistance to *Pseudomonas syringae*

Transient transformation of Col-0 leaves via agroinfiltration with *Agrobacterium tumefaciens* carrying the GG-*egfp*^{hp}GUS T-DNA vector may not confer localised resistance to infection with *Pseudomonas syringae*.

As shown by our results for our first localised infiltration, we successfully achieved disease symptoms, but the introduction of the hairpin did not provide a protective effect against *P. syringae*. The first localised infiltration experiment clearly indicated that infiltration with *P. syringae* significantly impacted the level of leaf damage exhibited by infiltrated plants, as the GFP.M treatment group, which did not receive any *P. syringae*, showed significantly lower leaf damage compared to those groups that were infected. This indicated that infiltration with *P. syringae* successfully induced disease symptoms. The success of the infection is further supported by the Water. I group, which was infiltrated with MiliQ mixed with sterile infiltration solution followed by *P. syringae*, this group showed statistically similar levels of leaf damage to GFP.I and EHA105.I, the groups that had been infiltrated with both *A. tumefaciens* and *P. syringae*. As each of these treatments had significantly higher leaf damage compared to GFP.M, it can be concluded that the increase in leaf damage was the result of infiltration with *P. syringae*.

Niehl *et al.* (2016) reported a priming effect, where treatment with Poly(I:C) (a dsRNA analog) triggers ethylene accumulation and subsequent upregulation of antiviral pathways in Col-0. It is worth noting, however, that this study also reports variable sensitivity to Poly(I:C) in different *A. thaliana* ascensions, with Col-0 showing a low log-fold change of ethylene production compared to other lines. Furthermore, Lee *et al.* (2016) reported that bacterial derived RNAs had to be intact to elicit an immune response in Col-0, when assaying for PTI responses elicited by treatment with *P. syringae* derived RNAs. This could, in part, explain why this priming effect may not have been triggered in *A. thaliana* when hairpins were introduced via agroinfiltration as T-DNA. There have been several proposed mechanisms of nonself RNA recognition by PRRs in plants: extracellular sensing, endomembrane sensing and intracellular sensing (Niehl *et al.* 2019), so logically, if the T-DNA vectors have successfully integrated the hairpin into the plant cells' genome then the foreign RNA hairpins they encode should

be sensed at some point between its transcription in the nucleus to its translation in the cytosol. However, as there was no reduction in the disease symptoms developed after infection with *P. syringae* in leaves that had been agroinfiltrated with GG-*egfp*^{hp}GUS, it appears that the RNA hairpins were not sensed by the recipient Col-0. This may have been due to the hairpins being degraded into siRNAs before they were sensed by PRRs, and they may not elicit this priming effect in this form, as the siRNA sequences may be too ambiguous to be recognised as non-self. This is a possibility as RNA sensing by PRRs has been shown to occur in a DCL-independent manner (Niehl *et al.* 2016; Das *et al.* 2020; Huang *et al.* 2022) and DCLs 1-4, which are responsible for producing mi- and siRNAs from dsRNA hairpins (Niehl *et al.* 2016), are localised to the nucleus (Schauer *et al.* 2002; Papp *et al.* 2003; Gasciolli *et al.* 2005; Hiraguri *et al.* 2005) which is not a region of the cell that has been proposed to be involved in PRR-mediated recognition of foreign RNAs. Therefore, it is possible the GG-*egfp*^{hp}GUS hairpin may have been broken down into siRNAs by the plant RNAi machinery before being trafficked to a region of the cells where it would otherwise be sensed as a PAMP by the transformed cells. Ultimately, transformation with agroinfiltration was proven to transfer the hairpin T-DNA vectors to *A. thaliana*, and disease symptoms were achieved when infiltrating with *P. syringae* in the first localised infiltrations so the fact that there appeared to be no protective effect conferred by the presence of non-self dsRNAs may not be due to a unsuccessful expression but, instead a lack of detection of the RNA hairpins by the transformant leaves. Alternatively, it is possible that the double-stranded GG-*egfp*^{hp}GUS RNA hairpin does not induce an immune response. This is possible, as a previous study using dsRNAs to target the *cyp3* gene in *Fusarium graminearum* does not elicit the PTI response in *Hordeum vulgare* (Koch *et al.* 2016). Another possibility is that enhanced disease resistance was not observed in Col-0 infiltrated with GG-*egfp*^{hp}GUS as the introduction of the hairpin did not induce an upregulation in any pathways relevant to defence against bacterial pathogens. Previous studies have demonstrated that dsRNA is perceived as a PAMP for the antiviral response (Niehl *et al.* 2016; Niehl *et al.* 2019; Amari *et al.* 2020), however this is a distinctly different pathway from the antibacterial response (Huang *et al.* 2021). Therefore, the introduction of GG-*egfp*^{hp}GUS may have elicited antiviral associated pathways which did not hinder the progress of disease when Col-0 was infected with *P. syringae*.

While the experimental procedures were optimised for each step, the combined infiltration disease assay system developed in this study is limited in terms of reproducibility. In this study, we found that infiltration with *A. tumefaciens* can variably elicit chlorosis. Plants in our second localized infiltration experiment which had been infiltrated with *A. tumefaciens* showed a significantly higher level of chlorosis than plants in the Water.I groups

which only received MiliQ mixed with infiltration solution before they were infected with *P. syringae*. This contrasted with our first localised infiltration experiment, where chlorosis post-agroinfiltration was not observed. Mixed model analysis revealed that the scores obtained for leaf damage and chlorosis, pre-infiltration with *P. syringae*, significantly impacted the variation of the scores obtained post-infiltration. This indicates that symptom scores associated with *A. tumefaciens* infiltrations confounded the results of the *P. syringae* disease assay. It is unclear from our results why *A. tumefaciens* seems to elicit chlorosis in some cases but not others, however *A. tumefaciens* has been reported to variably cause a hypersensitive response in plants. *A. tumefaciens* is known to induce plant defences such as induction of mitogen-activated protein kinases (*MAPK*s), defence gene expression, production of reactive oxygen species (ROS), necrosis of infiltrated tissue and hormonal adjustments (Kuta and Tripathi, 2005; Pitzschke, 2013a) which is a major drawback of methods that utilize it (Raman *et al.* 2022). A study similar to ours, Buscaill *et al.* (2021) used *Nicotina benthamiana* in an combined infiltration protocol which they named the "Agromonas" system. In their study they acknowledge that, despite being non-oncogenic, the strain of *A. tumefaciens* used in this study can still trigger immune responses in *N. benthamiana*, such as cytokinin upregulation, which can confound the results of a disease assay with *P. syringae* (Buscaill *et al.* 2021) as one of the key indicative symptoms of *P. syringae* infiltration is chlorosis, but cytokinin overproduction induced by *A. tumefaciens* can also induce chlorosis in the leaves of *A. thaliana* (Wang *et al.* 2015).

In conclusion, the results of the first localised infiltrations indicated that agroinfiltration of Col-0 leaves with GG-*egfp*^{hp}GUS does not confer protection against *P. syringae*, however the reproducibility of these results is uncertain due to the highly variable results from the repeat experiments. Future work should aim to optimise the agroinfiltration step, to identify the causes of leaf damage and chlorosis 5 d.p.i and adjust the combined infiltration disease assay protocols to limit the impact of these confounding variables.

5.6 Systemic Acquired Resistance to *Pseudomonas syringae* was not observed in Col-0 leaves infiltrated with hairpin-carrying *Agrobacterium tumefaciens*

Disease symptoms were not achieved in the systemic infiltration experiment, as leaves infiltrated with *P. syringae* in all infected treatments (GFP.I, Ctrl.HP.I, Water.I and EHA105.I) did not show significant leaf damage or chlorosis symptoms when compared to the mock inoculated treatment (GFP.M).

Visual inspection of the infiltrated leaves (Appendix 5), showed that most of the samples that were infiltrated with *P. syringae* did not show the expected symptoms of a water-soaked lesion 1 d.p.i followed by chlorosis of the leaves 5 d.p.i. The lack of any symptoms indicates that the infiltration with *P. syringae* was unsuccessful. Post-hoc analysis of both the leaf damage scores and the chlorosis scores showed no significant difference between the average scores for all treatment groups reaffirming the lack of variation in the data.

The insignificant difference between the average leaf damage and chlorosis scores across treatment groups that had only received the infiltration solution prior to infection with *P. syringae* (Water.I) compared to the groups that received both *A. tumefaciens* and *P. syringae,* means that the hypothesis could not be tested in this experiment.

Future work on this project, should ensure the *P.* syringae inoculum is tested for viability before performing the systemic infiltration to ensure disease symptoms are achieved in the leaves 5 d.p.i.

5.7 Use of Host-Induced Gene Silencing to improve *Arabidopsis thaliana* resistance to *Sclerotinia sclerotiorum*

To investigate the baseline transcriptional changes that occur in the host plant when expressing pathogen-targeting RNA hairpins (HIGS), RNASeq data was taken from a study by Walker *et al.* (2023) which compared the response of two *Arabidopsis thaliana* lines to infection with *Sclerotinia sclerotiorum* (white mold), one that was wild-type (Col-0) and a mutant line (*AT1703*) which expressed a hairpin tageting the *Anhydrolase-3* gene. In the study, it was observed that *AT1703* plants were able to mount a more effective response to infection with the fungal pathogen than wild type plants. Walker *et al.*'s (2023) primary focus was the difference in *AT1703* and Col-0's expression profiles, post-infection with *S. sclerotiorum.* They concluded that differences seen on 2-3 d.p.i. caused *AT1703*'s improved resistance to the fungus. However, our results, focussing on 0 d.p.i (pre-infection) and 2 d.p.i, show that the *AT1703* line differs in baseline RNA metabolism from Col-0 even during normal plant metabolism.

We hypothesised that expressing *Anhydrolase-3* targeting RNAi hairpins in *AT1703* plants before infection with *S. sclerotiorum* would shift their expression profiles, delay fungal colonisation and allow for a faster defence response. This would have been reflected in the differentially expressed genes and pathways, with *AT1703* showing an earlier downregulation of auxin-regulated pathways and an earlier upregulation of stress resistance and detoxification pathways. The DEGs analysis supported this hypothesis, as it was observed that

PSEUDORECEPTOR REGULATOR 3 (PRR3) was upregulated on 0 d.p.i. PRR3 interacts with TIMING OF CAB EXPRESSION 1 (TOC1), a circadian-clock associated transcription factor which functions during the evening photoperiod by repressing the CIRCADIAN CLOCK-ASSOCIATED 1 (CCA1) morning photoperiod circadian regulator, with PRR3 maintaining TOC1's stability (Hsu and Harmer, 2014). PRR3 has also been demonstrated to physically associate with TOPLESS (TPLs) and TPL-related transcriptional repressor proteins, potentially forming part of a corepressor complex with TPLs (Wang *et al.* 2013; Li *et al.* 2019). TPLs and TPL-related repressor proteins function in plant immunity to balance the growth-defence trade-off, by complexing with a vast array of other transcription factors to regulate jasmonate and auxin signalling, during stress and immune responses (Saini *et al.* 2022). The fact that PRR3 was upregulated at 0 d.p.i in *AT1703* indicates the plants' stress response pathways had already been induced, requiring TOPLESS and PRR3 to help balance growth with defence pathways. This is consistent with the pathways enrichment analysis which shows the activation of stress and defence-related pathways in *AT1703* at 0 d.p.i. Overexpression of PRR3 has been linked to a delay in flowering time under long-day conditions (Murakami, Yamashino and Mizuno, 2004), however early flowering time is a widely adopted strategy by plants to ensure successful reproduction even under environmental (Kazan *et al.* 2016) and biotic stress (Korves *et al.* 2003). The fact that PRR3 was upregulated at a time when defence and stress related pathways were being upregulated supports our other evidence that the plants had begun to shift their metabolism away from prioritising growth and upregulated their defence pathways even before infection, at 0 d.p.i. However, it is unclear if this early upregulation of defence pathways and downregulation of photosynthesis and growth is caused by the expression of the hairpin or the disruption of native DNA from insertion of the hairpin T-DNA.

Our results for GO pathway analysis 2 d.p.i for *AT1703* shows a significant downregulation in: auxin response, plant growth, the cell cycle and cell wall biomolecule synthesis, following this similar trend of reduced auxin and stunted growth in response to infection, indicating that *AT1703* plants can mount a more effective immune response to *S. sclerotiorum* than Col-0, likely because the plants defence pathways are being upregulated sooner than in Col-0. This is consistent with previously reported literature, as early pathogen detection is important for mounting an effective disease response in plants (Bigini *et al.* 2021). Furthermore, pathogens that evade early detection, have improved virulence in their host. For example: *A. thaliana* perception of *Botrytis cinerea* has been linked to the *RAC FAMILY-7* (*RAC7*) GTPase gene which, when overexpressed, leads to a delay in pathogen perception during infection, enhancing fungal colonisation and even making the *RAC7*-overexpessing (*RAC7-OX*)

lines more susceptible to bacterial infections (García-Soto *et al.* 2024). Another example is *Ralstonia solanacearum*, a gram-negative bacteria, which evades early detection by its host, through use of a Type-III Secretion System (T3SS) to secrete effector molecules into host cells, supressing recognition and response pathways (Chachar *et al.* 2025). Because of its virulence and ability to evade early detection, *R. solanacearum* infects over 310 species of plants, belonging to 42 plant families, causing annual crop yield losses that range from 20 to 100% (Wang *et al.* 2023). Other species such as *P. syringae* use mechanisms such as antigenic variation, secreting the alkaline protease (AprA) enzyme to break down its cell-surface flagellin monomers to evade detection by the *FLS2* receptors (Pel *et al.* 2014; Pascale *et al.* 2020). This was shown by Pel *et al.* (2014) which showed that AprA-deficient strains evoked a significantly higher level of expression of the host defence-related genes *FLG22-INDUCED RECEPTOR-LIKE 1* (*FRK1*) (Yeh *et al.* 2015) and *PATHOGENESIS-RELATED-1* (*PR-1)* (Pape *et al.* 2010) than the wild-type DC3000, demonstrating how the timing of detection by the host plant can improve or reduce *P. syringae*'s virulence during infection. *Xylella fastidiosa* is another pathogen, which primarily infects grapevine, and evades early detection of the pathogen by synthesizing a high molecular weight O-antigen as part of its cell-surface lipopolysaccharides, extending 30 nm away from the cell surface effectively masking the cells from detection by host cell PRRs to delay PTI (Rapicavoli *et al.* 2018). Rapicavoli *et al.* (2018) demonstrates the importance of early detection, as O-antigen deficient (*wzy*) mutant strains of *X. fastidiosa* were detected 8 hours post-infection and elicited the typical antibacterial pathways such as reactive oxygen species (ROS) bursts, activation of salicylic acid (SA)-mediated pathways, and upregulation of pathogenesis-related (PR) genes, whereas wild-type *X. fastidiosa* was not detected until 24 hours post-infection and instead of triggering antibacterial pathways, its colonisation of the xylem triggers abiotic stress pathways such as drought and wounding response pathways, which greatly improved the bacteria's colonisation of the host plant.

In the study by Walker *et al.* (2023), *S. sclerotiorum* may have been detected earlier by *AT1703* because the inhibition of *Anhydrolase-3* impaired its ability to colonise its host. *S. sclerotiorum* is a rapidly progressing disease in the leaf tissue, with symptoms being observed 1-5 d.p.i depending on the host plant (Huang *et al.* 2008; Abuyusuf *et al.* 2018; Xie *et al.* 2023). *S. sclerotiorum* evades early detection by secreting extracellular enzymes such as *Anhydrolase-3*, a phospholipase enzyme which breaks down the cell walls of its host during early infection, making them more permeable to other secreted pathogenicity factors such as oxalic acid (Walker *et al.* 2023). Oxalic acid is a key pathogenicity factor which increases host susceptibility to *S. sclerotiorum* by inhibiting the ROS burst response (Cessna *et al.* 2000) and supressing SA production leading to an overexpression of auxin

(Walker *et al.* 2023). Overexpression of auxin has been linked to susceptibility to various pathogens in different plant species, as it supresses the PTI response (Navarrete *et al.* 2021). As such, auxin modulation is a common mode of attack by various pathogens. For instance, pre-stressing Zea mays seedlings with Bipolaris spp. resulted in high levels of auxin present in the growing plants' tissues, leading to subsequent colonisation by the fungus (Yousaf *et al.* 2021). *Ustilago maydis* is another pathogen which uses auxin modulation, by secreting an effector protein *Naked1* (*Nkd1*) that binds to auxin transcriptional co-repressors TOPLESS/TOPLESS-related (TPL/TPRs) leading to de-repression of auxin in maize plants, increasing host susceptibility to (hemi)biotrophic pathogens (Navarrete *et al.* 2021). Because of the role *Anhydrolase-3* has in auxin modulation, hypothetically *S. sclerotiorum* should have been less able to colonise the invaded tissue in *AT1703* due to the inhibition of pathogens *Anhydrolase-3* by the 1703 RNAi-hairpin (Walker *et al.* 2023). Indeed, their first figure (Figure 20) shows a visible reduction in lesion formation in the leaves of *AT1703* compared to Col-0 (Walker *et al.* 2023). Increased resistance to fungal colonisation by *S. sclerotiorum* in *AT1703* is further supported by the large ratios of genes related to auxin-signalling and auxin-controlled pathways that are being downregulated 2 d.p.i. compared to Col-0. This indicates that the *AT1703* plants detected the pathogen earlier and, in response, shifted their metabolism away from growth, downregulating auxin production and prioritising defence metabolism. A reduction in auxin signalling and pathways is a key plant disease response, as various hosts infected with different pathogens show downregulation of auxin signalling. For example, previous studies with rice plants demonstrated that infection with *Magnaporthe spp.* fungi leads to dwarfism and reduced cell elongation, which was associated with a decrease in auxin biosynthesis gene expression and a significant increase in auxin signalling inhibition related genes (Domingo *et al.* 2009; Jiang *et al.* 2017). Similarly, studies on Clubroot disease (*Plasmodiophora brassicae*) in *Brassica napus* plants carrying clubroot resistance gene *Rcr1* show a significant downregulation of auxin biosynthesis and cell growth, morphogenesis and development, while immunity related pathways controlled by jasmonate and ethylene and other defensive pathways such as deposition of callose and biosynthesis of indole-containing compounds showed a significant upregulation (Chu *et al.* 2014).

On 2-3 d.p.i for Col-0, defence responses in the plant such as: toxin response/detoxification, sulphur and indole metabolism, and glutathione pathways are activated. These pathways are all controlled by JA and ethylene signalling (Zhang *et al.* 2011, 2018; Srivastava *et al.* 2015), which are the phytohormones responsible for controlling responses to necrotrophic fungi (Padmanabhan, Zhang and Jin, 2009; Nguyen, Nguyen and Nguyen, 2024). The expression profile at 2 d.p.i to 3 d.p.i in Col-0 which indicates the plants were mounting a defence

response against a necrotrophic pathogen. This fits with the findings of previous literature, where it was reported that oxalic acid is secreted at low levels during early infection (the biotrophic phase) and is heavily upregulated during late infection (the necrotrophic phase) (Liang *et al.* 2018). This is further supported by results of the pathways analysis from *AT1703* compared to Col-0 from 2 d.p.i onwards which indicates that oxalic acid was being produced in the apoplast by the fungus, as there is a strong upregulation of oxoacid metabolism. The DEGs from the 2 d.p.i timepoint also indicate that the plant is responding to the fungal necrotrophic phase. For example, the ACD6 was downregulated 2 d.p.i. This protein associates with cell surface receptors such as FLS2 and acts as a membrane channel for Ca^{2+} ions, its activity regulated by SA levels within the cell, which are in turn, augmented by Ca^{2+} levels controlled by channels such as ACD6, creating a positive feedback loop potentiating SA signalling in the cell (Lundberg *et al.* 2025). Lundberg *et al.* (2025) also notes that ACD6 hyperactivity in plants leads to a reduction in growth, faster leaf senescence and fewer seeds being produced, leading to an overall reduction in reproductive fitness. ACD6 gain-of-function mutants show an enhanced resistance to *P. syringae* phenotype, along with spontaneous patches of cell death across the leaves, and show a sharp upregulation of defence pathways which require SA as the sole activator or as a crucial coactivator (Rate *et al.* 1999). On 2 d.p.i, ACD6 was downregulated in *AT1703* plants, suggesting a decrease in SA signalling, as this would have led to a decrease in ACD6 expression. (Lu *et al.* 2003; Zhang *et al.* 2014). This is consistent with the pathway analysis as on 2 d.p.i oxoacid metabolism pathways are being upregulated, indicating the plant is responding to oxalic acid present in the infected tissue, which inhibits SA production (Cessna *et al.* 2000; Walker *et al.* 2023), indicating that *AT1703* was successfully infected, and engaged in a host-pathogen crosstalk interaction, with *S. sclerotiorum*.

Hypothetically, if *AT1703* was unable to inhibit *Anhydrolase-3*, then it would be just as susceptible as Col-0 to the inhibitory effect that oxalic acid, secreted by *S. sclerotiorum*, has on salicylic acid, which would cause an upregulation of auxin signalling and a downregulation of stress and detoxification response pathways. However, the DEGs analysis shows a clear upregulation of GSTU3 and GSTU7 at 2 d.p.i indicating that detoxification is being upregulated. GSTU3's specific function has yet to be fully characterised, but broadly speaking GSTs are highly versatile enzymes, which work in detoxification pathways by catalysing the conjugation of xenobiotic glutathione-fatty acids (GSH) to electrophilic compounds forming more soluble peptide derivatives (Labrou *et al.* 2015), which are then sequestered in the vacuoles for further hydrolytic degradation (Cummins *et al.* 2011; Ugalde *et al.* 2021). GSTU7 is better characterised, with recent studies providing evidence that it is often upregulated in response to oxidative stress, characterised by the release of ROS (Ugalde *et al.* 2021). GSTU7 has also been

demonstrated to be induced by an increase of salicylic acid levels in the cells (Sappl *et al.* 2004), and has been observed to be upregulated in *A. thaliana* infected with the fungal pathogen *Alternaria brassicicola*. During infection with *A. brassicicola,* GSTU7 has been reported to be involved in host defence of *A. thaliana* by mediating the catalytic breakdown of the fungal cell wall (Mukherjee *et al.* 2010). Oxalic acid does not directly induce GST production, however it does cause redox imbalances by inducing late-stage ROS bursts (Singh *et al.* 2022), leaching of Ca^{2+} ions from the cell walls (Cessna *et al.* 2000), and programmed cell death (Kim, Min and Dickman, 2008). Each of these processes produce large amounts of secondary ROS as byproducts , which are scavenged by GSTs, including GSTU7 (Ali *et al.* 2024). GSTU3 and -7, which are controlled by SA, were upregulated at 2 d.p.i. when *S. sclerotiorum* likely started producing high levels of oxalic acid, which was taken up by cells in *AT1703* and affected their SA levels. Despite ACD6 inhibition, the cells still maintained SA signalling, indicating that *AT1703* plants were responding to the xenobiotic nature of the oxalic acid. This was further supported by the GO pathway analysis which revealed there was a significant upregulation of genes related to the response to oxoacid and detoxification pathways in *AT1703* compared to the wild-type Col-0 2d.p.i. There was also clearly a downregulation of auxin signalling 2 d.p.i, indicating that *AT1703* plants were able to metabolise and break down the oxalic acid being produced by the *S. sclerotiorum* before it reached a high enough concentration in the cytosol to significantly downregulate salicylic acid production. The results indicated that *AT1703* was still able to properly regulate auxin levels to shift metabolism towards immunity and stress-responses. This is in line with the immunity-growth trade-off described in previous studies, as the downregulation of these specific pathways: growth, auxin signalling, the cell cycle and cell wall biomolecule synthesis related pathways has been reported to be downregulated in favour of immunity-related pathways (Jubault *et al.* 2013; Chu *et al.* 2014; Jiang *et al.* 2017; A. Cao *et al.* 2022).

Further evidence that *AT1703* was able to overcome the effects of oxalic acid and mount an effective immune response to *S. sclerotiorum* is the upregulation of quercetin synthesis at the 2 d.p.i timepoint. Gene Ontology analysis revealed that the most significantly upregulated genes 2 d.p.i fell into one of three categories: *Quercetin 7-O-glucosyltransferase activity, Quercetin 3-O-glucosyltransferase* activity or manganese ion binding. Quercetin is a flavanol; a special subclass of flavonoids (Kim *et al.* 2018), the biosynthesis of which was shown to have been significantly upregulated 3 d.p.i in *AT1703* (Figure 21c). Flavonoids are directly and indirectly involved in various stress and signalling responses in plants (Singh *et al.* 2021). Quercetins, in particular, have been reported to be produced in response to oxidative stress, the release of reactive oxidative species (ROS), which occurs when

tissue homeostasis has been disturbed by factors such as surrounding cells undergoing programmed cell death, or when the plant is undergoing drought stress (Nakabayashi *et al.* 2014). Quercetins mitigate the effects of drought and oxidative stress, improving the host plant's tolerance in overproducing mutant lines of *A. thaliana*, by scavenging ROS in the vacuoles, chloroplast, cytoplasm, mitochondria, and cell wall, before they accumulate and become cytotoxic to plant cells (Junaid Rao *et al.* 2025). At 2 d.p.i with *S. sclerotiorum, AT1703* shows increased production of *Quercetin 3'- and 7'-o-glycosyltransferase enzymes*, which are part of the uridine diphosphate glycosyltransferase (UDP glycosyltransferase-71 or UGT71) class of enzymes which catalyses the transfer of glycan-sugars from activated donor molecules to quercetin, converting it into 3'- and 7'-O-Quercetin glucosides by adding glycosyl groups to the hydroxyl groups at positions 3' and 7' (Yang *et al.* 2024). Glycosylation at the 3'-hydroxyl (OH) position reduces quercetin's antioxidant activity (Magar *et al.* 2020) and changes its solubility, allowing quercetin to be transported from the endoplasmic reticulum (Li *et al.* 2018) to the cell wall (Agati *et al.* 2012). 3-O'-quercetin glucosides are known to be transported to the cell wall via ABC-transporter proteins which competitively blocks auxin transport to the cell walls (Agati *et al.* 2012), something that has been demonstrated to inhibit plant stature (Yin *et al.* 2014; Laoué, Fernandez and Ormeño, 2022). This indicates that the upregulation of glycosylation at the 3'OH and 7'OH positions of quercetins, was indirectly related to the inhibition of growth, allowing *AT1703* plants to switch into its detoxification pathways.

The purpose of the upregulation of manganese binding genes 2 d.p.i remains obscure. Similar studies with hemibiotrophic pathogens, such as *Verticillium dahliae* do report an accumulation of manganese ions, however the role of manganese binding remains unclear (He *et al.* 2022). Studies have shown an increase in manganese and zinc ions, with zinc being used as a defence against invading pathogens (Escudero *et al.* 2020). However, manganese does not seem to have the same cytotoxic effect on fungal pathogens as zinc (De *et al.* 2024). That said, manganese is known to activate enzyme-catalysed reactions including phosphorylation, decarboxylation, reduction and hydrolysis reactions affecting processes such as lignin biosynthesis (Burnell, 1988), which has been identified as a key defence against fungal infection, providing a physical barrier against fungal penetration (Barber *et al.* 1988; Ghazanfar *et al.* 2022). Lignification has been found to be significantly increased in response to *S. sclerotium* infection in various hosts (Oliveira *et al.* 2015; Liu *et al.* 2021; Cao *et al.* 2022), and *A. thaliana* is known to deposit lignin in response to pathogen infections (Liu *et al.* 2018). Therefore, we can hypothesise that lignin may have been deposited in response to infection with *S. sclerotium* in *AT1703* and this may explain the upregulation in manganese ion binding that was observed. However, there was no evidence from the DEGs

analysis that lignin deposition occurred in *AT1703*, so this cannot be concluded from the available data. To further investigate whether lignification was enhanced in *AT1703* compared to Col-0, the disease assay would have to be repeated using appropriate methods to visualise and quantify the level of lignification in infected leaf samples, such as Weisner staining followed by an acetyl bromide assay (Indu *et al.* 2022) or Fourier transform infrared spectroscopy (Le Thanh *et al.* 2017).

As for the outlier DEGs, it is possible that the insertion of the *Anhydrolase-3* targeting hairpin T-DNA disrupted the loci of *AT1G05333*, *AT3G44130* and *AT2G22121*. There have been genetically modified T-DNA insertion lines of *A. thaliana* reported to have inserts transferred from *A. tumefaciens* near the loci containing *AT1G05333* and *AT2G22121* (The Arabidopsis Information Resource (TAIR), 2007; National Center for Biotechnology Information, 2014). Therefore, it is possible that the insertion of the *Anhydrolase-3* targeting hairpin may have inserted near these outlier genes' loci and caused them to be more heavily downregulated in *AT1703* compared to WT (which has not been transformed), hence why they were identified as DEGs.

Walker *et al.* (2023) concluded that the enhanced resistance to *S. sclerotiorum* observed in *AT1703* was due to the expression of the *Anhydrolase-3* targeting hairpin, leading to an improved disease response 2-3 d.p.i. However, the results of our DEGs analysis illustrate that, on 0 d.p.i. (pre-infection), *AT1703* plants showed significant downregulation of photosynthesis and growth-related pathways and significant upregulation of stress response pathways compared to Col-0. The results also showed a significant difference in RNA metabolism in *AT1703* 0 d.p.i compared to Col-0. We concluded that the introduction of the *Anhydrolase-3* targeting hairpin, led to an upregulation of stress tolerance and defence pathways pre-infection in *AT1703*, which may have enhanced their general baseline immunity and contributed to their improved disease response upon infection with *S. sclerotiorum*.

5.8 Use of a strict False Discovery Rate when performing Differentially Expressed Genes analysis

A False Discovery Rate (FDR) describes the proportion of positive results obtained that may be false positives as a percentage of the overall number of results. Usually an FDR is set to 0.05. This would allow for 5% of the positive results to be false positives. However, the number of genes we identified after Variance Stabilizing Transformation (retaining genes with a minimum Counts Per Million of 0.5 and a presence in at least 2 libraries) was 20,233. Given the large size of the data set, an FDR of 0.05 could have led to ~1,012 genes that were not significantly differentially regulated to have been falsely identified as DEGs.

Therefore, a more conservative FDR of 0.01 which only allows for a maximum of 1% of the data to be falsely identified as DEGs, was used to ensure the results of our DEGs analysis represented true biological differences between Col-0 and the *Arabidopsis thaliana 1703 (AT1703)* Host-Induced Gene Silencing RNA-interference hairpin expressing line that was compared in this study.

5.9 The importance of off-target prediction and accounting for similar confounding variables

The outlier DEGs that were observed for top 50 p-adjusted values showed expression levels that fell outside of the range of -10 to 10 $\log_2$ fold change observed for the rest of the data. All outlier DEGs were part of the downregulated genes identified in the dataset. These outliers warranted further scrutiny as they experienced a much higher $\log_2$ fold change compared to the other downregulated DEGs which we believed may have been related to the introduction of the *Anhydrolase-3* hairpin into the *Arabidopsis thaliana* genome at these loci.

It is difficult to say anything conclusive as the function of these DEGs is largely unknown, barring *AT3G22121* and *AT3G44130*, the former of which has a regulatory role in cold acclimation (Tiwari *et al.* 2020) and the latter of which has been partly categorised as an F-box and associated interaction domains containing protein (National Center for Biotechnology Information, 2024), seemingly belonging to the F-box protein family which are involved in various regulatory pathways for photomorphogenesis, circadian clock regulation, self-incompatibility, and floral meristem and floral organ identity determination (Jain *et al.* 2007). However, it is clear that the outlier DEGs are all on chromosomes 1-3, indicating that they may be within neighbouring loci, and the fact that there are known T-DNA insertion lines of *Arabidopsis thaliana* within the loci containing *AT1G05523*, *AT1G05333* and *AT2G22121* (The Arabidopsis Information Resource (TAIR), 2007; National Center for Biotechnology Information, 2014), it is possible that the insertion of the *Anhydrolase-3* targeting RNAi hairpin has disrupted the loci containing these five outlier genes, or their regulatory genes, causing them to appear to be being highly downregulated in *AT1703* compared to Col-0. Since Col-0 was not transformed, if *AT1703* had some frameshift mutations as a result of T-DNA insertion, the expression profiles at these loci may have differed simply because Col-0 did not have these mutations. Future studies can look to verify this by sequencing the *AT1703* genome and looking for T-DNA insertion sites on chromosomes 1-3, and investigate whether these sites are within, or near the loci containing these outlier DEGs.

If the hairpin inserted into the loci of these five outlier genes, then this would highlight the importance of accounting for unintended side-effects on host plant genomes when introduction RNA hairpins for HIGS. While not the exact same thing, it was important in this project to predict any potential matches to the hairpin in both the Col-0 genome and *Verticillium dahliae* genome. Our results showed that, even though there were some predicted off-target matches in the Col-0 genome to the GG-*sge1*^{hp}GUS hairpin, further analysis with BLAST confirmed that this was in a non-coding region of the genome and therefore the hairpin did not bind to any other gene, other than its target. In the case of Walker *et al.* (2023) the only way to determine where in the *A. thaliana* genome the *Anhydrolase-3* hairpin T-DNA inserted into would be through whole genome sequencing of the *AT1703* plants and mapping the T-DNA insertion sites with matching the hairpin. The genome for *AT1703* was not fully sequenced by Walker *et al.* (2023) nor was the sequence of the *Anhydrolase-3* hairpin published, which leaves us unable to confirm whether the hairpin has inserted into or near the loci of the identified outlier DEGs.

Future studies should aim to fully sequence the *AT1703* genome and map the T-DNA insertion points and other unexpected changes to the genome caused by the introduction of the *Anhydrolase-3* hairpin through transformation with *Agrobacterium tumefaciens*. Additionally, future studies should aim to better characterise the functions of *AT1G05523*, *AT1G05333*, *AT3G44130* and *AT2G22121*, investigate why these genes might show heavy downregulation in *AT1703* before and during infection with *S. sclerotiorum* and test whether these genes are heavily downregulated in other hairpin-expressing lines of *A. thaliana* and to see if there's a causal link between hairpin T-DNA insertion and the function of these genes.

6. Conclusion

Our hypothesis was that the transient transformation of the non-self GG-*egfp*^{hp}GUS RNA hairpin into the leaves of *Arabidopsis thaliana* would greatly improve the plants' resistance to infection with *Pseudomonas syringae*. We also hypothesised that stable transformation of the *Anhydrolase-3* targeting RNA-interference hairpin into the genome of *Arabidopsis thaliana* by Walker *et al.* (2023) would cause an upregulation in baseline defence pathway expression, before infection with *Sclerotinia sclerotiorum*, contributing to the previously reported improved disease response observed in the hairpin-expressing *AT1703*.

Our results indicate that transformation via agroinfiltration with the GG-*egfp*^{hp}GUS hairpin does not confer improved localised resistance to infection with *P. syringae* in the leaves of Col-0, though further optimisation of the agroinfiltration and *P. syringae* infiltration steps of our combined infiltration disease assay protocol is required to account for confounding variables such as *A. tumefaciens*-elicited symptoms of leaf damage and chlorosis, pre-infection with *P. syringae*. Further optimisation of the *P. syringae* infiltration steps of our combined infiltration disease assay protocol is required to test whether this method of transient transformation can confer systemic acquired resistance to the pathogen.

Finally, we concluded that stable introduction of *Anhydrolase-3* targeting RNAi-hairpins did appear to induce a shift in the expression profile of *AT1703* compared to that of Col-0 pre-infection with *S. sclerotiorum* and this upregulation of stress and defence related pathways may have contributed to the overall enhanced disease resistance phenotype observed in Walker et al's (2023) study.

Finally, the results from our DEGs and GO pathways analysis expand on the findings of Walker *et al.* (2023) by demonstrating that there is a clear difference between the baseline defence metabolism of the *Anhydrolase-3* hairpin-expressing *AT1703* line of *A. thaliana* compared to Col-0, pre-infection with *S. sclerotiorum*. This difference may have contributed to the enhanced disease resistance phenotype observed for *AT1703* in the original study. Our results support the hypothesis that, not only does the *Anhydrolase-3* targeting RNAi hairpin have the desired effect of reducing the virulence of *S. sclerotiorum* in *AT1703* but that its introduction into the genome may have led to an overall upregulation of plant defence pathways prior to infection, during normal plant metabolism, generally improving the plants' overall resistance to infection.

The significance of this work is such that we have reported successful introduction of the T-DNA vectors for the GG-*egfp*^{hp}GUS, GG-*wc1*^{hp}GUS and GG-Kan^{R}GUS RNAi hairpins into the leaves of *A. thaliana*. Subsequently, the results of our combined infiltration disease assays for localised resistance indicate that agroinfiltration with GG-*egfp*^{hp}GUS T-DNA, does not confer resistance to *P. syringae* in *A. thaliana*. In contrast, our DEGs analysis of the data provided by Walker *et al.* (2023), indicates that stable introduction of RNAi hairpins targeting the *Anhydrolase-3* gene in *S. sclerotiorum* into *A. thaliana,* may induce the upregulation of defence pathways prior to infection, improving the overall response to infection. Overall, our results indicate that transient transformation of *A. thaliana* with RNAi hairpins by agroinfiltration may not confer a comparable level of disease resistance to stable transformation of *A. thaliana* as observed by Walker et al (2023).

The use of RNA-interference to prime *Arabidopsis*, either by stable or transient introduction of RNA hairpins, shows great potential for developing chemical-free methods for pathogen resistance in commercial crop plants. With the rise of antimicrobial resistance, particularly in fungi against fungicides, there is an urgent need for the agricultural sector to develop effective, chemical-free methods for disease mitigation in economically important crops. The appeal of transient transformation over stable methods is that they avoid the need for complicated genetic modification protocols, which are time-consuming, may require expensive specialist equipment and often produce a low yield of transformed seeds. We have observed, in previous our previous research, that *A. thaliana* lines stably transformed with non-specific RNAi-hairpins can potentially improve resistance to *Verticilium dahliae*. If this priming effect can be achieved in a model species such as *A. thaliana* transformed with a transient method of hairpin introduction, such as agroinfiltration, then it may inform future research into the development of transient transformation with RNAi-hairpins as a low-cost, chemical-free method to protect economically important crops from a wide range of pathogens (bacterial, fungal and viral alike). However, this system first needs to be optimised for use in *A. thaliana*. This project lays the groundwork for further optimisation of agroinfiltration to introduce non-pathogen targeting hairpin vector T-DNAs into *A. thaliana* leaves, to induce the upregulation of baseline defence pathways and prime the plant against subsequent infection with a model pathogen such as *P. syringae*.

7. Limitations

Our second localised infiltration results highlight the need for further optimisation of the combined infiltration disease assay protocol to limit the impact of confounding variables and ensure the reproducibility of the results from our first localised infiltration experiment. At present, the reproducibility of our results are limited, as successful introduction of GG-*egfp*^{hp}GUS T-DNA-carrying *Agrobacterium tumefaciens* to the leaves of *Arabidopsis thaliana* was only achieved occasionally and was sporadically accompanied by the presence of confounding variables such as leaf degradation from the emergence of fungus gnat larvae, rot and physical stress from repeat infiltrations as well as premature chlorosis pre-infiltration with *Pseudomonas syringae*. Furthermore, our reliance on PCR screenings to infer whether priming has occurred in *A. thaliana* leaves against *P. syringae* infection, was limited in the sense that we could only detect whether the GG-*egfp*^{hp}GUS T-DNA was present in the leaves – we could not differentiate whether it was from remaining *A. tumefaciens* in the leaves or if it had been integrated into the *A. thaliana* leaf cells' genomes.

To improve the reproducibility of the results, adjustments to the combined infiltration assays could include: a higher number of biological replicates to improve the precision and enhance statistical power of the disease scoring analysis, and injecting the leaves with double-stranded small RNAs derived from the GG-*egfp*^{hp}GUS hairpin, rather than application with *A. tumefaciens* to reduce the likelihood of observing confounding variables such as premature bacterial-induced chlorosis. Additionally, to help better detect whether the introduction of the GG-*egfp*^{hp}GUS in recipient *A. thaliana* leaves led to successful transient transformation, RNASeq could be used 5-days post-infiltration, to detect whether siRNAs derived from the hairpin sequence are present, which would indicate transient expression of the T-DNA vector.

Furthermore, our ability to assess disease progression and severity was limited by the use of visual symptoms, which were easily confounded by the presence of factors such as fungus gnats, rot and perforation damage from the syringe infiltration process. To improve our assessment of disease, after visual scoring of the infiltrated leaves, we could've taken the leaf samples and measured the titre of *P. syringae* present in the infected tissue to see if there was a significant difference between the titre of *P. syringae* bacteria observed between the mock infiltrated groups and the groups infiltrated with the hairpin.

8. References

Abuyusuf, Md. *et al.* (2018) 'Glucosinolate Profiling and Expression Analysis of Glucosinolate Biosynthesis Genes Differentiate White Mold Resistant and Susceptible Cabbage Lines', *International Journal of Molecular Sciences*, 19(12), p. 4037. Available at: https://doi.org/10.3390/ijms19124037.

Ádám, A.L. *et al.* (2018) 'Signals of Systemic Immunity in Plants: Progress and Open Questions', *International Journal of Molecular Sciences*, 19(4), p. 1146. Available at: https://doi.org/10.3390/ijms19041146.

Adam, L. and Somerville, S.C. (1996) 'Genetic characterization of five powdery mildew disease resistance loci in Arabidopsis thaliana', *The Plant Journal*, 9(3), pp. 341–356. Available at: https://doi.org/10.1046/j.1365-313X.1996.09030341.x.

Agati, G. *et al.* (2012) 'Flavonoids as antioxidants in plants: Location and functional significance', *Plant Science*, 196, pp. 67–76. Available at: https://doi.org/10.1016/j.plantsci.2012.07.014.

Ahuja, I., Kissen, R. and Bones, A.M. (2012) 'Phytoalexins in defense against pathogens', *Trends in Plant Science*, 17(2), pp. 73–90. Available at: https://doi.org/10.1016/j.tplants.2011.11.002.

Ali, I. *et al.* (2022) 'Simplified floral dip transformation method of *Arabidopsis thaliana*', *Journal of Microbiological Methods*, 197, p. 106492. Available at: https://doi.org/10.1016/j.mimet.2022.106492.

Ali, Q. *et al.* (2024) 'Antioxidant production promotes defense mechanism and different gene expression level in Zea mays under abiotic stress', *Scientific Reports*, 14, p. 7114. Available at: https://doi.org/10.1038/s41598-024-57939-6.

Altschul, S.F. *et al.* (1990) 'Basic local alignment search tool', *Journal of Molecular Biology*, 215(3), pp. 403–410. Available at: https://doi.org/10.1016/S0022-2836(05)80360-2.

Amari, K. and Niehl, A. (2020) 'Nucleic acid-mediated PAMP-triggered immunity in plants', *Current Opinion in Virology*, 42, pp. 32–39. Available at: https://doi.org/10.1016/j.coviro.2020.04.003.

Arnal Barbedo, J.G. (2013) 'Digital image processing techniques for detecting, quantifying and classifying plant diseases', *SpringerPlus*, 2(1), p. 660. Available at: https://doi.org/10.1186/2193-1801-2-660.

Arnold, D.L. and Preston, G.M. (2019) '*Pseudomonas syringae*: enterprising epiphyte and stealthy parasite', *Microbiology*, 165(3), pp. 251–253. Available at: https://doi.org/10.1099/mic.0.000715.

Aung, K. *et al.* (2020) 'Pathogenic Bacteria Target Plant Plasmodesmata to Colonize and Invade Surrounding Tissues', *The Plant Cell*, 32(3), pp. 595–611. Available at: https://doi.org/10.1105/tpc.19.00707.

Aung, K., Jiang, Y. and He, S.Y. (2018) 'The role of water in plant–microbe interactions', *The Plant Journal*, 93(4), pp. 771–780. Available at: https://doi.org/10.1111/tpj.13795.

Axtell, M.J. and Staskawicz, B.J. (2003) 'Initiation of *RPS2*-Specified Disease Resistance in *Arabidopsis* Is Coupled to the AvrRpt2-Directed Elimination of RIN4', *Cell*, 112(3), pp. 369–377. Available at: https://doi.org/10.1016/S0092-8674(03)00036-9.

Badel, J.L. *et al.* (2006) 'A *Pseudomonas syringae pv.* tomato avrE1/hopM1 Mutant Is Severely Reduced in Growth and Lesion Formation in Tomato', *Molecular Plant-Microbe Interactions®*, 19(2), pp. 99–111. Available at: https://doi.org/10.1094/MPMI-19-0099.

Baker, C.J. *et al.* (2005) 'Involvement of acetosyringone in plant–pathogen recognition', *Biochemical and Biophysical Research Communications*, 328(1), pp. 130–136. Available at: https://doi.org/10.1016/j.bbrc.2004.12.153.

Barber, M.S. and Ride, J.P. (1988) 'A quantitative assay for induced lignification in wounded wheat leaves and its use to survey potential elicitors of the response', *Physiological and Molecular Plant Pathology*, 32(2), pp. 185–197. Available at: https://doi.org/10.1016/S0885-5765(88)80015-8.

Bates, D. (2025) 'lme4: Linear Mixed-Effects Models using "Eigen" and S4'. (v1.1-37). Available at: https://cran.r-project.org/web/packages/lme4/index.html (Accessed: 1 May 2025).

Baudin, M. *et al.* (2017) 'Analysis of the ZAR1 Immune Complex Reveals Determinants for Immunity and Molecular Interactions', *Plant Physiology*, 174(4), pp. 2038–2053. Available at: https://doi.org/10.1104/pp.17.00441.

Béclin, C. *et al.* (2002) 'A Branched Pathway for Transgene-Induced RNA Silencing in Plants', *Current Biology*, 12(8), pp. 684–688. Available at: https://doi.org/10.1016/S0960-9822(02)00792-3.

Bender, C.L., Alarcón-Chaidez, F. and Gross, D.C. (1999) '*Pseudomonas syringae* Phytotoxins: Mode of Action, Regulation, and Biosynthesis by Peptide and Polyketide Synthetases', *Microbiology and Molecular Biology Reviews*, 63(2), pp. 266–292. Available at: https://doi.org/10.1128/mmbr.63.2.266-292.1999.

Benedetti, C.E. and Arruda, P. (2002) 'Altering the expression of the chlorophyllase gene ATHCOR1 in transgenic *Arabidopsis* caused changes in the chlorophyll-to-chlorophyllide ratio', *Plant Physiology*, 128(4), pp. 1255–1263. Available at: https://doi.org/10.1104/pp.010813.

Bentham, A. *et al.* (2017) 'Animal NLRs provide structural insights into plant NLR function', *Annals of Botany*, 119(5), pp. 698–702. Available at: https://doi.org/10.1093/aob/mcw171.

Bigeard, J., Colcombet, J. and Hirt, H. (2015) 'Signaling Mechanisms in Pattern-Triggered Immunity (PTI)', *Molecular Plant*, 8(4), pp. 521–539. Available at: https://doi.org/10.1016/j.molp.2014.12.022.

Bigini, V. *et al.* (2021) 'Biotechnological Resources to Increase Disease-Resistance by Improving Plant Immunity: A Sustainable Approach to Save Cereal Crop Production', *Plants*, 10(6), p. 1146. Available at: https://doi.org/10.3390/plants10061146.

Blanchette, R. (1982) 'New technique to measure tree defect using an image analyzer.', *Plant Disease*, 66(5), pp. 394–397. Available at: https://doi.org/10.1094/PD-66-394.

Boch, J. *et al.* (2002) 'Identification of *Pseudomonas syringae pv.* tomato genes induced during infection of *Arabidopsis thaliana*', *Molecular Microbiology*, 44(1), pp. 73–88. Available at: https://doi.org/10.1046/j.1365-2958.2002.02877.x.

Bock, C.H. *et al.* (2008) 'Visual Rating and the Use of Image Analysis for Assessing Different Symptoms of Citrus Canker on Grapefruit Leaves', *Plant Disease*, 92(4), pp. 530–541. Available at: https://doi.org/10.1094/PDIS-92-4-0530.

Boter, M. *et al.* (2004) 'Conserved MYC transcription factors play a key role in jasmonate signaling both in tomato and Arabidopsis', *Genes & Development*, 18(13), pp. 1577–1591. Available at: https://doi.org/10.1101/gad.297704.

Bråte, J. *et al.* (2018) 'Unicellular Origin of the Animal MicroRNA Machinery', *Current Biology*, 28(20), pp. 3288-3295.e5. Available at: https://doi.org/10.1016/j.cub.2018.08.018.

Burnell, J.N. (1988) 'The Biochemistry of Manganese in Plants', in R.D. Graham, R.J. Hannam, and N.C. Uren (eds) *Manganese in Soils and Plants: Proceedings of the International Symposium on 'Manganese in Soils and Plants' held at the Waite Agricultural Research Institute, The University of Adelaide, Glen Osmond, South*

Australia, August 22–26, 1988 as an Australian Bicentennial Event. Dordrecht: Springer Netherlands (Developments in Plant and Soil Sciences), pp. 125–137. Available at: https://doi.org/10.1007/978-94-009-2817-6_10.

Buscaill, P. *et al.* (2021) 'Agromonas: a rapid disease assay for *Pseudomonas syringae* growth in agroinfiltrated leaves', *The Plant Journal*, 105(3), pp. 831–840. Available at: https://doi.org/10.1111/tpj.15056.

Cao, A. *et al.* (2022) 'Genomics and Pathways Involved in Maize Resistance to Fusarium Ear Rot and Kernel Contamination With Fumonisins', *Frontiers in Plant Science*, 13, p. 866478. Available at: https://doi.org/10.3389/fpls.2022.866478.

Cao, Y. *et al.* (2022) 'Knockout of the lignin pathway gene BnF5H decreases the S/G lignin compositional ratio and improves Sclerotinia sclerotiorum resistance in Brassica napus', *Plant, Cell & Environment*, 45(1), pp. 248–261. Available at: https://doi.org/10.1111/pce.14208.

Caracuel, Z. *et al.* (2005) '*Fusarium oxysporum* gas1 Encodes a Putative β-1, 3-Glucanosyltransferase Required for Virulence on Tomato Plants', *Molecular Plant-Microbe Interactions*®, 18(11), pp. 1140–1147. Available at: https://doi.org/10.1094/MPMI-18-1140.

Carrère, S. *et al.* (2023) 'A fully sequenced collection of homozygous EMS mutants for forward and reverse genetic screens in *Arabidopsis thaliana*'. [Preprint]: bioRxiv, p. 2023.10.26.564234. Available at: https://doi.org/10.1101/2023.10.26.564234.

Catoni, M. *et al.* (2018) 'Virus-mediated export of chromosomal DNA in plants', *Nature Communications*, 9(1), p. 5308. Available at: https://doi.org/10.1038/s41467-018-07775-w.

Cessna, S.G. *et al.* (2000) 'Oxalic Acid, a Pathogenicity Factor for *Sclerotinia sclerotiorum* , Suppresses the Oxidative Burst of the Host Plant', *The Plant Cell*, 12(11), pp. 2191–2199. Available at: https://doi.org/10.1105/tpc.12.11.2191.

Chachar, Z. *et al.* (2025) 'Key mechanisms of plant-*Ralstonia solanacearum* interaction in bacterial wilt pathogenesis', *Frontiers in Microbiology*, 16, p. 1521422. Available at: https://doi.org/10.3389/fmicb.2025.1521422.

Chang, M. *et al.* (2022) 'PTI and ETI: convergent pathways with diverse elicitors', *Trends in Plant Science*, 27(2), pp. 113–115. Available at: https://doi.org/10.1016/j.tplants.2021.11.013.

Chang, S.S. *et al.* (1994) 'Stable genetic transformation of *Arabidopsis thaliana* by *Agrobacterium* inoculation *in planta*', *The Plant Journal*, 5(4), pp. 551–558. Available at: https://doi.org/10.1046/j.1365-313X.1994.05040551.x.

Chaturvedi, R. *et al.* (2012) 'An abietane diterpenoid is a potent activator of systemic acquired resistance', *The Plant Journal*, 71(1), pp. 161–172. Available at: https://doi.org/10.1111/j.1365-313X.2012.04981.x.

Chen, H. *et al.* (2021) 'To Fight or to Grow: The Balancing Role of Ethylene in Plant Abiotic Stress Responses', *Plants*, 11(1), p. 33. Available at: https://doi.org/10.3390/plants11010033.

Cheng, A.-P. *et al.* (2023) 'Extracellular RNAs released by plant-associated fungi: from fundamental mechanisms to biotechnological applications', *Applied Microbiology and Biotechnology*, 107(19), pp. 5935–5945. Available at: https://doi.org/10.1007/s00253-023-12718-7.

Chi, Y. *et al.* (2021) 'Flg22-induced Ca2+ increases undergo desensitization and resensitization', *Plant, Cell & Environment*, 44(12), pp. 3793–3805. Available at: https://doi.org/10.1111/pce.14186.

Chincinska, I.A. (2021) 'Leaf infiltration in plant science: old method, new possibilities', *Plant Methods*, 17(1), p. 83. Available at: https://doi.org/10.1186/s13007-021-00782-x.

Chini, A. *et al.* (2007) 'The JAZ family of repressors is the missing link in jasmonate signalling', *Nature*, 448(7154), pp. 666–671. Available at: https://doi.org/10.1038/nature06006.

Chini, A. *et al.* (2018) 'An OPR3-independent pathway uses 4,5-didehydrojasmonate for jasmonate synthesis', *Nature Chemical Biology*, 14(2), pp. 171–178. Available at: https://doi.org/10.1038/nchembio.2540.

Chu, M. *et al.* (2014) 'Fine mapping of Rcr1 and analyses of its effect on transcriptome patterns during infection by Plasmodiophora brassicae', *BMC Genomics*, 15(1), p. 1166. Available at: https://doi.org/10.1186/1471-2164-15-1166.

Chung, E.-H. *et al.* (2011) 'Specific Threonine Phosphorylation of a Host Target by Two Unrelated Type III Effectors Activates a Host Innate Immune Receptor in Plants', *Cell Host & Microbe*, 9(2), pp. 125–136. Available at: https://doi.org/10.1016/j.chom.2011.01.009.

Chungu, C. *et al.* (1997) 'Assessment of ear rot symptom development in maize hybrids inoculated with *Fusarium graminearum*', *Canadian Journal of Plant Pathology*, 19(4), pp. 390–396. Available at: https://doi.org/10.1080/07060669709501065.

Clay, N.K. *et al.* (2009) 'Glucosinolate Metabolites Required for an Arabidopsis Innate Immune Response', *Science*, 323(5910), pp. 95–101. Available at: https://doi.org/10.1126/science.1164627.

Clough, S.J. and Bent, A.F. (1998) 'Floral dip: a simplified method for *Agrobacterium*-mediated transformation of *Arabidopsis thaliana*', *The Plant Journal: For Cell and Molecular Biology*, 16(6), pp. 735–743. Available at: https://doi.org/10.1046/j.1365-313x.1998.00343.x.

Coursey, T., Regedanz, E. and Bisaro, D.M. (2018) '*Arabidopsis* RNA Polymerase V Mediates Enhanced Compaction and Silencing of Geminivirus and Transposon Chromatin during Host Recovery from Infection', *Journal of Virology*, 92(7), pp. e01320-17. Available at: https://doi.org/10.1128/jvi.01320-17.

Couto, D. and Zipfel, C. (2016) 'Regulation of pattern recognition receptor signalling in plants', *Nature Reviews Immunology*, 16(9), pp. 537–552. Available at: https://doi.org/10.1038/nri.2016.77.

Cui, H., Tsuda, K. and Parker, J.E. (2015) 'Effector-Triggered Immunity: From Pathogen Perception to Robust Defense', *Annual Review of Plant Biology*, 66(2015), pp. 487–511. Available at: https://doi.org/10.1146/annurev-arplant-050213-040012.

Cummins, I. *et al.* (2011) 'Multiple roles for plant glutathione transferases in xenobiotic detoxification', *Drug Metabolism Reviews*, 43(2), pp. 266–280. Available at: https://doi.org/10.3109/03602532.2011.552910.

Cunnac, S., Lindeberg, M. and Collmer, A. (2009) '*Pseudomonas syringae* type III secretion system effectors: repertoires in search of functions', *Current Opinion in Microbiology*, 12(1), pp. 53–60. Available at: https://doi.org/10.1016/j.mib.2008.12.003.

Dalio, R.J.D. *et al.* (2021) 'Hypersensitive response: From NLR pathogen recognition to cell death response', *Annals of Applied Biology*, 178(2), pp. 268–280. Available at: https://doi.org/10.1111/aab.12657.

Das, A. *et al.* (2020) 'Chapter 8 - Genetic transformation', in M. Singh (ed.) *Chickpea: Crop Wild Relatives for Enhancing Genetic Gains*. Academic Press, pp. 205–224. Available at: https://doi.org/10.1016/B978-0-12-818299-4.00008-7.

Das, P.R. and Sherif, S.M. (2020) 'Application of Exogenous dsRNAs-induced RNAi in Agriculture: Challenges and Triumphs', *Frontiers in Plant Science*, 11, p. 946. Available at: https://doi.org/10.3389/fpls.2020.00946.

De, A. *et al.* (2024) 'Combating plant diseases through transition metal allocation', *New Phytologist*, 245(5), pp. 1833–1842. Available at: https://doi.org/10.1111/nph.20366.

Desfeux, C., Clough, S.J. and Bent, A.F. (2000) 'Female reproductive tissues are the primary target of *Agrobacterium*-mediated transformation by the *Arabidopsis* floral-dip method', *Plant Physiology*, 123(3), pp. 895–904. Available at: https://doi.org/10.1104/pp.123.3.895.

Dexheimer, P.J. and Cochella, L. (2020) 'MicroRNAs: From Mechanism to Organism', *Frontiers in Cell and Developmental Biology*, 8, p. 409. Available at: https://doi.org/10.3389/fcell.2020.00409.

Dharmasiri, N., Dharmasiri, S. and Estelle, M. (2005) 'The F-box protein TIR1 is an auxin receptor', *Nature*, 435(7041), pp. 441–445. Available at: https://doi.org/10.1038/nature03543.

Domingo, C. *et al.* (2009) 'Constitutive Expression of OsGH3.1 Reduces Auxin Content and Enhances Defense Response and Resistance to a Fungal Pathogen in Rice', *Molecular Plant-Microbe Interactions®*, 22(2), pp. 201–210. Available at: https://doi.org/10.1094/MPMI-22-2-0201.

Donati, I. *et al.* (2020) '*Pseudomonas syringae pv. actinidiae*: Ecology, Infection Dynamics and Disease Epidemiology', *Microbial Ecology*, 80(1), pp. 81–102. Available at: https://doi.org/10.1007/s00248-019-01459-8.

Du, J. *et al.* (2019) 'Identification of microRNAs regulated by tobacco curly shoot virus co-infection with its betasatellite in *Nicotiana benthamiana*', *Virology Journal*, 16(1), p. 130. Available at: https://doi.org/10.1186/s12985-019-1234-5.

Duanis-Assaf, D. *et al.* (2022) 'Double-stranded RNA targeting fungal ergosterol biosynthesis pathway controls *Botrytis cinerea* and postharvest grey mould', *Plant Biotechnology Journal*, 20(1), pp. 226–237. Available at: https://doi.org/10.1111/pbi.13708.

Dubey, S.M. *et al.* (2023) 'The AFB1 auxin receptor controls the cytoplasmic auxin response pathway in *Arabidopsis thaliana*', *Molecular Plant*, 16(7), pp. 1120–1130. Available at: https://doi.org/10.1016/j.molp.2023.06.008.

El Jarroudi, M. *et al.* (2015) 'A comparison between visual estimates and image analysis measurements to determine septoria leaf blotch severity in winter wheat', *Plant Pathology*, 64(2), pp. 355–364. Available at: https://doi.org/10.1111/ppa.12252.

Ellendorff, U. *et al.* (2009) 'RNA silencing is required for *Arabidopsis* defence against Verticillium wilt disease', *Journal of Experimental Botany*, 60(2), pp. 591–602. Available at: https://doi.org/10.1093/jxb/ern306.

English, J.J. *et al.* (1997) 'Requirement of sense transcription for homology-dependent virus resistance and trans-inactivation', *The Plant Journal*, 12(3), pp. 597–603. Available at: https://doi.org/10.1046/j.1365-313X.1997.00597.x.

Escudero, V. *et al.* (2020) 'Arabidopsis thaliana Zn2+-efflux ATPases HMA2 and HMA4 are required for resistance to the necrotrophic fungus Plectosphaerella cucumerina BMM'. [Preprint]: bioRxiv, p. 2020.08.10.243014. Available at: https://doi.org/10.1101/2020.08.10.243014.

Fahad, M. *et al.* (2025) 'MicroRNA gatekeepers: Orchestrating rhizospheric dynamics', *Journal of Integrative Plant Biology*, 67(3), pp. 845–876. Available at: https://doi.org/10.1111/jipb.13860.

Feldmann, K.A. and David Marks, M. (1987) 'Agrobacterium-mediated transformation of germinating seeds of Arabidopsis thaliana: A non-tissue culture approach', *MGG Molecular & General Genetics*, 208(1–2), pp. 1–9. Available at: https://doi.org/10.1007/BF00330414.

Felix, G. *et al.* (1999) 'Plants have a sensitive perception system for the most conserved domain of bacterial flagellin', *The Plant Journal*, 18(3), pp. 265–276. Available at: https://doi.org/10.1046/j.1365-313X.1999.00265.x.

Fernandez, J.C. and Gilroy, S. (2023) 'Chapter Sixteen - Imaging systemic calcium response and its molecular dissection using virus-induced gene silencing', in J. Jez (ed.) *Methods in Enzymology*. Academic Press (Biochemical Pathways and Environmental Responses in Plants: Part B), pp. 439–459. Available at: https://doi.org/10.1016/bs.mie.2022.08.006.

Friesner, J.D. *et al.* (2025) 'In defense of funding foundational plant science', *The Plant Cell*, 37(5), p. koaf106. Available at: https://doi.org/10.1093/plcell/koaf106.

Fusaro, A.F. *et al.* (2006) 'RNA interference-inducing hairpin RNAs in plants act through the viral defence pathway', *EMBO Reports*, 7(11), pp. 1168–1175. Available at: https://doi.org/10.1038/sj.embor.7400837.

Gallego-Bartolomé, J. *et al.* (2019) 'Co-targeting RNA Polymerases IV and V Promotes Efficient *De Novo* DNA Methylation in *Arabidopsis*', *Cell*, 176(5), pp. 1068-1082.e19. Available at: https://doi.org/10.1016/j.cell.2019.01.029.

Gao, X. *et al.* (2013) 'Bifurcation of Arabidopsis NLR Immune Signaling via Ca2+-Dependent Protein Kinases', *PLoS Pathogens*. Edited by S. He, 9(1), p. e1003127. Available at: https://doi.org/10.1371/journal.ppat.1003127.

Garabagi, F., McLean, M.D. and Hall, J.C. (2012) 'Transient and stable expression of antibodies in *Nicotiana* species', *Methods in Molecular Biology (Clifton, N.J.)*, 907, pp. 389–408. Available at: https://doi.org/10.1007/978-1-61779-974-7_23.

García-Soto, I. *et al.* (2024) 'AtRAC7/ROP9 Small GTPase Regulates *A. thaliana* Immune Systems in Response to *B. cinerea* Infection', *International Journal of Molecular Sciences*, 25(1), p. 591. Available at: https://doi.org/10.3390/ijms25010591.

Gasciolli, V. *et al.* (2005) 'Partially Redundant Functions of *Arabidopsis* DICER-like Enzymes and a Role for DCL4 in Producing *trans*-Acting siRNAs', *Current Biology*, 15(16), pp. 1494–1500. Available at: https://doi.org/10.1016/j.cub.2005.07.024.

Ghazanfar, M.U. *et al.* (2022) 'RELATIONSHIP BETWEEN INDUCED RESISTANCE AND MANGANESE ZINC AND COPPER CONTENTS OF SUSCEPTIBLE CHICKPEA CULTIVARS AFTER THEIR INOCULATION WITH ASCOCHYTA RABIEI', *Pakistan Journal of Phytopathology*, 34(2), pp. 135–145. Available at: https://doi.org/10.33866/phytopathol.034.02.0768.

Gibbs, A.J. *et al.* (2008) 'The Prehistory of Potyviruses: Their Initial Radiation Was during the Dawn of Agriculture', *PLoS ONE*. Edited by B. Lindenbach, 3(6), p. e2523. Available at: https://doi.org/10.1371/journal.pone.0002523.

Gimenez-Ibanez, S. *et al.* (2014) 'The bacterial effector HopX1 targets JAZ transcriptional repressors to activate jasmonate signaling and promote infection in *Arabidopsis*', *PLoS biology*, 12(2), p. e1001792. Available at: https://doi.org/10.1371/journal.pbio.1001792.

Grimsley, N. *et al.* (1986) '"Agroinfection," an alternative route for viral infection of plants by using the Ti plasmid', *Proceedings of the National Academy of Sciences*, 83(10), pp. 3282–3286. Available at: https://doi.org/10.1073/pnas.83.10.3282.

Hartmann, M. *et al.* (2018) 'Flavin Monooxygenase-Generated N-Hydroxypipecolic Acid Is a Critical Element of Plant Systemic Immunity', *Cell*, 173(2), pp. 456-469.e16. Available at: https://doi.org/10.1016/j.cell.2018.02.049.

He, L. *et al.* (2022) 'Advanced genes expression pattern greatly contributes to divergence in Verticillium wilt resistance between *Gossypium barbadense* and *Gossupium hirsutum*', *Frontiers in Plant Science*, 13, p. 979585. Available at: https://doi.org/10.3389/fpls.2022.979585.

Hernández, I. *et al.* (2022) 'Assessment of downy mildew in grapevine using computer vision and fuzzy logic. Development and validation of a new method', *OENO One*, 56(3), pp. 41–53. Available at: https://doi.org/10.20870/oeno-one.2022.56.3.5359.

Hewedy, O.A. *et al.* (2023) 'Jasmonic acid regulates plant development and orchestrates stress response during tough times', *Environmental and Experimental Botany*, 208, p. 105260. Available at: https://doi.org/10.1016/j.envexpbot.2023.105260.

Hiraguri, A. *et al.* (2005) 'Specific interactions between Dicer-like proteins and HYL1/DRB- family dsRNA-binding proteins in *Arabidopsis thaliana*', *Plant Molecular Biology*, 57(2), pp. 173–188. Available at: https://doi.org/10.1007/s11103-004-6853-5.

Hofgen, R. and Willmitzer, L. (1988) 'Storage of competent cells for *Agrobacterium transformation*', *Nucleic Acids Research*, 16(20), pp. 9877–9877. Available at: https://doi.org/10.1093/nar/16.20.9877.

Hsu, P.Y. and Harmer, S.L. (2014) 'Wheels within wheels: the plant circadian system', *Trends in Plant Science*, 19(4), pp. 240–249. Available at: https://doi.org/10.1016/j.tplants.2013.11.007.

Hu, L. *et al.* (2024) 'Ontogenic stage-associated SA response contributes to leaf age-dependent resistance in Arabidopsis and cotton', *Frontiers in Plant Science*, 15, p. 1398770. Available at: https://doi.org/10.3389/fpls.2024.1398770.

Hu, Y. *et al.* (2013) 'Evolution of RNA interference proteins dicer and argonaute in *Basidiomycota*', *Mycologia*, 105(6), pp. 1489–1498. Available at: https://doi.org/10.3852/13-171.

Hu, Y. *et al.* (2022) 'Bacterial effectors manipulate plant abscisic acid signaling for creation of an aqueous apoplast', *Cell Host & Microbe*, 30(4), pp. 518-529.e6. Available at: https://doi.org/10.1016/j.chom.2022.02.002.

Huang, C. *et al.* (2021) 'Suppression of a dsRNA-induced plant immunity pathway by viral movement protein'. [Preprint]: bioRxiv, p. 2021.10.30.466425. Available at: https://doi.org/10.1101/2021.10.30.466425.

Huang, C. *et al.* (2022) 'dsRNA-induced immunity targets plasmodesmata and is suppressed by viral movement proteins'. [Preprint]: bioRxiv, p. 2022.11.21.517408. Available at: https://doi.org/10.1101/2022.11.21.517408.

Huang, J., Yang, M. and Zhang, X. (2016) 'The function of small RNAs in plant biotic stress response', *Journal of Integrative Plant Biology*, 58(4), pp. 312–327. Available at: https://doi.org/10.1111/jipb.12463.

Huang, L. *et al.* (2008) 'Ultrastructural and cytochemical studies on the infection process of *Sclerotinia sclerotiorum* in oilseed rape', *Journal of Plant Diseases and Protection*, 115(1), pp. 9–16. Available at: https://doi.org/10.1007/BF03356233.

Ichinose, Y., Taguchi, F. and Mukaihara, T. (2013) 'Pathogenicity and virulence factors of *Pseudomonas syringae*', *Journal of General Plant Pathology*, 79(5), pp. 285–296. Available at: https://doi.org/10.1007/s10327-013-0452-8.

Indu, M. *et al.* (2022) '"Priming" protects *Piper nigrum L.* from *Phytophthora capsici* through reinforcement of phenylpropanoid pathway and possible enhancement of Piperine biosynthesis', *Frontiers in Plant Science*, 13, p. 1072394. Available at: https://doi.org/10.3389/fpls.2022.1072394.

Ishiga, Y. *et al.* (2011) 'Arabidopsis seedling flood-inoculation technique: a rapid and reliable assay for studying plant-bacterial interactions', *Plant Methods*, 7(1), p. 32. Available at: https://doi.org/10.1186/1746-4811-7-32.

Ishihara, T. *et al.* (2008) 'Overexpression of the *Arabidopsis thaliana* EDS5 gene enhances resistance to viruses', *Plant Biology (Stuttgart, Germany)*, 10(4), pp. 451–461. Available at: https://doi.org/10.1111/j.1438-8677.2008.00050.x.

Iwakawa, H. and Tomari, Y. (2022) 'Life of RISC: Formation, action, and degradation of RNA-induced silencing complex', *Molecular Cell*, 82(1), pp. 30–43. Available at: https://doi.org/10.1016/j.molcel.2021.11.026.

Jackel, J.N. *et al.* (2016) '*Arabidopsis* RNA Polymerases IV and V Are Required To Establish H3K9 Methylation, but Not Cytosine Methylation, on Geminivirus Chromatin', *Journal of Virology*, 90(16), pp. 7529–7540. Available at: https://doi.org/10.1128/JVI.00656-16.

Jacob, F., Vernaldi, S. and Maekawa, T. (2013) 'Evolution and Conservation of Plant NLR Functions', *Frontiers in Immunology*, 4, p. 297. Available at: https://doi.org/10.3389/fimmu.2013.00297.

Jain, M. *et al.* (2007) 'F-Box Proteins in Rice. Genome-Wide Analysis, Classification, Temporal and Spatial Gene Expression during Panicle and Seed Development, and Regulation by Light and Abiotic Stress', *Plant Physiology*, 143(4), pp. 1467–1483. Available at: https://doi.org/10.1104/pp.106.091900.

Jiang, C.-J. *et al.* (2017) 'Stunted Growth Caused by Blast Disease in Rice Seedlings Is Associated with Changes in Phytohormone Signaling Pathways', *Frontiers in Plant Science*, 8, p. Article 1558. Available at: https://doi.org/10.3389/fpls.2017.01558.

Jiménez-Guerrero, I. *et al.* (2022) 'The Rhizobial Type 3 Secretion System: The Dr. Jekyll and Mr. Hyde in the Rhizobium–Legume Symbiosis', *International Journal of Molecular Sciences*, 23(19), p. 11089. Available at: https://doi.org/10.3390/ijms231911089.

Jin, L. *et al.* (2022) 'RNAi-Based Antiviral Innate Immunity in Plants', *Viruses*, 14(2), p. 432. Available at: https://doi.org/10.3390/v14020432.

Jones, H.D. (2003) 'GENETIC MODIFICATION | Transformation, General Principles', in B. Thomas (ed.) *Encyclopedia of Applied Plant Sciences*. Oxford: Elsevier, pp. 377–382. Available at: https://doi.org/10.1016/B0-12-227050-9/00197-6.

Jones, J.D.G. and Dangl, J.L. (2006) 'The plant immune system', *Nature*, 444(7117), pp. 323–329. Available at: https://doi.org/10.1038/nature05286.

Jubault, M. *et al.* (2013) 'Partial resistance to clubroot in Arabidopsis is based on changes in the host primary metabolism and targeted cell division and expansion capacity', *Functional & Integrative Genomics*, 13(2), pp. 191–205. Available at: https://doi.org/10.1007/s10142-013-0312-9.

Junaid Rao, M. *et al.* (2025) 'Antioxidant Defense System in Plants: Reactive Oxygen Species Production, Signaling, and Scavenging During Abiotic Stress-Induced Oxidative Damage', *Horticulturae*, 11, p. 477. Available at: https://doi.org/10.3390/horticulturae11050477.

Kachroo, A. and Kachroo, P. (2020) 'Mobile signals in systemic acquired resistance', *Current Opinion in Plant Biology*, 58, pp. 41–47. Available at: https://doi.org/10.1016/j.pbi.2020.10.004.

Kapila, J. *et al.* (1997) 'An *Agrobacterium*-mediated transient gene expression system for intact leaves', *Plant Science*, 122(1), pp. 101–108. Available at: https://doi.org/10.1016/S0168-9452(96)04541-4.

Katagiri, F., Thilmony, R. and He, S.Y. (2002) 'The *Arabidopsis thaliana-Pseudomonas syringae* Interaction', *The Arabidopsis Book / American Society of Plant Biologists*, 1, p. e0039. Available at: https://doi.org/10.1199/tab.0039.

Kaur, R.P. and Devi, S. (2019) '*In Planta* Transformation in Plants: A Review', *Agricultural Reviews*, 40(3), pp. 159–174. Available at: https://doi.org/10.18805/ag.R-1597.

Kazan, K. and Lyons, R. (2016) 'The link between flowering time and stress tolerance', *Journal of Experimental Botany*, 67(1), pp. 47–60. Available at: https://doi.org/10.1093/jxb/erv441.

Khan, U.M. *et al.* (2022) 'Optimization of Regeneration and Agrobacterium-Mediated Transformation Protocols for Bi and Multilocular Varieties of *Brassica rapa*', *Plants*, 12(1), p. 161. Available at: https://doi.org/10.3390/plants12010161.

Kileeg, Z., Wang, P. and Mott, G.A. (2024) 'Chromosome-Scale Assembly and Annotation of Eight *Arabidopsis thaliana* Ecotypes', *Genome Biology and Evolution*, 16(8), p. evae169. Available at: https://doi.org/10.1093/gbe/evae169.

Kim, C.-Y., Song, H. and Lee, Y.-H. (2022) 'Ambivalent response in pathogen defense: A double-edged sword?', *Plant Communications*, 3(6), p. 100415. Available at: https://doi.org/10.1016/j.xplc.2022.100415.

Kim, J.K. and Park, S.U. (2018) 'Quercetin and its role in biological functions: an updated review', *EXCLI Journal*, 17, pp. 856–863. Available at: https://doi.org/10.17179/excli2018-1538.

Kim, K.S., Min, J.-Y. and Dickman, M.B. (2008) *Oxalic Acid Is an Elicitor of Plant Programmed Cell Death during* Sclerotinia sclerotiorum *Disease Development*, *https://doi.org/10.1094/MPMI-21-5-0605*. The American Phytopathological Society. Available at: https://doi.org/10.1094/MPMI-21-5-0605.

Koch, A. *et al.* (2016) 'An RNAi-Based Control of *Fusarium graminearum* Infections Through Spraying of Long dsRNAs Involves a Plant Passage and Is Controlled by the Fungal Silencing Machinery', *PLOS Pathogens*. Edited by S.P. Dinesh-Kumar, 12(10), p. e1005901. Available at: https://doi.org/10.1371/journal.ppat.1005901.

Koornneef, M. and Meinke, D. (2010) 'The development of *Arabidopsis* as a model plant', *The Plant Journal*, 61(6), pp. 909–921. Available at: https://doi.org/10.1111/j.1365-313X.2009.04086.x.

Korves, T.M. and Bergelson, J. (2003) 'A Developmental Response to Pathogen Infection in Arabidopsis', *Plant Physiology*, 133(1), pp. 339–347. Available at: https://doi.org/10.1104/pp.103.027094.

Köster, P., DeFalco, T.A. and Zipfel, C. (2022) 'Ca2+ signals in plant immunity', *The EMBO Journal*, 41(12), p. e110741. Available at: https://doi.org/10.15252/embj.2022110741.

Kunkel, B.N. *et al.* (1993) 'RPS2, an Arabidopsis disease resistance locus specifying recognition of Pseudomonas syringae strains expressing the avirulence gene avrRpt2.', *The Plant Cell*, 5(8), pp. 865–875. Available at: https://doi.org/10.1105/tpc.5.8.865.

Kurihara, Y. and Watanabe, Y. (2004) '*Arabidopsis* micro-RNA biogenesis through Dicer-like 1 protein functions', *Proceedings of the National Academy of Sciences of the United States of America*, 101(34), pp. 12753–12758. Available at: https://doi.org/10.1073/pnas.0403115101.

Kuta, D. and Tripathi, L. (2005) '*Agrobacterium*-induced hypersensitive necrotic reaction in plant cells: A resistance response against *Agrobacterium*-mediated DNA transfer', *AFRICAN JOURNAL OF BIOTECHNOLOGY*, 4, pp. 752–757.

Labrou, N.E. *et al.* (2015) 'Plant GSTome: structure and functional role in xenome network and plant stress response', *Food Biotechnology • Plant Biotechnology*, 32, pp. 186–194. Available at: https://doi.org/10.1016/j.copbio.2014.12.024.

Lacerda, A. *et al.* (2014) 'Antifungal defensins and their role in plant defense', *Frontiers in Microbiology*, 5. Available at: https://doi.org/10.3389/fmicb.2014.00116.

Laflamme, B. *et al.* (2020) 'The pan-genome effector-triggered immunity landscape of a host-pathogen interaction', *Science*, 367(6479), pp. 763–768. Available at: https://doi.org/10.1126/science.aax4079.

Laibach, F. (1907) 'Zur Frage nach der Individualität der Chromosomen im Pflanzenreich.', *Beihefte zum botanischen Centralblatt* [Preprint]. Available at: https://cir.nii.ac.jp/crid/1370298336630845955.

Laoué, J., Fernandez, C. and Ormeño, E. (2022) 'Plant Flavonoids in Mediterranean Species: A Focus on Flavonols as Protective Metabolites under Climate Stress', *Plants*, 11(2), p. 172. Available at: https://doi.org/10.3390/plants11020172.

Le Thanh, T. *et al.* (2017) 'Salicylic acid-induced accumulation of biochemical components associated with resistance against *Xanthomonas oryzae pv. oryzae* in rice', *Journal of Plant Interactions*, 12(1), pp. 108–120. Available at: https://doi.org/10.1080/17429145.2017.1291859.

Lee, B. *et al.* (2016) 'Bacterial RNAs activate innate immunity in *Arabidopsis*', *New Phytologist*, 209(2), pp. 785–797. Available at: https://doi.org/10.1111/nph.13717.

Lee, D. *et al.* (2015) 'Phosphorylation of the Plant Immune Regulator RPM1-INTERACTING PROTEIN4 Enhances Plant Plasma Membrane H^+-ATPase Activity and Inhibits Flagellin-Triggered Immune Responses in *Arabidopsis*', *The Plant Cell*, 27(7), pp. 2042–2056. Available at: https://doi.org/10.1105/tpc.114.132308.

Lee, R.C., Feinbaum, R.L. and Ambros, V. (1993) 'The C. elegans heterochronic gene *lin-4* encodes small RNAs with antisense complementarity to *lin-14*', *Cell*, 75(5), pp. 843–854. Available at: https://doi.org/10.1016/0092-8674(93)90529-Y.

Lee, S. *et al.* (2022) 'Functional role of formate dehydrogenase 1 (FDH1) for host and nonhost disease resistance against bacterial pathogens', *PLOS ONE*. Edited by R.A. Wilson, 17(5), p. e0264917. Available at: https://doi.org/10.1371/journal.pone.0264917.

Leutwiler, L.S., Hough-Evans, B.R. and Meyerowitz, E.M. (1984) 'The DNA of *Arabidopsis thaliana*', *Molecular and General Genetics MGG*, 194, pp. 15–23. Available at: https://doi.org/10.1007/BF00383491.

Leuzinger, K. *et al.* (2013) 'Efficient Agroinfiltration of Plants for High-level Transient Expression of Recombinant Proteins', *Journal of Visualized Experiments : JoVE*, (77), p. 50521. Available at: https://doi.org/10.3791/50521.

Li, C. *et al.* (2023) 'Involvement of a receptor-like kinase complex of Fv*FLS2* and FvBAK1 in brassinosteroids-induced immunity in postharvest strawberry fruit', *Postharvest Biology and Technology*, 198, p. 112266. Available at: https://doi.org/10.1016/j.postharvbio.2023.112266.

Li, M.-W. *et al.* (2019) 'Characterization of Two Growth Period QTLs Reveals Modification of PRR3 Genes During Soybean Domestication', *Plant and Cell Physiology*, 60(2), pp. 407–420. Available at: https://doi.org/10.1093/pcp/pcy215.

Li, Q. *et al.* (2018) 'Ectopic expression of glycosyltransferase UGT76E11 increases flavonoid accumulation and enhances abiotic stress tolerance in Arabidopsis', *Plant Biology*, 20(1), pp. 10–19. Available at: https://doi.org/10.1111/plb.12627.

Liang, X. and Rollins, J.A. (2018) 'Mechanisms of Broad Host Range Necrotrophic Pathogenesis in *Sclerotinia sclerotiorum*', *Phytopathology* [Preprint]. Available at: https://doi.org/10.1094/PHYTO-06-18-0197-RVW.

Lim, G.-H. *et al.* (2020) 'The plant cuticle regulates apoplastic transport of salicylic acid during systemic acquired resistance', *Science Advances*, 6(19), p. eaaz0478. Available at: https://doi.org/10.1126/sciadv.aaz0478.

Lin, J.-Y. *et al.* (2016) 'Development of an *In Planta* system to monitor phosphorus status by agroinfiltration and agroinjection', *Plant and Soil*, 409(1), pp. 313–328. Available at: https://doi.org/10.1007/s11104-016-2959-1.

Liu, D. *et al.* (2021) 'Overexpression of Cinnamoyl-CoA Reductase 2 in Brassica napus Increases Resistance to Sclerotinia sclerotiorum by Affecting Lignin Biosynthesis', *Frontiers in Plant Science*, 12. Available at: https://doi.org/10.3389/fpls.2021.732733.

Liu, J. *et al.* (2011) 'A Receptor-like Cytoplasmic Kinase Phosphorylates the Host Target RIN4, Leading to the Activation of a Plant Innate Immune Receptor', *Cell Host & Microbe*, 9(2), pp. 137–146. Available at: https://doi.org/10.1016/j.chom.2011.01.010.

Liu, Q., Luo, L. and Zheng, L. (2018) 'Lignins: Biosynthesis and Biological Functions in Plants', *International Journal of Molecular Sciences*, 19(2), p. 335. Available at: https://doi.org/10.3390/ijms19020335.

Lloyd, A.M. *et al.* (1986) 'Transformation of *Arabidopsis thaliana* with *Agrobacterium tumefaciens*', *Science*, 234(4775), pp. 464–466. Available at: https://doi.org/10.1126/science.234.4775.464.

Locci, F. and Parker, J.E. (2024) 'Plant NLR immunity activation and execution: a biochemical perspective', *Open Biology*, 14(1), p. 230387. Available at: https://doi.org/10.1098/rsob.230387.

Lu, H. *et al.* (2003) 'ACD6, a Novel Ankyrin Protein, Is a Regulator and an Effector of Salicylic Acid Signaling in the *Arabidopsis* Defense Response', *The Plant Cell*, 15(10), pp. 2408–2420. Available at: https://doi.org/10.1105/tpc.015412.

Lu, J. *et al.* (2024) 'RIN4 immunity regulators mediate recognition of the core effector RipE1 of Ralstonia solanacearum by the receptor Ptr1', *Plant Physiology*, 197(1), p. kiae514. Available at: https://doi.org/10.1093/plphys/kiae514.

Lück, S. *et al.* (2019) 'siRNA-Finder (si-Fi) Software for RNAi-Target Design and Off-Target Prediction', *Frontiers in Plant Science*, 10. Available at: https://doi.org/10.3389/fpls.2019.01023.

Lundberg, D.S. *et al.* (2025) 'A major trade-off between growth and defense in *Arabidopsis thaliana* can vanish in field conditions', *PLOS Biology*, 23(7), p. e3003237. Available at: https://doi.org/10.1371/journal.pbio.3003237.

Luo, C. *et al.* (2024) 'Plant microRNAs regulate the defense response against pathogens', *Frontiers in Microbiology*, 15. Available at: https://doi.org/10.3389/fmicb.2024.1434798.

Mackey, D. *et al.* (2003) '*Arabidopsis* RIN4 Is a Target of the Type III Virulence Effector AvrRpt2 and Modulates RPS2-Mediated Resistance', *Cell*, 112(3), pp. 379–389. Available at: https://doi.org/10.1016/S0092-8674(03)00040-0.

Magar, R.T. and Sohng, J.K. (2020) 'A Review on Structure, Modifications and Structure-Activity Relation of Quercetin and Its Derivatives', *Journal of Microbiology and Biotechnology*, 30(1), pp. 11–20. Available at: https://doi.org/10.4014/jmb.1907.07003.

Majumdar, R., Rajasekaran, K. and Cary, J.W. (2017) 'RNA Interference (RNAi) as a Potential Tool for Control of Mycotoxin Contamination in Crop Plants: Concepts and Considerations', *Frontiers in Plant Science*, 8. Available at: https://doi.org/10.3389/fpls.2017.00200.

Marc Carlson (2024) ‘GO.db: A set of annotation maps describing the entire Gene Ontology’. Online: Bioconductor. Available at: https://bioconductor.org/packages/GO.db (Accessed: 18 August 2025).

Marques, M.J.M. *et al.* (2024) ‘Plant Doctor: A hybrid machine learning and image segmentation software to quantify plant damage in video footage’. [Preprint]: arXiv. Available at: https://doi.org/10.48550/ARXIV.2407.02853.

Martinez-Trujillo, M. *et al.* (2004) ‘Improving transformation efficiency of *Arabidopsis thaliana* by modifying the floral dip method’, *Plant Molecular Biology Reporter*, 22(1), pp. 63–70. Available at: https://doi.org/10.1007/BF02773350.

Maruri-López, I. *et al.* (2019) ‘Intra and Extracellular Journey of the Phytohormone Salicylic Acid’, *Frontiers in Plant Science*, 10, p. 423. Available at: https://doi.org/10.3389/fpls.2019.00423.

Mathieu, L. *et al.* (2024) ‘SeptoSympto: a precise image analysis of Septoria tritici blotch disease symptoms using deep learning methods on scanned images’, *Plant Methods*, 20, p. 18. Available at: https://doi.org/10.1186/s13007-024-01136-z.

McCann, H.C. *et al.* (2013) ‘Genomic Analysis of the Kiwifruit Pathogen *Pseudomonas syringae pv. actinidiae* Provides Insight into the Origins of an Emergent Plant Disease’, *PLOS Pathogens*, 9(7), p. e1003503. Available at: https://doi.org/10.1371/journal.ppat.1003503.

Meinke, D.W. and Sussex, I.M. (1979) ‘Isolation and characterization of six embryo-lethal mutants of *Arabidopsis thaliana*’, *Developmental Biology*, 72(1), pp. 62–72. Available at: https://doi.org/10.1016/0012-1606(79)90098-8.

Melotto, M. *et al.* (2006) ‘Plant Stomata Function in Innate Immunity against Bacterial Invasion’, *Cell*, 126(5), pp. 969–980. Available at: https://doi.org/10.1016/j.cell.2006.06.054.

Meyerowitz, E.M. and Pruitt, R.E. (1985) ‘*Arabidopsis thaliana* and Plant Molecular Genetics.’, *Science (New York, N.Y.)*, 229(4719), pp. 1214–1218. Available at: https://doi.org/10.1126/science.229.4719.1214.

Mittal, S. and Davis, K.R. (1995) ‘Role of the phytotoxin coronatine in the infection of Arabidopsis thaliana by Pseudomonas syringae pv. tomato’, *Molecular plant-microbe interactions: MPMI*, 8(1), pp. 165–171. Available at: https://doi.org/10.1094/mpmi-8-0165.

Morris, C.E. *et al.* (2019) 'The overlapping continuum of host range among strains in the *Pseudomonas syringae* complex', *Phytopathology Research*, 1(1), p. 4. Available at: https://doi.org/10.1186/s42483-018-0010-6.

Mouyna, I. *et al.* (2005) 'Deletion of GEL2 encoding for a β(1–3)glucanosyltransferase affects morphogenesis and virulence in *Aspergillus fumigatus*', *Molecular Microbiology*, 56(6), pp. 1675–1688. Available at: https://doi.org/10.1111/j.1365-2958.2005.04654.x.

Muhammad, T. *et al.* (2019) 'RNA Interference: A Natural Immune System of Plants to Counteract Biotic Stressors', *Cells*, 8(1), p. 38. Available at: https://doi.org/10.3390/cells8010038.

Mukherjee, A.K. *et al.* (2010) 'Proteomics of the response of *Arabidopsis thaliana* to infection with *Alternaria brassicicola*', *Journal of Proteomics*, 73(4), pp. 709–720. Available at: https://doi.org/10.1016/j.jprot.2009.10.005.

Munkvold, K.R. *et al.* (2009) 'Pseudomonas syringae pv. tomato DC3000 type III effector HopAA1-1 functions redundantly with chlorosis-promoting factor PSPTO4723 to produce bacterial speck lesions in host tomato', *Molecular plant-microbe interactions: MPMI*, 22(11), pp. 1341–1355. Available at: https://doi.org/10.1094/MPMI-22-11-1341.

Murakami, M., Yamashino, T. and Mizuno, T. (2004) 'Characterization of Circadian-Associated APRR3 Pseudo-Response Regulator Belonging to the APRR1/TOC1 Quintet in *Arabidopsis thaliana*', *Plant and Cell Physiology*, 45(5), pp. 645–650. Available at: https://doi.org/10.1093/pcp/pch065.

Nabi, Z. *et al.* (2024) 'Pattern-Triggered Immunity and Effector-Triggered Immunity: crosstalk and cooperation of PRR and NLR-mediated plant defense pathways during host–pathogen interactions', *Physiology and Molecular Biology of Plants*, 30(4), pp. 587–604. Available at: https://doi.org/10.1007/s12298-024-01452-7.

Nagle, M. *et al.* (2018) 'Opportunities for Innovation in Genetic Transformation of Forest Trees', *Frontiers in Plant Science*, 9. Available at: https://doi.org/10.3389/fpls.2018.01443.

Nakabayashi, R. *et al.* (2014) 'Enhancement of oxidative and drought tolerance in Arabidopsis by overaccumulation of antioxidant flavonoids', *The Plant Journal*, 77(3), pp. 367–379. Available at: https://doi.org/10.1111/tpj.12388.

Nakano, Y. (2017) ‘Effect of Acetosyringone on *Agrobacterium*-mediated Transformation of *Eustoma grandiflorum* Leaf Disks’, *Japan Agricultural Research Quarterly: JARQ*, 51(4), pp. 351–355. Available at: https://doi.org/10.6090/jarq.51.351.

National Center for Biotechnology Information (2014) ‘SALKseq_047059.2 Arabidopsis thaliana TDNA insertion lines - TDNA_seq Arabidopsis thaliana genomic clone SALK_047059, genomic survey sequence’. Available at: http://www.ncbi.nlm.nih.gov/nuccore/KO368438.1 (Accessed: 8 July 2025).

National Center for Biotechnology Information (2024) *F-box and associated interaction domains-containing protein [Arabidopsis thaliana (thale cress)] - Gene - NCBI*, *Gene[Internet]*. Available at: https://www.ncbi.nlm.nih.gov/gene/823534 (Accessed: 8 July 2025).

Návarová, H. *et al.* (2012) ‘Pipecolic Acid, an Endogenous Mediator of Defense Amplification and Priming, Is a Critical Regulator of Inducible Plant Immunity’, *The Plant Cell*, 24(12), pp. 5123–5141. Available at: https://doi.org/10.1105/tpc.112.103564.

Navarrete, F. *et al.* (2021) ‘TOPLESS promotes plant immunity by repressing auxin signaling and is targeted by the fungal effector Naked1’, *Plant Communications*, 3(2), p. 100269. Available at: https://doi.org/10.1016/j.xplc.2021.100269.

Navarro, L. *et al.* (2006) ‘A Plant miRNA Contributes to Antibacterial Resistance by Repressing Auxin Signaling’, *Science*, 312(5772), pp. 436–439. Available at: https://doi.org/10.1126/science.1126088.

Necira, K. *et al.* (2024) ‘Comparative analysis of RNA interference and pattern-triggered immunity induced by dsRNA reveals different efficiencies in the antiviral response to potato virus X’, *Molecular Plant Pathology*, 25(9), p. e70008. Available at: https://doi.org/10.1111/mpp.70008.

Ngou, B.P.M. *et al.* (2021) ‘Mutual potentiation of plant immunity by cell-surface and intracellular receptors’, *Nature*, 592(7852), pp. 110–115. Available at: https://doi.org/10.1038/s41586-021-03315-7.

Nguyen, N.H. *et al.* (2022) ‘Camalexin accumulation as a component of plant immunity during interactions with pathogens and beneficial microbes’, *Planta*, 255(6), p. 116. Available at: https://doi.org/10.1007/s00425-022-03907-1.

Nguyen, N.H., Nguyen, H.D. and Nguyen, T. (2024) 'Roles of phytohormones in regulation of plant immunity against pathogens', *South Asian Journal of Agricultural Sciences*, 4(1), pp. 222–226. Available at: https://doi.org/10.22271/27889289.2024.v4.i1c.132.

Niehl, A. *et al.* (2016) 'Double-stranded RNAs induce a pattern-triggered immune signaling pathway in plants', *New Phytologist*, 211(3), pp. 1008–1019. Available at: https://doi.org/10.1111/nph.13944.

Niehl, A. and Heinlein, M. (2019) 'Perception of double-stranded RNA in plant antiviral immunity', *Molecular Plant Pathology*, 20(9), pp. 1203–1210. Available at: https://doi.org/10.1111/mpp.12798.

Noh, S.W. *et al.* (2021) 'Two Arabidopsis Homologs of Human Lysine-Specific Demethylase Function in Epigenetic Regulation of Plant Defense Responses', *Frontiers in Plant Science*, 12, p. 688003. Available at: https://doi.org/10.3389/fpls.2021.688003.

Norkunas, K. *et al.* (2018) 'Improving agroinfiltration-based transient gene expression in *Nicotiana benthamiana*', *Plant Methods*, 14(1), p. 71. Available at: https://doi.org/10.1186/s13007-018-0343-2.

Nosaki, S. and Miura, K. (2021) 'Chapter Nine - Transient expression of recombinant proteins in plants', in W.B. O'Dell and Z. Kelman (eds) *Methods in Enzymology*. Academic Press (Recombinant Protein Expression: Eukaryotic Hosts), pp. 193–203. Available at: https://doi.org/10.1016/bs.mie.2021.04.021.

Obbard, D.J. *et al.* (2009) 'The evolution of RNAi as a defence against viruses and transposable elements', *Philosophical Transactions of the Royal Society B: Biological Sciences*, 364(1513), pp. 99–115. Available at: https://doi.org/10.1098/rstb.2008.0168.

O'Brien, H.E. *et al.* (2012) 'Extensive remodeling of the *Pseudomonas syringae pv. avellanae* type III secretome associated with two independent host shifts onto hazelnut', *BMC Microbiology*, 12(1), p. 141. Available at: https://doi.org/10.1186/1471-2180-12-141.

Oliveira, M.B. *et al.* (2015) 'Analysis of genes that are differentially expressed during the Sclerotinia sclerotiorum–Phaseolus vulgaris interaction', *Frontiers in Microbiology*, 6, p. 1162. Available at: https://doi.org/10.3389/fmicb.2015.01162.

Olmstead, J.W., Lang, G.A. and Grove, G.G. (2001) 'Assessment of Severity of Powdery Mildew Infection of Sweet Cherry Leaves by Digital Image Analysis', *HortScience*, 36(1), pp. 107–111. Available at: https://doi.org/10.21273/HORTSCI.36.1.107.

Padmanabhan, C., Zhang, X. and Jin, H. (2009) 'Host small RNAs are big contributors to plant innate immunity', *Current Opinion in Plant Biology*, 12(4), pp. 465–472. Available at: https://doi.org/10.1016/j.pbi.2009.06.005.

Pape, S., Thurow, C. and Gatz, C. (2010) 'The *Arabidopsis* PR-1 Promoter Contains Multiple Integration Sites for the Coactivator NPR1 and the Repressor SNI1', *Plant Physiology*, 154(4), pp. 1805–1818. Available at: https://doi.org/10.1104/pp.110.165563.

Papp, I. *et al.* (2003) 'Evidence for Nuclear Processing of Plant Micro RNA and Short Interfering RNA Precursors', *Plant Physiology*, 132(3), pp. 1382–1390. Available at: https://doi.org/10.1104/pp.103.021980.

Park, S.-W. *et al.* (2007) 'Methyl Salicylate Is a Critical Mobile Signal for Plant Systemic Acquired Resistance', *Science*, 318(5847), pp. 113–116. Available at: https://doi.org/10.1126/science.1147113.

Pascale, A. *et al.* (2020) 'Modulation of the Root Microbiome by Plant Molecules: The Basis for Targeted Disease Suppression and Plant Growth Promotion', *Frontiers in Plant Science*, 10, p. 1741. Available at: https://doi.org/10.3389/fpls.2019.01741.

Pel, M.J.C. *et al.* (2014) '*Pseudomonas syringae* Evades Host Immunity by Degrading Flagellin Monomers with Alkaline Protease AprA', *Molecular Plant-Microbe Interactions®*, 27(7), pp. 603–610. Available at: https://doi.org/10.1094/MPMI-02-14-0032-R.

Philip L. Walker *et al.* (2023) 'Control of white mold (*Sclerotinia sclerotiorum*) through plant-mediated RNA interference', *Scientific Reports*, 13(1), p. 6477. Available at: https://doi.org/10.1038/s41598-023-33335-4.

Pitzschke, A. (2013a) '*Agrobacterium* infection and plant defense—transformation success hangs by a thread', *Frontiers in Plant Science*, 4. Available at: https://doi.org/10.3389/fpls.2013.00519.

Pitzschke, A. (2013b) '*Tropaeolum* Tops Tobacco – Simple and Efficient Transgene Expression in the Order *Brassicales*', *PLoS ONE*. Edited by J.-H. Liu, 8(9), p. e73355. Available at: https://doi.org/10.1371/journal.pone.0073355.

Pooggin, M. (2013) 'How Can Plant DNA Viruses Evade siRNA-Directed DNA Methylation and Silencing?', *International Journal of Molecular Sciences*, 14(8), pp. 15233–15259. Available at: https://doi.org/10.3390/ijms140815233.

Pougy, K.C. *et al.* (2025) 'Phase separation as a key mechanism in plant development, environmental adaptation, and abiotic stress response', *The Journal of Biological Chemistry*, 301(6), p. 108548. Available at: https://doi.org/10.1016/j.jbc.2025.108548.

Pride, L., Vallad, G. and Agehara, S. (2020) 'How to Measure Leaf Disease Damage Using Image Analysis in ImageJ: HS1382, 9/2020', *EDIS*, 2020(5). Available at: https://doi.org/10.32473/edis-hs1382-2020.

Qamar, F. *et al.* (2022) 'Germline transformation of *Artemisia annuaL.* plant via in planta transformation technology "Floral dip"', *Biotechnology Reports*, 36, p. e00761. Available at: https://doi.org/10.1016/j.btre.2022.e00761.

Qi, D. and Innes, R.W. (2013) 'Recent Advances in Plant NLR Structure, Function, Localization, and Signaling', *Frontiers in Immunology*, 4. Available at: https://doi.org/10.3389/fimmu.2013.00348.

Raman, V. *et al.* (2022) 'Agrobacterium expressing a type III secretion system delivers Pseudomonas effectors into plant cells to enhance transformation', *Nature Communications*, 13(1), p. 2581. Available at: https://doi.org/10.1038/s41467-022-30180-3.

Rapicavoli, J.N. *et al.* (2018) 'Lipopolysaccharide O-antigen delays plant innate immune recognition of *Xylella fastidiosa*', *Nature Communications*, 9(1), p. 390. Available at: https://doi.org/10.1038/s41467-018-02861-5.

Rate, D.N. *et al.* (1999) 'The gain-of-function *Arabidopsis* acd6 mutant reveals novel regulation and function of the salicylic acid signaling pathway in controlling cell death, defenses, and cell growth.', *The Plant cell*, 11(9), pp. 1695–1708. Available at: https://doi.org/10.1105/tpc.11.9.1695.

Ratu, S.T.N. *et al.* (2021) 'Multiple Domains in the Rhizobial Type III Effector Bel2-5 Determine Symbiotic Efficiency With Soybean', *Frontiers in Plant Science*, 12. Available at: https://doi.org/10.3389/fpls.2021.689064.

Rekhter, D. *et al.* (2019) 'Isochorismate-derived biosynthesis of the plant stress hormone salicylic acid', *Science (New York, N.Y.)*, 365(6452), pp. 498–502. Available at: https://doi.org/10.1126/science.aaw1720.

Saini, R. and Nandi, A.K. (2022) 'TOPLESS in the regulation of plant immunity', *Plant Molecular Biology*, 109(1), pp. 1–12. Available at: https://doi.org/10.1007/s11103-022-01258-9.

Saleem, M., Fariduddin, Q. and Castroverde, C.D.M. (2021) 'Salicylic acid: A key regulator of redox signalling and plant immunity', *Plant Physiology and Biochemistry*, 168, pp. 381–397. Available at: https://doi.org/10.1016/j.plaphy.2021.10.011.

Sappl, P.G. *et al.* (2004) 'Proteomic Analysis of Glutathione S-Transferases of *Arabidopsis thaliana* Reveals Differential Salicylic Acid-Induced Expression of the Plant-Specific Phi and Tau Classes', *Plant Molecular Biology*, 54(2), pp. 205–219. Available at: https://doi.org/10.1023/B:PLAN.0000028786.57439.b3.

Schauer, S.E. *et al.* (2002) 'DICER-LIKE1: blind men and elephants in *Arabidopsis* development', *Trends in Plant Science*, 7(11), pp. 487–491. Available at: https://doi.org/10.1016/S1360-1385(02)02355-5.

Schöb, H., Kunz, C. and Meins Jr., F. (1997) 'Silencing of transgenes introduced into leaves by agroinfiltration: a simple, rapid method for investigating sequence requirements for gene silencing', *Molecular and General Genetics MGG*, 256(5), pp. 581–585. Available at: https://doi.org/10.1007/s004380050604.

Schott, A. and Strahl, S. (2011) 'Chapter Seventeen - Methods to Study Stromal-Cell Derived Factor 2 in the Context of ER Stress and the Unfolded Protein Response in *Arabidopsis thaliana*', in P.M. Conn (ed.) *Methods in Enzymology*. Academic Press (The Unfolded Protein Response and Cellular Stress, Part B), pp. 295–319. Available at: https://doi.org/10.1016/B978-0-12-385114-7.00017-9.

Schweizer, F. *et al.* (2013) 'Arabidopsis Basic Helix-Loop-Helix Transcription Factors MYC2, MYC3, and MYC4 Regulate Glucosinolate Biosynthesis, Insect Performance, and Feeding Behavior[W][OPEN]', *The Plant Cell*, 25(8), pp. 3117–3132. Available at: https://doi.org/10.1105/tpc.113.115139.

Serrano-Jamaica, L.M. *et al.* (2021) 'Effect of Fragmented DNA From Plant Pathogens on the Protection Against Wilt and Root Rot of Capsicum annuum L. Plants', *Frontiers in Plant Science*, 11. Available at: https://doi.org/10.3389/fpls.2020.581891.

Seybold, H. *et al.* (2014) 'Ca2+ signalling in plant immune response: from pattern recognition receptors to Ca2+ decoding mechanisms', *New Phytologist*, 204(4), pp. 782–790. Available at: https://doi.org/10.1111/nph.13031.

Shabalina, S.A. and Koonin, E.V. (2008) 'Origins and evolution of eukaryotic RNA interference', *Trends in ecology & evolution*, 23(10), pp. 578–587. Available at: https://doi.org/10.1016/j.tree.2008.06.005.

Shine, M.B. *et al.* (2019) 'Glycerol-3-phosphate mediates rhizobia-induced systemic signaling in soybean', *Nature Communications*, 10(1), p. 5303. Available at: https://doi.org/10.1038/s41467-019-13318-8.

Sigma-Aldrich Co.LLC (2016) *ß-Glucuronidase Reporter Gene Staining Kit*. Technical Bulletin GUSS. Bioassy Section: Sigma-Aldrich Co.LLC, p. 2. Available at: https://www.sigmaaldrich.com/deepweb/assets/sigmaaldrich/product/documents/155/752/gussbul.pdf (Accessed: 17 September 2024).

Singh, M. *et al.* (2022) 'Early oxidative burst and anthocyanin-mediated antioxidant defense mechanism impart resistance against *Sclerotinia sclerotiorum* in Indian mustard', *Physiological and Molecular Plant Pathology*, 120, p. 101847. Available at: https://doi.org/10.1016/j.pmpp.2022.101847.

Singh, P. *et al.* (2021) 'The role of quercetin in plants', *Plant Physiology and Biochemistry*, 166, pp. 10–19. Available at: https://doi.org/10.1016/j.plaphy.2021.05.023.

Song, C. *et al.* (2022) 'The Multifaceted Roles of MYC2 in Plants: Toward Transcriptional Reprogramming and Stress Tolerance by Jasmonate Signaling', *Frontiers in Plant Science*, 13. Available at: https://doi.org/10.3389/fpls.2022.868874.

Song, Y. and Thomma, B.P.H.J. (2016) 'Host-induced gene silencing compromises Verticillium wilt in tomato and *Arabidopsis*', *Molecular Plant Pathology*, 19(1), pp. 77–89. Available at: https://doi.org/10.1111/mpp.12500.

Sozzani, R. and Benfey, P.N. (2011) 'High-throughput phenotyping of multicellular organisms: finding the link between genotype and phenotype', *Genome Biology*, 12(3), p. 219. Available at: https://doi.org/10.1186/gb-2011-12-3-219.

Sparkes, I. *et al.* (2006) 'Rapid, transient expression of fluorescent fusion proteins in tobacco plants and generation of stably transformed plants', *Nature Protocols*, 1, pp. 2019–25. Available at: https://doi.org/10.1038/nprot.2006.286.

Spoel, S.H. and Dong, X. (2012) 'How do plants achieve immunity? Defence without specialized immune cells', *Nature Reviews Immunology*, 12(2), pp. 89–100. Available at: https://doi.org/10.1038/nri3141.

Srivastava, S. *et al.* (2015) 'Transcriptomics profiling of Indian mustard (*Brassica juncea*) under arsenate stress identifies key candidate genes and regulatory pathways', *Frontiers in Plant Science*, 6. Available at: https://doi.org/10.3389/fpls.2015.00646.

Stotz, H.U., Thomson ‚James and and Wang, Y. (2009) 'Plant defensins: Defense, development and application', *Plant Signaling & Behavior*, 4(11), pp. 1010–1012. Available at: https://doi.org/10.4161/psb.4.11.9755.

Stukenbrock, E. and McDonald, B. (2008) 'The Origins of Plant Pathogens in Agro-Ecosystems', *Annual review of phytopathology*, 46, pp. 75–100. Available at: https://doi.org/10.1146/annurev.phyto.010708.154114.

Su, J. *et al.* (2018) 'Active photosynthetic inhibition mediated by MPK3/MPK6 is critical to effector-triggered immunity', *PLOS Biology*, 16(5), p. e2004122. Available at: https://doi.org/10.1371/journal.pbio.2004122.

Sun, Y.-W. *et al.* (2015) 'Attenuation of Histone Methyltransferase KRYPTONITE-mediated transcriptional gene silencing by Geminivirus', *Scientific Reports*, 5, p. 16476. Available at: https://doi.org/10.1038/srep16476.

Suzuki, K. *et al.* (2009) 'Ti and Ri Plasmids', in E. Schwartz (ed.) *Microbial Megaplasmids*. Berlin, Heidelberg: Springer, pp. 133–147. Available at: https://doi.org/10.1007/978-3-540-85467-8_6.

Tarkowski, P. and Vereecke, D. (2014) 'Threats and opportunities of plant pathogenic bacteria', *Biotechnology Advances*, 32(1), pp. 215–229. Available at: https://doi.org/10.1016/j.biotechadv.2013.11.001.

The Arabidopsis Genome Initiative (2000) 'Analysis of the genome sequence of the flowering plant *Arabidopsis thaliana*.', *Nature*, 408(6814), pp. 796–815. Available at: https://doi.org/10.1038/35048692.

The Arabidopsis Information Resource (TAIR) (2007) 'Polymorphism: SAIL_384_E04.V1'. https://www.arabidopsis.org/: The Arabidopsis Information Resource (TAIR). Available at: https://www.arabidopsis.org/polyallele?key=500329009 (Accessed: 8 July 2025).

Thermo Fisher Scientific, Inc (2014) *Phire Plant Direct PCR Kit*. Lab Protocol MAN0013358. USA: Thermo Fisher Scientific, Inc, p. 2. Available at: https://assets.thermofisher.com/TFS-Assets/LSG/manuals/MAN0013358_Phire_Plant_Direct_PCR_UG.pdf (Accessed: 3 September 2024).

Thulasi Devendrakumar, K., Li, X. and Zhang, Y. (2018) 'MAP kinase signalling: interplays between plant PAMP- and effector-triggered immunity', *Cellular and Molecular Life Sciences: CMLS*, 75(16), pp. 2981–2989. Available at: https://doi.org/10.1007/s00018-018-2839-3.

Tian, H. *et al.* (2024) 'Salicylic acid: The roles in plant immunity and crosstalk with other hormones', *Journal of Integrative Plant Biology*, 67(3), pp. 773–785. Available at: https://doi.org/10.1111/jipb.13820.

Tiwari, B. *et al.* (2020) 'Identification of small RNAs during cold acclimation in Arabidopsis thaliana', *BMC Plant Biology*, 20, p. 298. Available at: https://doi.org/10.1186/s12870-020-02511-3.

Tsikou, D. *et al.* (2018) 'Systemic control of legume susceptibility to rhizobial infection by a mobile microRNA', *Science*, 362(6411), pp. 233–236. Available at: https://doi.org/10.1126/science.aat6907.

Tsuda, K. and Katagiri, F. (2010) 'Comparing signaling mechanisms engaged in pattern-triggered and effector-triggered immunity', *Current Opinion in Plant Biology*, 13(4), pp. 459–465. Available at: https://doi.org/10.1016/j.pbi.2010.04.006.

Ugalde, J.M. *et al.* (2021) 'A dual role for glutathione transferase U7 in plant growth and protection from methyl viologen-induced oxidative stress', *Plant Physiology*, 187(4), pp. 2451–2468. Available at: https://doi.org/10.1093/plphys/kiab444.

Uppalapati, S.R. *et al.* (2005) 'The phytotoxin coronatine and methyl jasmonate impact multiple phytohormone pathways in tomato', *The Plant Journal*, 42(2), pp. 201–217. Available at: https://doi.org/10.1111/j.1365-313X.2005.02366.x.

Val-Torregrosa, B. *et al.* (2022) 'Phosphate-induced resistance to pathogen infection in *Arabidopsis*', *The Plant Journal*, 110(2), pp. 452–469. Available at: https://doi.org/10.1111/tpj.15680.

Veluthambi, K. and Sunitha, S. (2021) 'Targets and Mechanisms of Geminivirus Silencing Suppressor Protein AC2', *Frontiers in Microbiology*, 12, p. 645419. Available at: https://doi.org/10.3389/fmicb.2021.645419.

Vlot, A.C., Dempsey, D.A. and Klessig, D.F. (2009) 'Salicylic Acid, a Multifaceted Hormone to Combat Disease', *Annual Review of Phytopathology*, 47(Volume 47, 2009), pp. 177–206. Available at: https://doi.org/10.1146/annurev.phyto.050908.135202.

Volko, S.M., Boller, T. and Ausubel, F.M. (1998) 'Isolation of New Arabidopsis Mutants With Enhanced Disease Susceptibility to Pseudomonas syringae by Direct Screening', *Genetics*, 149(2), pp. 537–548. Available at: https://doi.org/10.1093/genetics/149.2.537.

Wang, B. *et al.* (2018) 'Ta*MAPK*4 Acts as a Positive Regulator in Defense of Wheat Stripe-Rust Infection', *Frontiers in Plant Science*, 9, p. 152. Available at: https://doi.org/10.3389/fpls.2018.00152.

Wang, B. *et al.* (2022) 'High-quality *Arabidopsis thaliana* Genome Assembly with Nanopore and HiFi Long Reads', *Genomics, Proteomics & Bioinformatics*, 20(1), pp. 4–13. Available at: https://doi.org/10.1016/j.gpb.2021.08.003.

Wang, C. *et al.* (2014) 'Free Radicals Mediate Systemic Acquired Resistance', *Cell Reports*, 7(2), pp. 348–355. Available at: https://doi.org/10.1016/j.celrep.2014.03.032.

Wang, C. *et al.* (2019) 'Extracellular pyridine nucleotides trigger plant systemic immunity through a lectin receptor kinase/BAK1 complex', *Nature Communications*, 10(1), p. 4810. Available at: https://doi.org/10.1038/s41467-019-12781-7.

Wang, J. *et al.* (2019) 'Jasmonate action in plant defense against insects', *Journal of Experimental Botany*, 70(13), pp. 3391–3400. Available at: https://doi.org/10.1093/jxb/erz174.

Wang, L., Kim, J. and Somers, D.E. (2013) 'Transcriptional corepressor TOPLESS complexes with pseudoresponse regulator proteins and histone deacetylases to regulate circadian transcription', *Proceedings of the National Academy of Sciences*, 110(2), pp. 761–766. Available at: https://doi.org/10.1073/pnas.1215010110.

Wang, M. *et al.* (2016) 'Bidirectional cross-kingdom RNAi and fungal uptake of external RNAs confer plant protection', *Nature Plants*, 2, p. 16151. Available at: https://doi.org/10.1038/nplants.2016.151.

Wang, S. *et al.* (2016) 'Chloroplast RNA-Binding Protein RBD1 Promotes Chilling Tolerance through 23S rRNA Processing in *Arabidopsis*', *PLoS Genetics*, 12. Available at: https://doi.org/10.1371/journal.pgen.1006027.

Wang, X.-B. *et al.* (2011) 'The 21-Nucleotide, but Not 22-Nucleotide, Viral Secondary Small Interfering RNAs Direct Potent Antiviral Defense by Two Cooperative Argonautes in *Arabidopsis thaliana*', *The Plant Cell*, 23(4), pp. 1625–1638. Available at: https://doi.org/10.1105/tpc.110.082305.

Wang, Y. *et al.* (2015) 'Endogenous Cytokinin Overproduction Modulates ROS Homeostasis and Decreases Salt Stress Resistance in *Arabidopsis thaliana*', *Frontiers in Plant Science*, 6, p. 1004. Available at: https://doi.org/10.3389/fpls.2015.01004.

Wang, Y. *et al.* (2021) 'Regulation and Function of Defense-Related Callose Deposition in Plants', *International Journal of Molecular Sciences*, 22(5), p. 2393. Available at: https://doi.org/10.3390/ijms22052393.

Wang, Y., Yaghmaiean, H. and Zhang, Y. (2020) 'High transformation efficiency in Arabidopsis using extremely low Agrobacterium inoculum', *F1000Research*, 9, p. 356. Available at: https://doi.org/10.12688/f1000research.23449.1.

Wang, Z. *et al.* (2023) '*Ralstonia solanacearum* – A soil borne hidden enemy of plants: Research development in management strategies, their action mechanism and challenges', *Frontiers in Plant Science*, 14, p. 1141902. Available at: https://doi.org/10.3389/fpls.2023.1141902.

W.C. James (1971) 'AN ILLUSTRATED SERIES OF ASSESSMENT KEYS FOR PLANT DISEASES, THEIR PREPARATION AND USAGE'', *Journal Canadian Plant Disease Survey*, 51(2), pp. 39–65.

Wenig, M. *et al.* (2019) 'Systemic acquired resistance networks amplify airborne defense cues', *Nature Communications*, 10(1), p. 3813. Available at: https://doi.org/10.1038/s41467-019-11798-2.

Whalen, M.C. *et al.* (1991) 'Identification of Pseudomonas syringae pathogens of Arabidopsis and a bacterial locus determining avirulence on both Arabidopsis and soybean.', *The Plant Cell*, 3(1), pp. 49–59. Available at: https://doi.org/10.1105/tpc.3.1.49.

Whitehead, K.A. *et al.* (2011) 'Silencing or Stimulation? siRNA Delivery and the Immune System', *Annual Review of Chemical and Biomolecular Engineering*, 2(1), pp. 77–96. Available at: https://doi.org/10.1146/annurev-chembioeng-061010-114133.

Wickham, H. (2016) *ggplot2: Elegant Graphics for Data Analysis*. 2nd ed. 2016. Cham: Springer International Publishing : Imprint: Springer (Use R!). Available at: https://doi.org/10.1007/978-3-319-24277-4.

Wightman, B., Ha, I. and Ruvkun, G. (1993) 'Posttranscriptional regulation of the heterochronic gene lin-14 by lin-4 mediates temporal pattern formation in *C. elegans*', *Cell*, 75(5), pp. 855–862. Available at: https://doi.org/10.1016/0092-8674(93)90530-4.

Wiktorek-Smagur, A., Hnatuszko-Konka, K. and Kononowicz, A.K. (2009) 'Flower bud dipping or vacuum infiltration—two methods of *Arabidopsis thaliana* transformation', *Russian Journal of Plant Physiology*, 56(4), pp. 560–568. Available at: https://doi.org/10.1134/S1021443709040177.

Wilson, R.C. and Doudna, J.A. (2013) 'Molecular Mechanisms of RNA Interference', *Annual Review of Biophysics*, 42(Volume 42, 2013), pp. 217–239. Available at: https://doi.org/10.1146/annurev-biophys-083012-130404.

Wroblewski, T., Tomczak, A. and Michelmore, R. (2005) 'Optimization of *Agrobacterium*-mediated transient assays of gene expression in lettuce, tomato and *Arabidopsis*', *Plant Biotechnology Journal*, 3(2), pp. 259–273. Available at: https://doi.org/10.1111/j.1467-7652.2005.00123.x.

Wu, Y. *et al.* (2012) 'The *Arabidopsis* NPR1 Protein Is a Receptor for the Plant Defense Hormone Salicylic Acid', *Cell Reports*, 1(6), pp. 639–647. Available at: https://doi.org/10.1016/j.celrep.2012.05.008.

Xie, L. *et al.* (2023) 'Screening of microRNAs and target genes involved in *Sclerotinia sclerotiorum* (Lib.) infection in *Brassica napus L.*', *BMC Plant Biology*, 23(1), p. 479. Available at: https://doi.org/10.1186/s12870-023-04501-7.

Xie, Z. *et al.* (2004) 'Genetic and Functional Diversification of Small RNA Pathways in Plants', *PLoS Biology*. Edited by Detlef Weigel, 2(5), p. e104. Available at: https://doi.org/10.1371/journal.pbio.0020104.

Xin, X.-F. *et al.* (2016) 'Bacteria establish an aqueous living space in plants crucial for virulence', *Nature*, 539(7630), pp. 524–529. Available at: https://doi.org/10.1038/nature20166.

Xin, X.-F., Kvitko, B. and He, S.Y. (2018) '*Pseudomonas syringae*: what it takes to be a pathogen', *Nature reviews. Microbiology*, 16(5), pp. 316–328. Available at: https://doi.org/10.1038/nrmicro.2018.17.

Xu, H.-J. *et al.* (2008) 'Exploration on the vacuum infiltration transformation of pakchoi', *Biologia plantarum*, 52(4), pp. 763–766. Available at: https://doi.org/10.1007/s10535-008-0148-7.

Yang, Y. *et al.* (2024) 'Characterization of UGT71, a major glycosyltransferase family for triterpenoids, flavonoids and phytohormones-biosynthetic in plants', *Forestry Research*, 4(1). Available at: https://doi.org/10.48130/forres-0024-0032.

Yao, J., Withers, J. and He, S.Y. (2013) 'Pseudomonas syringae infection assays in Arabidopsis', *Methods in Molecular Biology (Clifton, N.J.)*, 1011, pp. 63–81. Available at: https://doi.org/10.1007/978-1-62703-414-2_6.

Ye, G.-N. *et al.* (1999) 'Arabidopsis ovule is the target for *Agrobacterium* in planta vacuum infiltration transformation', *The Plant Journal*, 19(3), pp. 249–257. Available at: https://doi.org/10.1046/j.1365-313X.1999.00520.x.

Ye, J. *et al.* (2015) 'Geminivirus Activates ASYMMETRIC LEAVES 2 to Accelerate Cytoplasmic DCP2-Mediated mRNA Turnover and Weakens RNA Silencing in *Arabidopsis*', *PLOS Pathogens*. Edited by D.M. Bisaro, 11(10), p. e1005196. Available at: https://doi.org/10.1371/journal.ppat.1005196.

Yeh, Y.-H. *et al.* (2015) 'Enhanced *Arabidopsis* pattern-triggered immunity by overexpression of cysteine-rich receptor-like kinases', *Frontiers in Plant Science*, 6, p. 322. Available at: https://doi.org/10.3389/fpls.2015.00322.

Yin, R. *et al.* (2014) 'Kaempferol 3-O-rhamnoside-7-O-rhamnoside is an endogenous flavonol inhibitor of polar auxin transport in Arabidopsis shoots', *New Phytologist*, 201(2), pp. 466–475. Available at: https://doi.org/10.1111/nph.12558.

Yoneyama, K. and Natsume, M. (2010) '4.13 - Allelochemicals for Plant–Plant and Plant–Microbe Interactions', in H.-W. (Ben) Liu and L. Mander (eds) *Comprehensive Natural Products II*. Oxford: Elsevier, pp. 539–561. Available at: https://doi.org/10.1016/B978-008045382-8.00105-2.

Young, J.M. (2010) 'TAXONOMY OF *PSEUDOMONAS SYRINGAE*', *Journal of Plant Pathology*, 92, pp. S5–S14.

Yousaf, M.J. *et al.* (2021) 'Transformation of Endophytic *Bipolaris spp.* Into Biotrophic Pathogen Under Auxin Cross-Talk With Brassinosteroids and Abscisic Acid', *Frontiers in Bioengineering and Biotechnology*, 9, p. 657635. Available at: https://doi.org/10.3389/fbioe.2021.657635.

Yu, K. *et al.* (2013) 'A Feedback Regulatory Loop between G3P and Lipid Transfer Proteins DIR1 and AZI1 Mediates Azelaic-Acid-Induced Systemic Immunity', *Cell Reports*, 3(4), pp. 1266–1278. Available at: https://doi.org/10.1016/j.celrep.2013.03.030.

Yu, X. *et al.* (2017) 'From Chaos to Harmony: Responses and Signaling upon Microbial Pattern Recognition', *Annual Review of Phytopathology*, 55(Volume 55, 2017), pp. 109–137. Available at: https://doi.org/10.1146/annurev-phyto-080516-035649.

Yu, X.-Q. *et al.* (2024) 'PTI-ETI synergistic signal mechanisms in plant immunity', *Plant Biotechnology Journal*, 22(8), pp. 2113–2128. Available at: https://doi.org/10.1111/pbi.14332.

Yuan, M., Jiang, Z., *et al.* (2021) 'Pattern-recognition receptors are required for NLR-mediated plant immunity', *Nature*, 592(7852), pp. 105–109. Available at: https://doi.org/10.1038/s41586-021-03316-6.

Yuan, M., Ngou, B.P.M., *et al.* (2021) 'PTI-ETI crosstalk: an integrative view of plant immunity', *Current Opinion in Plant Biology*, 62, p. 102030. Available at: https://doi.org/10.1016/j.pbi.2021.102030.

Zambryski, P., Tempe, J. and Schell, J. (1989) 'Transfer and function of T-DNA genes from *Agrobacterium* Ti and Ri plasmids in plants', *Cell*, 56(2), pp. 193–201. Available at: https://doi.org/10.1016/0092-8674(89)90892-1.

Zarei, A. *et al.* (2011) 'Two GCC boxes and AP2/ERF-domain transcription factor ORA59 in jasmonate/ethylene-mediated activation of the PDF1.2 promoter in Arabidopsis', *Plant Molecular Biology*, 75(4), pp. 321–331. Available at: https://doi.org/10.1007/s11103-010-9728-y.

Zeng, W. and He, S.Y. (2010) 'A Prominent Role of the Flagellin Receptor FLAGELLIN-SENSING2 in Mediating Stomatal Response to *Pseudomonas syringae pv* tomato DC3000 in *Arabidopsis*', *Plant Physiology*, 153(3), pp. 1188–1198. Available at: https://doi.org/10.1104/pp.110.157016.

Zhang, K. *et al.* (2019) 'Isolation and characterization of the GbVIP1 gene and response to Verticillium wilt in cotton and tobacco', *Journal of Cotton Research*, 2(1), p. 2. Available at: https://doi.org/10.1186/s42397-019-0019-0.

Zhang, L. *et al.* (2011) 'The involvement of jasmonates and ethylene in *Alternaria alternata f. sp. lycopersici* toxin-induced tomato cell death', *Journal of Experimental Botany*, 62(15), pp. 5405–5418. Available at: https://doi.org/10.1093/jxb/err217.

Zhang, L. *et al.* (2017) 'Jasmonate signaling and manipulation by pathogens and insects', *Journal of Experimental Botany*, 68(6), pp. 1371–1385. Available at: https://doi.org/10.1093/jxb/erw478.

Zhang, L. *et al.* (2023) 'Plant cell surface immune receptors—Novel insights into function and evolution', *Current Opinion in Plant Biology*, 74, p. 102384. Available at: https://doi.org/10.1016/j.pbi.2023.102384.

Zhang, P. *et al.* (2024) 'Strategies for Enhancing Plant Immunity and Resilience Using Nanomaterials for Sustainable Agriculture', *Environmental Science & Technology*, 58(21), pp. 9051–9060. Available at: https://doi.org/10.1021/acs.est.4c03522.

Zhang, P. *et al.* (2025) 'Salicylic acid and jasmonic acid in plant immunity', *Horticulture Research*, p. uhaf082. Available at: https://doi.org/10.1093/hr/uhaf082.

Zhang, X. *et al.* (2006) '*Agrobacterium*-mediated transformation of *Arabidopsis thaliana* using the floral dip method', *Nature Protocols*, 1(2), pp. 641–646. Available at: https://doi.org/10.1038/nprot.2006.97.

Zhang, X. *et al.* (2019) 'Mechanisms and Functions of Long Non-Coding RNAs at Multiple Regulatory Levels', *International Journal of Molecular Sciences*, 20. Available at: https://doi.org/10.3390/ijms20225573.

Zhang, X.-N. *et al.* (2018) 'Metabolomics Analysis Reveals that Ethylene and Methyl Jasmonate Regulate Different Branch Pathways to Promote the Accumulation of Terpenoid Indole Alkaloids in Catharanthus roseus', *Journal of Natural Products*, 81(2), pp. 335–342. Available at: https://doi.org/10.1021/acs.jnatprod.7b00782.

Zhang, Y. *et al.* (2020) 'A Highly Efficient *Agrobacterium*-Mediated Method for Transient Gene Expression and Functional Studies in Multiple Plant Species', *Plant Communications*, 1(5), p. 100028. Available at: https://doi.org/10.1016/j.xplc.2020.100028.

Zhang, Z. *et al.* (2014) 'Salicylic Acid Signaling Controls the Maturation and Localization of the *Arabidopsis* Defense Protein ACCELERATED CELL DEATH6', *Molecular Plant*, 7(8), pp. 1365–1383. Available at: https://doi.org/10.1093/mp/ssu072.

Zheng, L. *et al.* (2021) 'An improved and efficient method of *Agrobacterium* syringe infiltration for transient transformation and its application in the elucidation of gene function in poplar', *BMC Plant Biology*, 21, p. 54. Available at: https://doi.org/10.1186/s12870-021-02833-w.

Zhu, Z. (2014) 'Molecular basis for jasmonate and ethylene signal interactions in Arabidopsis', *Journal of Experimental Botany*, 65(20), pp. 5743–5748. Available at: https://doi.org/10.1093/jxb/eru349.

Zipfel, C. and Felix, G. (2005) ‘Plants and animals: a different taste for microbes?’, *Current Opinion in Plant Biology*, 8(4), pp. 353–360. Available at: https://doi.org/10.1016/j.pbi.2005.05.004.

Zou, Y., Wang, S. and Lu, D. (2020) ‘MiR172b-TOE1/2 module regulates plant innate immunity in an age-dependent manner’, *Biochemical and Biophysical Research Communications*, 531(4), pp. 503–507. Available at: https://doi.org/10.1016/j.bbrc.2020.07.061.

8. Appendices

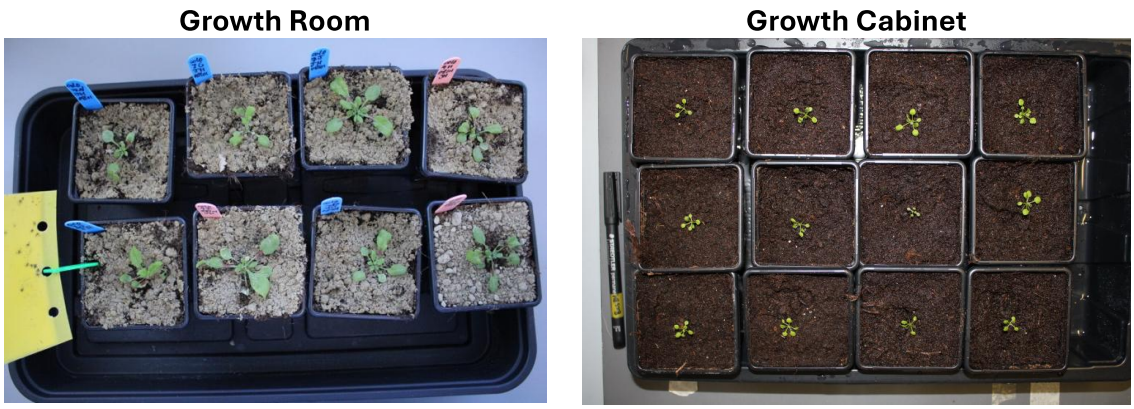

Appendix 1: Col-0 3-weeks post-sewing, grown under the same environmental conditions in a growth room (left) and in a growth cabinet (right).

	1 d.p.i	5 d.p.i
EHA105-I		
		
		
		
GFP-I		




GFP-M






Water-I



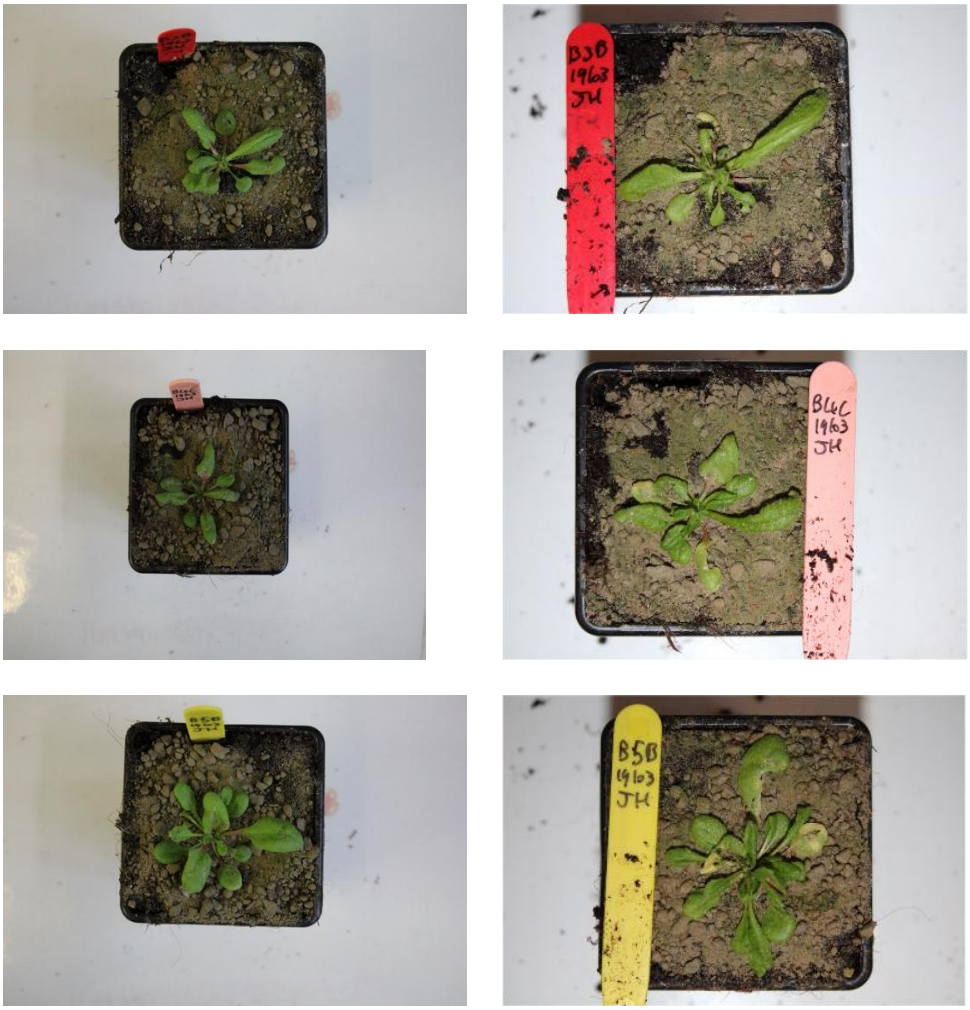

Appendix 3: Col-0 plants from the first round of local infiltrations. Plants have been infiltrated with: Agrobacterium tumefaciens either untransformed (EHA105.I) or carrying (GFP.I and GFP.M) or with sterile infiltration solution (Water.I). Figure shows plants 1 (a) and 5 days post-infection (b) with Pseudomonas syringae.

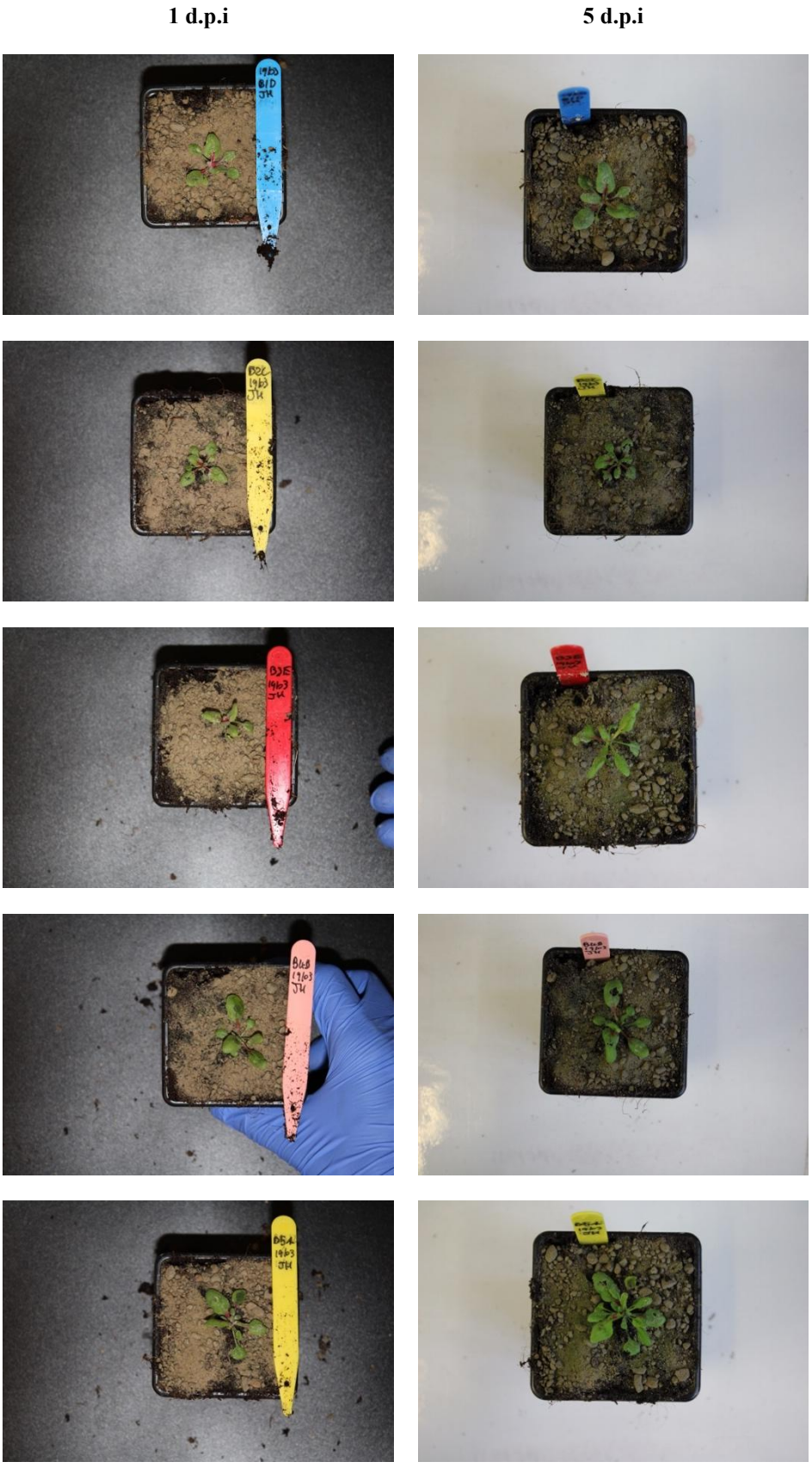

Appendix 4: Col-0 plants from the first round of localized infiltrations agroinfiltrated with GG-Kan^{R}GUS 1 d.p.i and 5 d.p.i

1 d.p.i	5 d.p.i
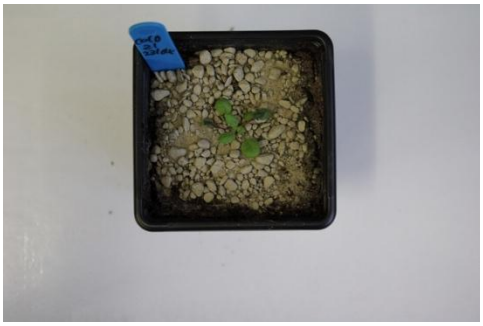	
	
	
	
	

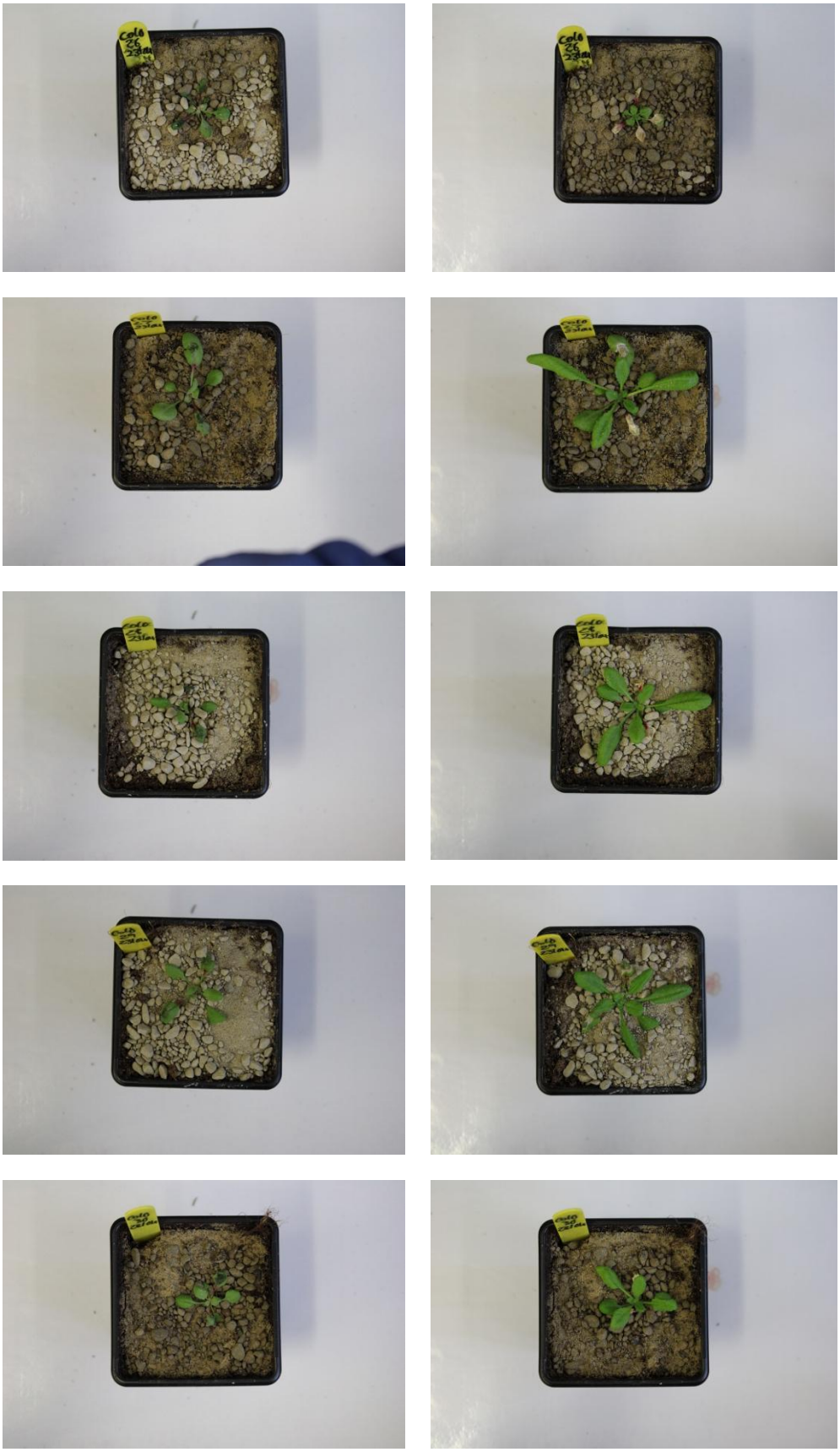

Appendix 5: Col-0 plants from the second round of localized infiltrations agroinfiltrated with GG-Kan^{R}GUS 1 d.p.i and 5 d.p.i

Appendix 6: Col-0 plants that have received hairpin carrying A. tumefaciens and P. syringae in alternating leaves (5 d.p.i with P .syringae)

1 d.p.i **5 d.p.i**

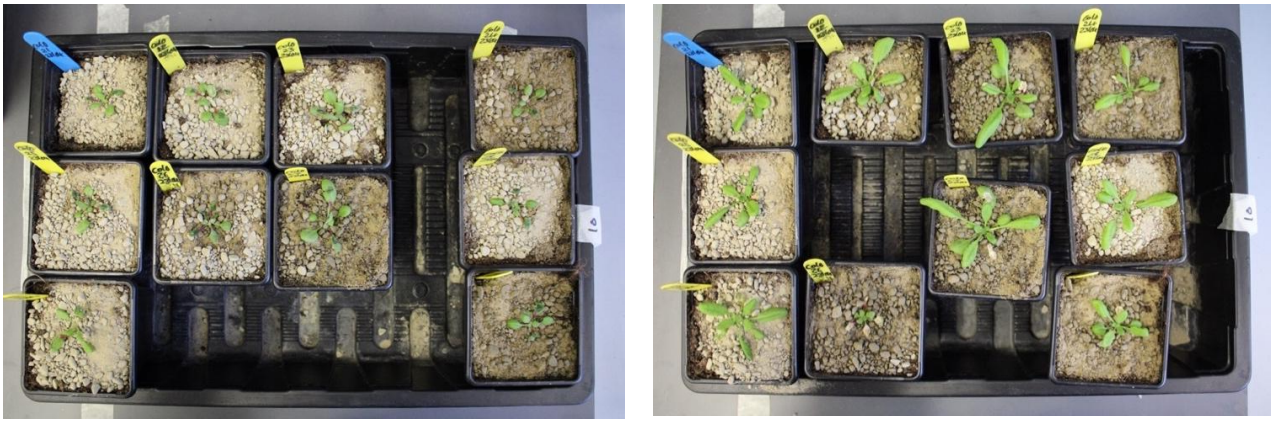

Appendix 7: Col-0 in the second round of localized infiltration, Col-0 replicates 21-29, infiltrated with A. tumefaciens carrying GG-Kan^{R}GUS. 1 d.p.i (left) and 5 d.p.i (right).

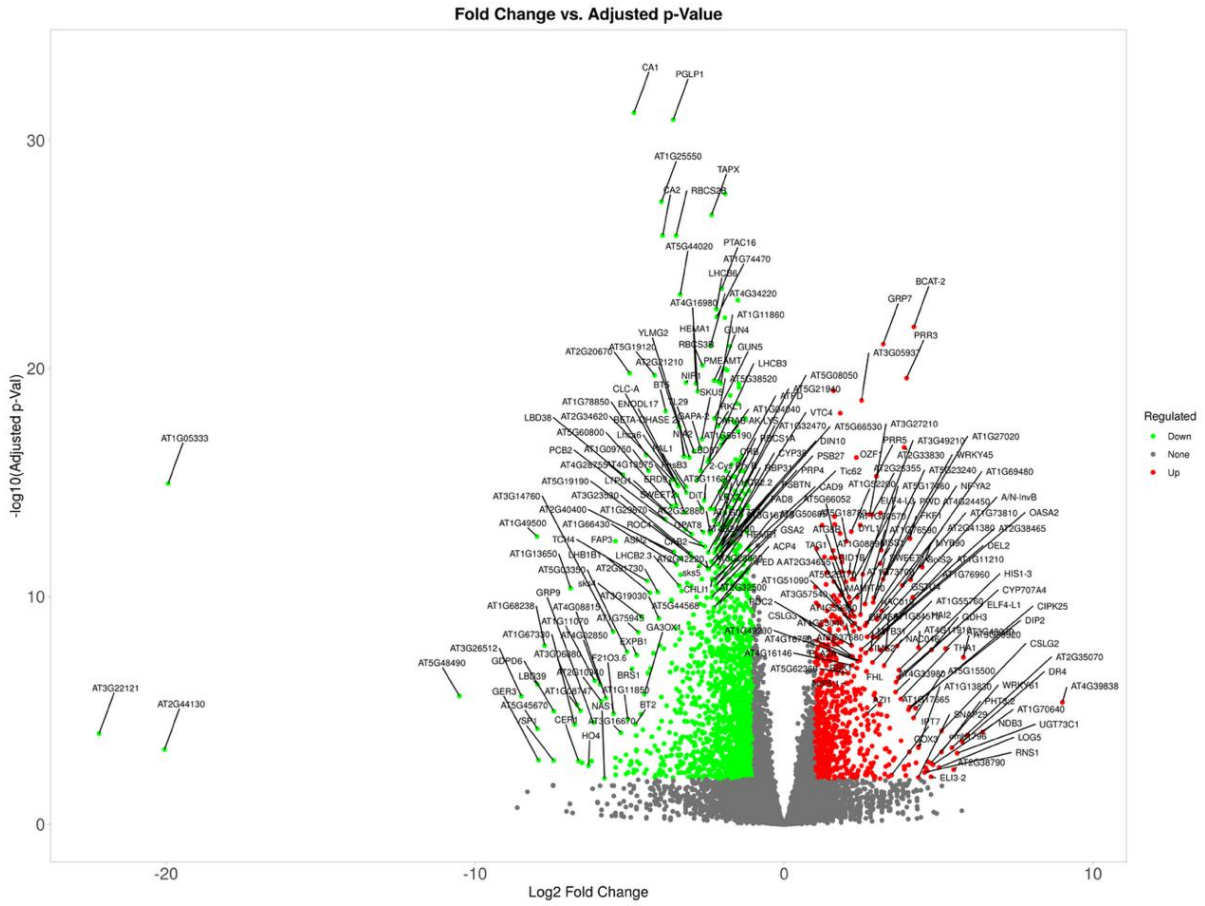

a)

b)

Appendix 8: A Volcano Plot of the Top 50 Differentially Expressed Genes of Col-0 vs *AT1703* on 0 d.p.i. (a) and 2 d.p.i (b) with and False Discovery Rate (FDR) of < 0.01. The magnitude of up/downregulation is given as Log2 Fold change (-20 to 10) shown on the X-axis and the significance of the change is given as -log10(adjusted *p*-value) (0-30) shown on the Y-axis. As shown above, there are genes that have been consistently up/downregulated across both time points.